Optimization methods for scheduling the charge of electric vehicles and planning their charging infrastructure

Biswarup Mukherjee

PSL UNIVERSITÉ PARIS

THÈSE DE DOCTORAT
DE L'UNIVERSITÉ PSL

Préparée à Mines Paris-PSL

Méthodes d'optimisation pour la programmation de la charge des véhicules électriques et la planification de leur infrastructure de charge
Optimization methods for scheduling the charge of electric vehicles and planning their charging infrastructure

Soutenue par

Biswarup Mukherjee

Le 07 07 2023

École doctorale n°621

Ingénierie des Systèmes, Matériaux, Mécanique, Energétique

Spécialité

Energetique et Génie de Procédés

Composition du jury :

Federico Silvestro Professor, University of Genova	*Président*
Marie-Cecile Alvarez-Herault Maître de conférences, HDR, Université Grenoble Alpes	*Rapportrice*
Manuela Sechilariu Professeure des Universités, Université de Technologie de Compiègne	*Rapportrice*
Katarina Knezovic Senior Scientist, Hitachi Energy	*Examinatrice*
Marc Petit Professeur des Universités, Centrale-Supélec	*Examinateur*
Fabrizio Sossan Associate Professor, HES-SO	*Examinateur*
Georges Kariniotakis Directeur de Recherche, Mines Paris - PSL	*Directeur de thèse*

MINES PARIS | PSL

Abstract

The growing number of electric vehicles (EVs) poses a significant challenge for distribution grid operators (DSOs) due to the increased power demand required for EV charging. This surge in demand raises concerns as it can lead to violations of operational and physical constraints within the grid, such as voltage levels, line currents, and substation transformer power flows. This thesis addresses the issue by developing algorithmic solutions to assist DSOs in effectively managing high EV penetration while adhering to operational and physical constraints of the grid. The research focuses on two main aspects: scheduling EV charging and planning the necessary charging infrastructure. For scheduling the charge of EVs, the thesis focuses on the development of a unified algorithmic framework capable of accommodating various charging strategies while taking into account operational constraints of the distribution grid. This framework utilizes an optimal power flow (OPF) formulation, incorporating a linearized model of the grid to ensure convexity and improve computational efficiency. By employing this framework, different charging strategies, such as uncoordinated charging, grid-aware coordinated charging (V1G), reactive power support, and vehicle-to-grid (V2G) interactions, can be compared and analyzed for large penetration of EVs. To plan the charging infrastructure for large penetration of EVs, a mixed-integer linear programming (MILP) formulation is proposed, extending the proposed scheduling framework. Here the objective is to compute the number and the location of EV chargers by satisfying EVs' charging demand and the operational constraints of the distribution grid. The proposed formulation explicitly models flexibility of owners in plugging and unplugging their EVs, emphasizing the advantages of cooperative owners who promptly disconnect after charging completion. Additionally, the planning method considers the concept of single-port and multi-port chargers, highlighting their significance. Furthermore, an extension of the method is proposed to encourage PV self-consumption and incorporate V2G functionality. Validation of the proposed deployment plans demonstrates the superiority of optimally deployed chargers in achieving higher charging levels for EVs compared to uniform deployment scenarios.

Résumé en Français

Le nombre croissant de véhicules électriques (VE) représente un défi important pour les gestionnaires de réseaux de distribution (GRD) en raison de l'augmentation de la demande d'électricité nécessaire pour la recharge des VE. Cette augmentation de la demande soulève des inquiétudes car elle peut conduire à des violations des contraintes opérationnelles et physiques au sein du réseau, telles que les niveaux de tension, les courants de ligne et les flux de puissance des transformateurs des sous-stations. Cette thèse aborde le problème en développant des solutions algorithmiques pour aider les GRD à gérer efficacement la forte pénétration des VE tout en respectant les contraintes opérationnelles et physiques du réseau. La recherche se concentre sur deux aspects principaux : la programmation de la charge des VE et la planification de l'infrastructure de charge nécessaire. Pour la programmation de la charge des VE, la thèse se concentre sur le développement d'un cadre algorithmique unifié capable d'accommoder différentes stratégies de charge tout en prenant en compte les contraintes opérationnelles du réseau de distribution. Ce cadre utilise une formulation de flux de puissance optimal (OPF), incorporant un modèle linéarisé du réseau pour assurer la convexité et améliorer l'efficacité des calculs. En utilisant ce cadre, différentes stratégies de charge, telles que la charge non coordonnée, la charge coordonnée tenant compte du réseau (V1G), le soutien de la puissance réactive et les interactions véhicule-réseau (V2G), peuvent être comparées et analysées pour une grande pénétration des VE. Pour planifier l'infrastructure de charge pour une grande pénétration des VE, une formulation de programmation linéaire en nombres entiers mixtes (MILP) est proposée, étendant le cadre d'ordonnancement proposé. L'objectif est ici de calculer le nombre et l'emplacement des chargeurs de VE en satisfaisant la demande de charge des VE et les contraintes opérationnelles du réseau de distribution. La formulation proposée modélise explicitement la flexibilité des propriétaires dans le branchement et le débranchement de leurs VE, en soulignant les avantages des propriétaires coopératifs qui se débranchent rapidement après la fin de la charge. En outre, la méthode de planification prend en compte le concept de chargeurs à port unique et à ports multiples, en soulignant leur importance. En outre, une extension de la méthode est proposée pour encourager l'autoconsommation photovoltaïque et intégrer la fonctionnalité V2G. La validation des plans de déploiement proposés démontre la supériorité des chargeurs déployés de manière optimale pour atteindre des niveaux de charge plus élevés pour les VE par rapport aux scénarios de déploiement uniformes.

Acknowledgements

I would like to express my deep gratitude and appreciation to all those who have supported and guided me throughout my doctoral journey.

First and foremost, I extend my heartfelt thanks to my supervisors, Prof. Fabrizio Sossan and Prof. Georges Kariniotakis, for their unwavering guidance, encouragement, and support throughout my research. Their invaluable insights, wisdom, and expertise have significantly shaped the direction and focus of my work. Furthermore, I am deeply grateful to the EVA Project[1] for funding my Ph.D. studies. Their financial support has played a crucial role in facilitating the execution of my research and its successful completion.

I would like to extend my appreciation to the dedicated staff of Centre PERSEE for providing a stimulating and supportive research environment. Their expertise, professionalism, and unwavering commitment have been instrumental in creating an atmosphere conducive to academic growth and development.

I am forever indebted to Dr. Daniel Re, whose significant role in my life during my doctoral journey cannot be overstated. Lastly, I would like to express my deepest gratitude to my grandma, parents, and friends (especially Dr. Suman Maity) for their unwavering love, support, and encouragement throughout my academic journey. Their belief in my abilities, along with the extraordinary care provided by Dr. Re, has been a constant source of strength and inspiration.

Thank you all for your support and encouragement.

Biswarup
April, 2023

[1]Funding Agency: ERA-Net and European Union's Horizon 2020 Research and Innovation Programme (Grant Number: 775970)

List of Acronyms

AC	Alternate Current
AEV	Autonomous Electric Vehicle
AV	Autonomous Vehicle
BESS	Battery Energy Storage System
DC	Direct Current
DSO	Distribution System Operator
EU	European Union
EUCO	European Council
EV	Electric Vehicle
GHG	Greenhouse Gases
GS	Gauss-Seidel
HV	High Voltage
IEC	International Electrotechnical Commission
IEEE	Institute of Electrical and Electronics Engineers
LDVs	Light-Duty Vehicles
LP	Linear Programming
LV	Low Voltage
MCS	Monte Carlo simulation
MILP	Mixed-Integer Linear Programming
MIP	Mixed-Integer Programming
MOEA	Multi-Objective Evolutionary Algorithm
MONAA	Multi-Objective Natural Aggregation
MPC	Multi-Port Charger

MV	Medium Voltage
NLP	Nonlinear Programming
NR	Newton Raphson
NSGA	Non-Dominated Sorting Genetic Algorithm
OLTC	On-Load Tap Changer
OPF	Optimal Power Flow
QP	Quadratic Programming
RES	Renewable Energy Source
SAE	Society of Automotive Engineers
SAEV	Shared Autonomous Electric Vehicle
SC	Sensitivity Coefficient
SG	Scenario Generation
SOC	State-Of-Charge
SOCP	Second-Order Cone Programming
SPC	Single-Port Charger
TSO	Transmission System Operator
V2B	Vehicle-to-Building
V2G	Vehicle-to-Grid
V2H	Vehicle-to-Home
V2X	Vehicle-to-Everything

Contents

List of Figures

List of Tables

Chapter 1

Introduction

Résumé en Français

Le chapitre introductif de la thèse donne un aperçu du contexte général et des questions clés qui entourent le sujet. Il aborde les défis liés à l'intégration des véhicules électriques (VE) dans les réseaux électriques. En outre, il explore le concept émergent de la mobilité autonome et ses implications pour l'intégration des VE dans les réseaux électriques. En outre, le chapitre présente une analyse de l'état de l'art, couvrant des sujets importants tels que les modèles de charge des batteries de VE, les techniques d'écoulement optimal de l'énergie et la modélisation des réseaux électriques. En outre, le chapitre présente les questions de recherche et les objectifs scientifiques qui guident l'étude, établissant une direction claire pour la thèse. Enfin, le chapitre conclut en décrivant la structure et les contributions de la thèse, en soulignant ses perspectives et ses idées uniques, fournissant une base solide pour les chapitres suivants.

Summary

The introductory chapter of the thesis provides an overview of the general context and key issues surrounding the subject. It addresses the challenges involved in integrating electric vehicles (EVs) into power grids. Furthermore, it explores the emerging concept of autonomous mobility and its implications for EV-grid integration. Additionally, the chapter presents a state-of-the-art analysis, covering important topics such as EV battery charging models, optimal power flow techniques, and power grid modeling. Moreover, the chapter presents the research questions and scientific objectives that guide the study, setting a clear direction for the thesis. Finally, the chapter concludes by outlining the structure and contributions of the thesis, highlighting its unique perspectives and insights, providing a solid foundation for the subsequent chapters.

1.1 General context and issues of Thesis subject

Over the past decade, the world has witnessed the consequences of climate change and global warming. According to the 2021 assessment report by the IPCC (Intergovernmental Panel on Climate Change), global temperatures will continue to rise for many decades, primarily due to the greenhouse gases (GHG) produced by human activities [9]. As global warming has significantly impacted society, countries worldwide have initiated energy transition programs to reduce GHG emissions [10]. The climate transition is a key priority for the European Council (EUCO) and the Council of the European Union (EU). In December 2008, the European Commission published the climate and energy package to address objectives that ensure the EU achieves its climate targets by 2020, including a 20% reduction in greenhouse gas emissions, a 20% improvement in energy efficiency, and a 20% share of renewables in the EU energy mix [11]. The EU has also set a target to achieve at least a 40% reduction in GHG emissions by 2030 and to lower GHG emissions by 80-95% below the 1990 level by 2050, which aligns with the goals of the Paris Agreement to keep global warming below 2°C [12]. Although the Covid-19 pandemic resulted in a significant decrease in emissions from the transport sector, it was reported in [13] that in Europe, 27% of greenhouse gas emissions in 2017 were attributed to the transport sector. Between 2018 and 2019, the EU's domestic transport emissions increased by 0.8%. The transport sector is the only sector in which emissions have been consistently increasing since 1990. In France, the transport sector accounts for 40% of GHG emissions, with 95% of those emissions originating from road transport [3].

It has been reported in [14] that light-duty vehicles (LDVs) across the world account for 47% of transport energy usage, and by 2050, the stock of LDVs is projected to reach 2 billion, indicating a doubling of energy usage. Over the past two decades, the European Union (EU) has successfully improved the fuel economy rate for LDVs. LDVs primarily use internal combustion engines that rely on petroleum fuels. While biofuels can be cost-effective, the most promising approach to reducing greenhouse gas (GHG) emissions from LDVs lies in full hybridization, plug-in hybrids, and eventually the adoption of electric vehicles (EVs) [14]. Currently, EVs are considered the primary solution to curtail GHG emissions from road transportation. According to the IEA, with smart charging (see Section 1.2.3) of EVs, it will be possible to reduce CO2 emissions by 50% with increased consumer awareness and better policy frameworks [4]. Although EVs have been around for more than 100 years, their history includes several achievements [15]. The market share of EVs is growing rapidly in France and globally [3]. China is the largest market with 2.6 million EVs, followed by the United States with 1.1 million EVs [2]. Therefore, the implementation of EVs in the transport sector is expected to not only reduce CO2 emissions but also decrease dependency on fossil fuels in the future. Figure 1.1 displays the global distribution of EV stock by region and technology from 2013 to 2019. The plot demonstrates the increasing popularity and adoption of EV technologies worldwide. The widespread adoption of electric vehicles will play a central role in decarbonizing road transportation [2, 16–18]. According to Germany's Solar Energy and Hydrogen Research Centre (ZSW), there were 5.6 million EVs on the road by the beginning of 2019 [2]. Currently, there are three main types of electric vehicles available in the market: fully electric vehicles, fuel cell electric vehicles,

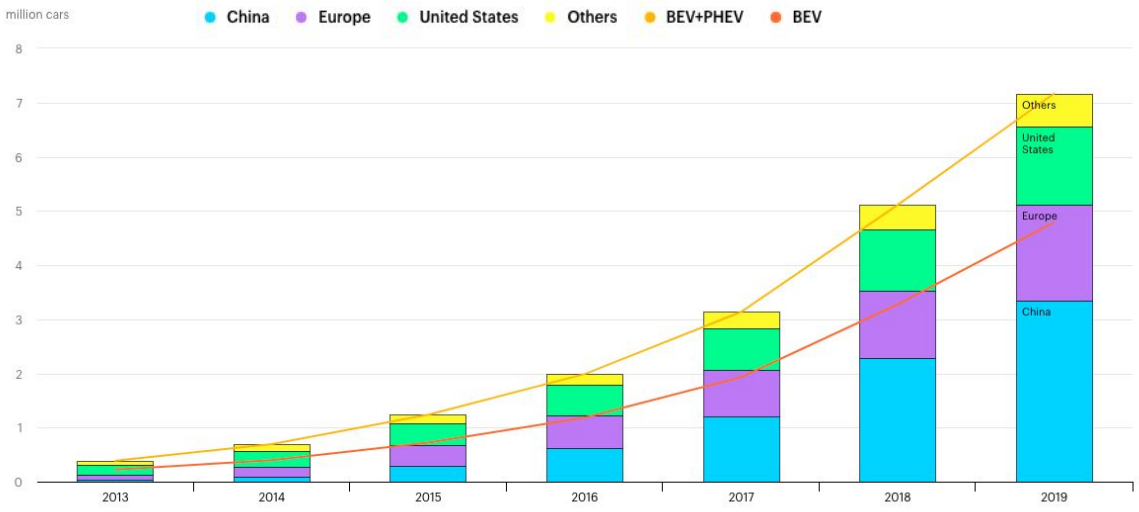

Figure 1.1: Electric vehicles stock by region and technology during 2013-2019. Source: IEA

and hybrid electric vehicles [19]. In this thesis, we will consider fully electric vehicles. As it will be discussed more thoroughly later, a concern related to the massive diffusion of EVs is the recharging process from the power grid, which might overload the existing grid infrastructure. Various charging methodologies have been discussed by authors in [20], such as fast charging, standard charging, and slow charging, which impact the charging time of EVs ranging from 20 minutes to 10 hours, depending on the available charger capacity. To meet the increasing demand for charging electric vehicle fleets, generating more power from renewable sources, such as wind power and solar power, can be considered as a solution to reduce CO2 emissions and develop a sustainable transportation system [15].

The EV technology combines both the transport and energy sectors and acts as a paradigm shift for them [2]. With the increase in the number of EV owners, the demand for EV charging increases, which has an impact on the power and energy sector. Recent advancements in EV technologies, such as charging technologies and shared autonomous driving, within the transportation sector have created further opportunities for conducting research on EVs, particularly on the charging impacts of EV integration with modern power systems.

1.2 Challenges of integrating EVs in power grids

1.2.1 Impact of EV charging on the power grid

There are primarily two impacts of EV integration from a grid perspective. Firstly, with an increase in the number of EV owners, the charging demand of EVs also increases, as it needs to satisfy their driving demand. Secondly, the increased power demand from EVs affects the operation of the grid at both the distribution and transmission levels [5]. EVs can be considered as controllable loads for the power system, and depending on their driving demand, charging patterns, and different charging

methods, the power system experiences variability in the overall load profile [15]. One disadvantage of integrating EVs with the power system is that their charging process requires a significant amount of power. While charging a small number of vehicles may not significantly affect the power system, when a large population of EVs is recharged simultaneously, their charging profiles can lead to overloading, power losses, and wear on grid components, especially in distribution grids.

The impacts of uncontrolled EV charging processes on the distribution network are shown in Fig. 1.2. At the distribution level, distribution system operators (DSOs) are responsible for ensuring

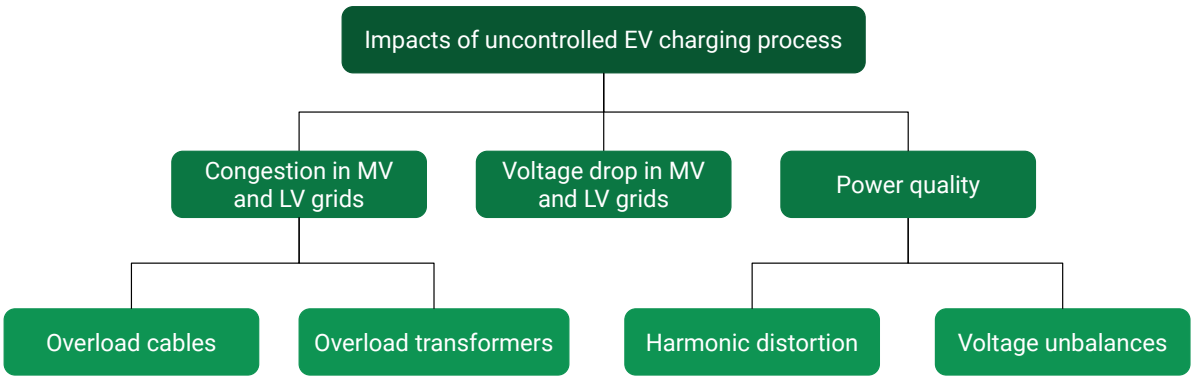

Figure 1.2: Impacts of uncontrolled EV charging process in the distribution network [1].

efficient and reliable power supply to customers through flexibility services, which mainly involve four operations: (a) congestion prevention, (b) loss reduction, (c) voltage magnitude regulation, and (d) voltage unbalance reduction. Through these voltage services, DSOs maximize the integration of renewable energy sources (RES) to facilitate the EV charging process.

In the literature, it has been summarized that the percentage of peak load increases for different EV penetration rates[1] due to the uncontrolled[2] EV charging process at both the transmission and distribution levels [1]. This makes congestion handling in distribution networks a critical task. In addition to congestion and adverse voltage effects, high EV penetration also causes power quality issues, including harmonic distortion and voltage unbalances [1]. Voltage unbalances are common in the distribution grid as the loads are unequally distributed per phase, and single-phase EV charging contributes to this imbalance [1]. The location of EV charging is another reason for voltage unbalances; EVs have a negligible impact on voltage unbalances if connected at the beginning of the feeder but can have a significant impact if connected towards the end [21]. The EV chargers have nonlinear characteristics, and with high EV penetration, they cause harmonic distortions that impose stress on the grid components. This can reduce the lifetime of the grid components and significantly increase their replacement cost. Therefore, DSOs often need to undertake expensive

[1] One way to define the penetration rate is the ratio between the number of EVs and the number of houses under any observed feeder [1].

[2] Different EV charging strategies are explained in the next section.

grid reinforcements [1]. In the thesis, power quality issues have not been investigated for the charging algorithms as it has been assumed that EVs charge at different grid nodes of a balanced medium voltage (MV) grid (see Chapter 2).

1.2.2 EV charging standards

In the case of EV charging, there are typically two types of power supply: AC or DC. The charging process involves supplying direct current (DC) to the battery pack. Since electricity distribution systems provide alternating current (AC) power, a rectifier is required to convert the power to DC for the battery. EVs can be charged in three ways: (a) conductive charging, (b) inductive charging, and (c) battery swap [5]. The most common practice for EV charging is the conductive process, specifically using a wire or charging cable to transfer power from the source to the EV. Conductive charging can be either AC or DC. In the case of an AC EV charger, the AC power is delivered to the EV's onboard charger, which converts it to DC. On the other hand, a DC EV charger performs the power conversion externally and directly supplies DC power to the battery, bypassing the onboard charger [5, 22]. Organizations such as SAE (Society of Automotive Engineers), IEC (International Electrotechnical Commission), and IEEE (Institute of Electrical and Electronics Engineers) develop EV charging standards that comply with power grids. These standards ensure the interoperability and compatibility of EV supply equipment for EVs [22]. Understanding these standards is crucial when differentiating between EV charging levels and charging modes.

SAE defines the power levels of charging outlets and also specifies the supply types, which can be either AC or DC [1]. Table 1.1 summarizes the specifications for both AC and DC supply levels in EV charging as defined by SAE-J1772 [8].

Table 1.1: Electric vehicle supply power levels [8].

	Supply Type	*Power level*	*Maximum current*
Level 1	AC	1.4 kW	12 A
	AC	1.9kW	80 A
	DC	up to 36 kW	80 A
Level 2	AC	2.4 kW	10 A
	AC	3.8kW	16 A
	AC	7.7kW	32 A
	AC	19.2kW	80 A
	DC	up to 90 kW	200 A
Level 3	AC	$\geq$ 19.2kW	not-yet-defined
	DC	up to 240 kW	400 A

Charging an EV is possible in four different modes as specified by IEC. These different EV charging modes describe the safety communication protocol between the EV and the EV charger [1].

- Mode 1: Standard AC charging through a socket without protection, allowing a current of up to 16 A. The charging can be either in single-phase or three-phase.
- Mode 2: Standard AC charging with protection, allowing a current of up to 32 A. The charging can be either in single-phase or three-phase.
- Mode 3: AC charging with a dedicated EV charger, allowing 32 A (loose cable) and 63 A (fixed cable). The charger provides the control pilot signal.
- Mode 4: Wired DC off-board charging, allowing a current of up to 400 A.

1.2.3 EV charging strategies

In general, EV charging strategies can be categorized into three types: (a) uncontrolled or uncoordinated or dumb charging, (b) passive charging, and (c) active or smart charging, as shown in Figure 1.3. In this thesis, the performance of uncontrolled and some smart charging strategies has been modeled and compared for a large population of EVs charging in a medium voltage (MV) distribution grid (See Chapter 2). In the case of uncontrolled or dumb charging, EVs start recharging as soon as they are connected to a charging point, using the rated power of the charger based on battery conditions such as temperature, state-of-health, and voltage conditions. The implementation of uncontrolled charging is easy as it does not require active interaction between operators and EV owners. However, this process can lead to overloading in the power grid. A report suggests that uncontrolled charging of EVs will result in a 50% increase in investment costs for low-voltage grids and transformers in Germany by 2035 [23]. In the case of passive charging, EV owners are encouraged to shift their charging to off-peak hours by utilizing "Time-of-Use" tariffs [1]. During off-peak hours, electricity prices are lower, which motivates EV owners to charge their vehicles at a more affordable rate. However, it has been reported in [24] that passive charging can pose a threat to the successful integration of EVs with the power grid. It can put significant pressure on existing grid infrastructures, requiring high peak power capacities when all EVs start charging almost simultaneously during off-peak hours, leading to a sudden increase in demand [1, 24]. As a result, while passive charging may be a feasible solution for small EV populations, as the market share of EVs increases, adopting smart charging strategies becomes necessary [1]. The continuous growth of EV penetration in the power network will render passive charging obsolete in the future, as it will have a substantial impact due to the rapid increase in load.

In the previous section, it was discussed how the uncontrolled EV charging process can impact the power grid. To mitigate the impact of uncoordinated charging of multiple EVs, smart charging strategies have been widely proposed in the existing literature. These strategies aim to distribute the charging demand of EVs over a longer time horizon, enabling effective congestion management [2, 19]. Smart charging involves adapting the charging cycle of EVs based on the conditions of the power system and the preferences of vehicle owners [2]. According to [3], smart charging has the potential to save approximately 0.9 billion Euros annually in France, and this can be achieved through a simple form of smart charging. By using advanced smart charging devices, an additional

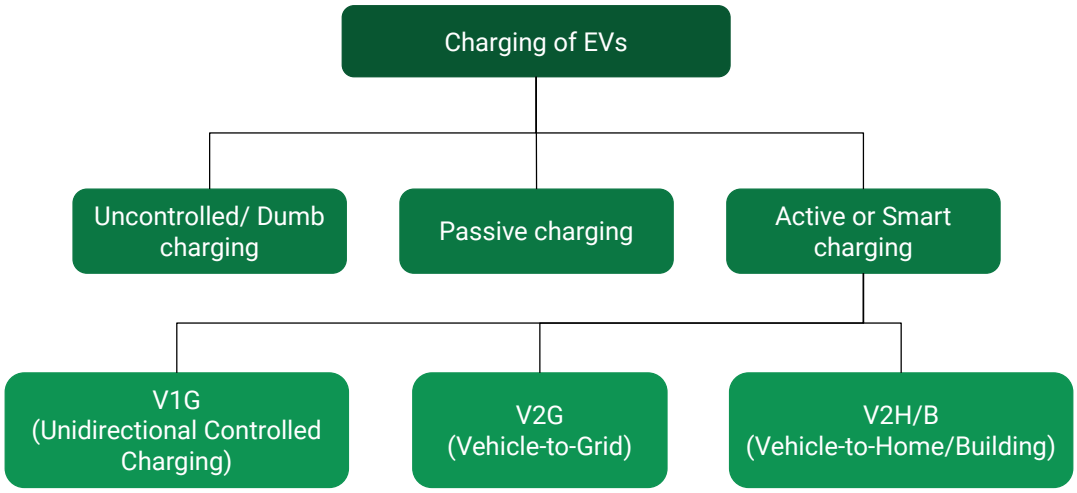

Figure 1.3: Different EV charging strategies [2, 3].

saving of nearly 0.3 billion Euros per year is possible. Ideally, smart charging can be classified into three types: (a) V1G or unidirectional controlled charging, which modulates the rate of EV charging by increasing or decreasing it; (b) V2G or vehicle-to-grid or bidirectional charging, where EVs have the capability to provide power back to the grid. In this scenario, utility or transmission system operators may purchase energy from customers during periods of peak demand and utilize the EV battery capacity to offer various flexibility services; and (c) V2H/B or vehicle-to-building or home, where EVs supply power back to the building or home during power outages or to enhance local energy consumption. However, advanced smart charging, such as charging management combined with PV self-consumption with or without bi-directional functionality, further improves flexibility [3, 25]. Figure 1.4 presents a comparison of CO2 emissions (plotted on the Y-axis) between smart charging and evening peak charging in major markets, including the EU [4]. It is observed that the implementation of smart charging in all markets results in nearly a 50% reduction in CO2 production.

The main advantage of active or smart charging processes is their ability to enhance both local and system flexibility in power systems operations, benefiting distribution system operators (DSOs) and transmission system operators (TSOs) respectively, as explained below. To improve power system flexibility, the V1G option, as reported in [25], can be considered. This option involves controlling the EV charging profiles to adjust the demand during peak hours and provide real-time balancing services for the power grid. V2G is particularly relevant for slow charging, especially in areas with a large population of EVs, such as large EV parking areas [2]. With V2G, it becomes possible to inject electricity back into the power grid. EVs can also provide ancillary services to TSOs, such as voltage management and emergency power during outages, thereby improving system flexibility. The two key features of V2G services, namely battery charging and discharging of EVs, contribute to grid management. In the event of a grid failure, EVs can be utilized as a power source

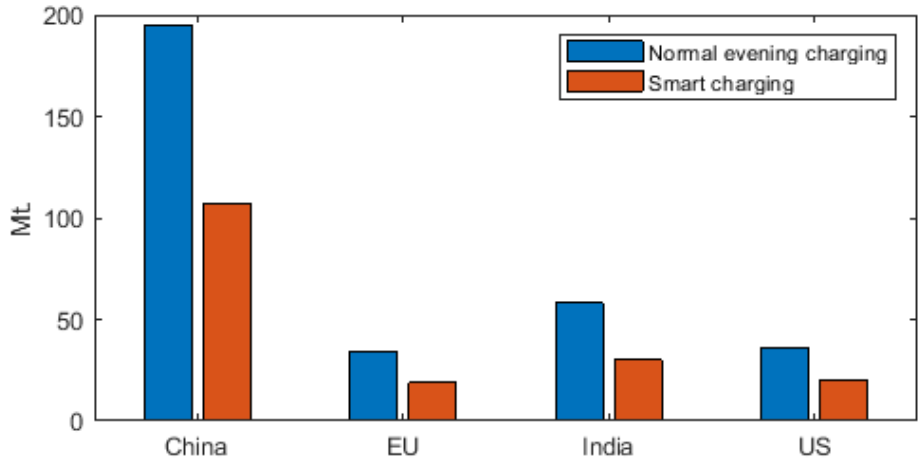

Figure 1.4: Impact of smart charging on CO2. Adapted from [4].

to support the grid by discharging their batteries. For example, EVs can participate in demand-side management by selectively discharging their batteries to "shave-the-peak," as depicted in Fig.1.5, effectively acting as a micro-grid system. Additionally, the charging schedule during peak hours can be shifted to off-peak times to avoid grid congestion, thereby improving local flexibility for DSOs. Reactive power support, along with V2G, provided by traditional EVs, is another means to assist grid management. Both unidirectional and bidirectional chargers can supply reactive power to the grid, which can be utilized for local voltage regulation, as demonstrated in [26, 27].

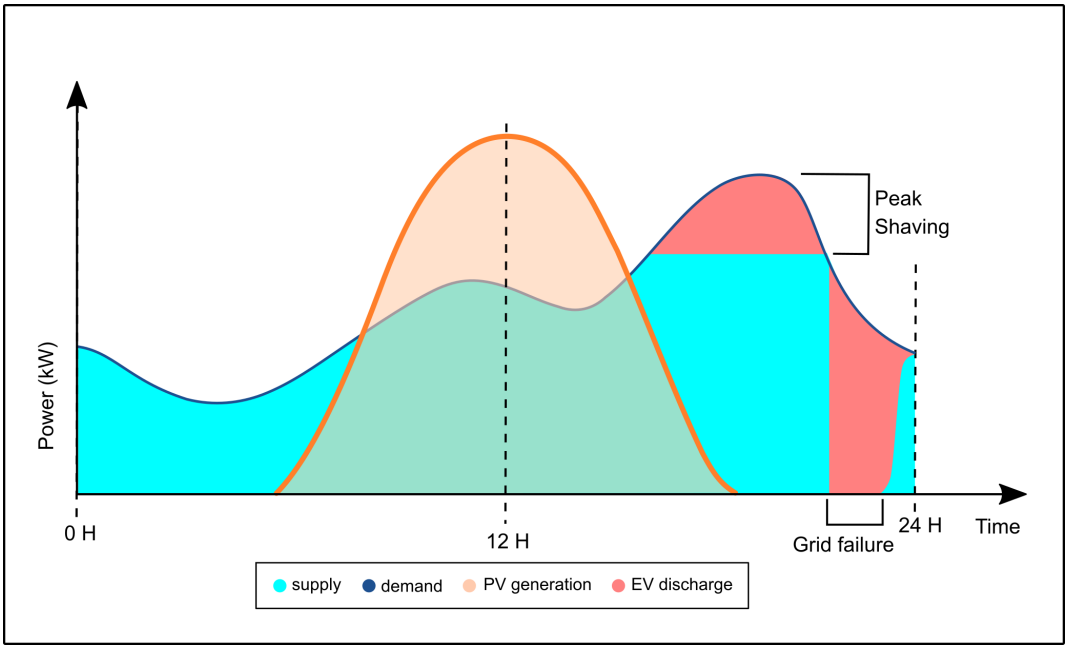

Figure 1.5: EV support for grid balancing. Source:[2]

Charging point power ratings determine the speed of battery charging, categorized as slow, fast, or ultra-fast charging. These power ratings can vary significantly depending on the installation location, such as homes, workplaces, or public areas. Slow chargers typically have power ratings up to 22 kilowatts (kW) and are commonly found in residential or office settings for EV charging [25]. It has also been reported in the literature [1, 3] that slow chargers can be rated between 3.7 kW and 7.4 kW. The main advantage of charging EVs from slow chargers is that EV batteries can remain connected to the grid for a longer period, increasing the potential to provide flexibility services for power system operations [2]. Fast chargers, on the other hand, are predominantly used in direct current systems along highways and for street charging, such as Paris' Belib [2]. Fast chargers typically have power ratings up to 50 kW or higher. Ultra-fast chargers have power ratings above 150 kW and are often installed on highways or motorways, where power ratings can reach as high as 350 kW, as reported in [3]. While fast and ultra-fast chargers offer quick charging to meet EVs' demands, they have some disadvantages. Firstly, these charging processes do not allow EVs to remain connected to the grid for an extended period to provide flexibility services. Secondly, the high power transfer associated with fast and ultra-fast charging can strain the grid within a short time frame. To mitigate the impact of fast and ultra-fast charging on the power system, these chargers need to be installed in areas with low demand and congestion during peak hours of the day [2]. To enhance the flexibility of charging stations near the power grid, fast charging stations can be combined with slow chargers, battery storage, and renewable energy sources. Fig.1.6 presents a generic diagram illustrating different charging strategies and charger typologies, showcasing how system operators can achieve various levels of flexibility for EV charging. This concept has been integrated within the planning problem context, where the proposed joint formulation accommodates both slow and fast charging infrastructures in an MV distribution grid (refer to Chapter 3).

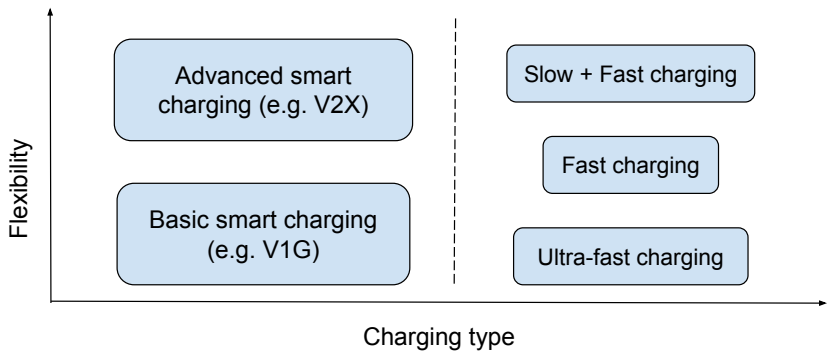

Figure 1.6: Flexibility diagram for different charging strategies.

1.2.4 Control architectures for smart charging

In the existing literature, a wide range of algorithms for smart charging control architectures have been proposed. One such approach is the decentralised unidirectional droop control method proposed in [28], which addresses under-voltage problems by adjusting the EV charging rate based

on local voltage measurements. This method ensures that the charging process does not cause voltage drops beyond acceptable limits. Another distributed approach for voltage regulation has been proposed in [29], which utilizes game theory. This approach employs an iterative algorithm where all EVs send their charging profiles to an EV aggregator. The aggregator then computes voltage levels and sends the data back to the individual EVs. The EV aggregator plays a crucial role in managing a certain number of EVs whose charging profiles can be controlled, enabling the provision of various flexibility services on their behalf [1]. These proposed control architectures demonstrate different strategies to enhance voltage regulation and optimize the charging process in smart charging systems.

Several strategies to address loading issues have been proposed in the literature. One such strategy is a market-based coordination approach suggested in [30] for congestion management involving EVs. This approach introduces EV fleet operators (FOs) to enable flexible coordination between the EV charging process and the power system operator. The coordination between FOs and DSOs (Distribution System Operators) can be facilitated through the distribution grid capacity market, which not only helps manage congestion but also maximizes the integration of renewable energy into the network. In addition to congestion management, demand flexibility (DF) can be utilized to reduce peak loads in the distribution network [31]. This work also presents the concept of a transactive energy (TE) system for aggregated EVs. The TE operator serves as a facilitator for interaction between the DSO and aggregators, enabling effective management of demand flexibility and promoting a more efficient use of resources.

Figure 1.7 provides an overview of different EV control architectures for smart charging, including their respective advantages and disadvantages. The three control methods are as follows:

- **Centralised**: In the case of a centralised smart charging control architecture, a central scheduler (e.g., EV aggregator) collects all the required information from each EV using a communication link and provides an optimized solution for scheduling the EV charging profile. The communication link typically involves a high level of complexity; however, it allows for the achievement of a highly optimal solution for the objective. Typically, an algorithm is employed to achieve the objective within the corresponding control area [1, 5].

- **Decentralised**: The decentralised method is a local control approach where the decision-making process occurs locally at the individual EV level [1]. In this case, the EV charging profile is computed using locally measured data without requiring external communication links, significantly reducing the cost of communication establishment.

- **Distributed**: The distributed control method is a hybrid approach that combines elements of both centralised and decentralised control methods. This coordination method is also known as “Hierarchical” control.

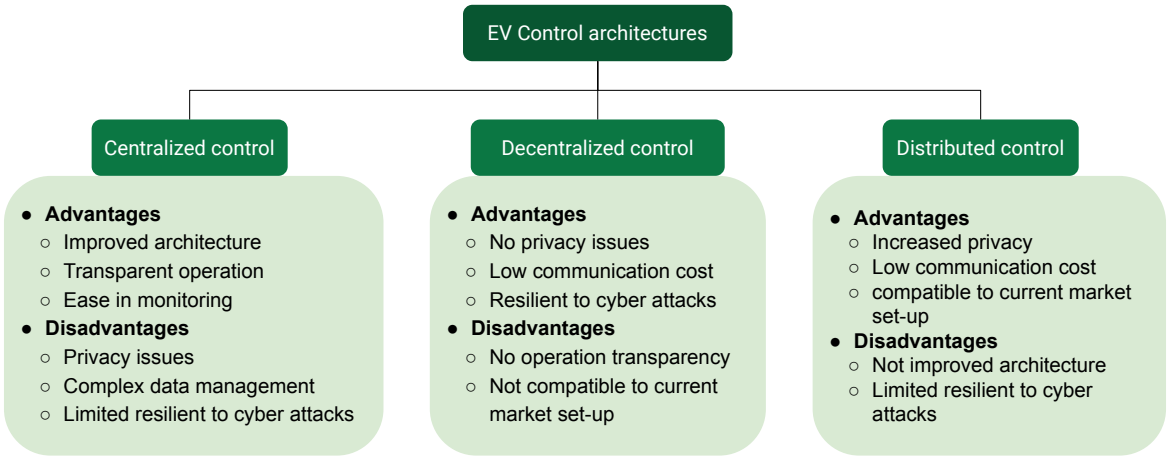

Figure 1.7: Advantages and disadvantages of different smart charging control architectures for traditional EVs [1, 5].

1.2.5 The planning of EV charging infrastructures

This section presents the motivation and research gaps identified in the existing literature regarding the planning of EV charging infrastructures. The increasing population of electric vehicles has driven the need for an expanded charging infrastructure. For instance, in France, it is estimated that 2 billion euros will be required to deploy 7 million public and private chargers by 2030 [17, 32]. Similarly, in the United States, it is projected that over 2 billion dollars will be necessary between 2019 and 2025 to improve public and residential charging infrastructure in major metropolitan areas [33]. Simultaneous arrival of a large number of EVs at charging stations can lead to increased power flows, potentially violating operational constraints of distribution grids, such as voltage levels, line capacities, and substation transformer ratings. Thus, in addition to the investment required for developing charging infrastructures, there may be a need for additional investments to upgrade and reinforce distribution grid infrastructure. This motivates the planning of EV charging infrastructure, taking into account grid constraints and the driving demand of EV owners, including their preferences for charging at different locations.

As mentioned in [5], the impact of EV charging on residential grids can be minimized by diversifying charging locations, such as at workplaces and public parking spots. Another solution to reduce grid congestion and losses while improving the carbon footprint is to charge EVs using electricity generated from local renewable sources. The concept of photovoltaic (PV) self-consumption has been advocated in the literature to integrate more PV into distribution grids, thus delaying the need for expensive grid reinforcement [34–36]. In this thesis, the idea of PV self-consumption is incorporated into the planning context to promote the direct utilization of PV power for EV charging. Additionally, multiple charger typologies and EV owners' flexibility in plugging and unplugging their EVs are considered to investigate the charging impacts on the planning process, while promoting PV self-consumption. The problem of planning the charging infrastructure for EVs has received

significant attention in recent years. However, certain aspects have been overlooked in previous works. For example, in [37] and [38], distribution grid and traffic flow models were considered to identify suitable locations for EV charging stations using a genetic algorithm, but renewable self-consumption and explicit models of EV owners' flexibility were not included. In [39], a data-driven approach was proposed to identify driving demand and charger locations, but grid constraints were not taken into account. The authors in [40, 41] proposed a two-stage optimization framework to co-optimize the charging infrastructure of EVs in combination with the operations of the power and gas networks. However, their work does not specifically address drivers' flexibility and PV self-consumption. Similarly, the works in [42, 43] focused on planning the charging infrastructure without considering grid constraints, PV self-consumption, and EV owners' flexibility. Another research study [44] proposes joint planning of EV charging stations and distribution capacity expansion but does not model EV owners' flexibility and PV self-consumption. In [45], the authors modeled the bounded rational charging behavior of EV drivers and applied this behavior model to solve the planning problem for EV chargers; however, they did not investigate the impact of PV self-consumption. A multi-objective planning model for EV chargers is developed in [46], which considers renewable generation with wind power but does not explore the impacts of self-consumption of renewable sources or drivers' flexibility on the planning. Similarly, in [47], a multi-objective planning model for the layout of an electric vehicle charging station is proposed, but it does not consider the operational constraints of the distribution grid or the self-consumption of renewable sources. Recently, the work in [48] presented a stochastic planning model for EV chargers, including PV generation; however, it did not investigate the impact of PV self-consumption modeling on the planning process.

Table 1.2: Optimization approaches and solvers for planning EV charging stations.

Optimization approach	*Reference*	*Solver/Optimization algorithm*
Robust optimization	[49]	Gurobi
Robust optimization	[50]	CPLEX
Probabilistic model	[46]	SG-based MONAA
Probabilistic model	[51]	Monte Carlo simulation (MCS)/CPLEX
Probabilistic model and queuing theory	[52]	Gurobi
Probabilistic model	[48]	MCS
Probabilistic model	[48]	MOEA/D
Probabilistic model	[53, 54]	NSGA-II
Deterministic model	[55]	GAMS
Deterministic model	[56]	MOEA/D
Deterministic model	[7]	Gurobi

Table 1.2 provides a summary of different optimization approaches and solvers from the existing literature. While stochastic models can represent a complex system in a more realistic way, deterministic models are less complicated and allow for faster execution of simulations.

1.3 The advent of autonomous mobility

As reported in the literature, autonomous vehicles (AVs) have undergone extensive testing and are planned to be commercially available in the next decade [57]. It is expected that the emergence of AVs will provide customers with more leisure time, estimated to be at least 50 minutes a day, thus improving work efficiency [58]. AVs have the capability to autonomously pick up customers without the need for parking, optimize their state of charge (SOC), and manage their charging schedule while ensuring reliable service to users [59, 60]. AVs have the potential to significantly reduce greenhouse gas emissions, with estimates suggesting a reduction of 87%-94% compared to current private vehicles in the United States by 2030, and 63%-82% below projected 2030 hybrid vehicles [61]. In a study by [62], it is mentioned that 53 projects related to autonomous vehicles are being carried out by 9 shuttle manufacturers in 20 European countries, serving 45 cities. In comparison to non-autonomous electric vehicles, shared autonomous electric vehicles (SAEVs) can be more easily controlled and optimized for implementing fast and large-scale demand response [63]. Another significant advantage of SAEVs is their ability to autonomously move to designated charging stations, allowing for a direct connection to the high voltage (HV) transmission grid at specified points, without overloading the low voltage (LV) distribution networks [60]. The integration of autonomous electric vehicles (AEVs) into distribution grids is not yet thoroughly explored in the existing literature [64]. The charge scheduling problem for AEVs has recently been addressed in [60] with the aim of minimizing waiting times and electricity costs, but this work does not take network constraints into account. The planning of charging infrastructure for AEVs has been examined in [65, 66], considering mobility patterns. However, distribution grids are not considered in these works.

Considering the differences in charging processes between EVs and AEVs, it will have a further impact on distribution grid consumption patterns. Therefore, it is important to investigate the impact of AEV charging on distribution grids in order to identify their consumption patterns. With the large-scale integration of EVs into power grids, the ability to independently select the most suitable charging locations, such as those near renewable power plants or energy storage facilities, due to autonomous driving, will help avoid grid congestion. If future mobility relies on autonomous vehicles, the grid reinforcements and technological developments currently planned for non-autonomous EVs may become obsolete. For example, a distribution system operator (DSO) may prefer to invest in temporary solutions to mitigate congestion, such as battery energy storage systems, rather than expensive grid reinforcements that may become underused and cost-inefficient with the introduction of autonomous EVs.

1.4 State-of-the-art

1.4.1 EV battery charging model

The state-of-charge (SOC) of a battery indicates the available capacity resulting from its daily charging and discharging process. The SOC value ranges from 0 to 100%. A SOC of 100% indicates that the cell is fully charged, while a SOC of 0 indicates a completely discharged condition [67]. In

general, the dynamic SOC model of a vehicle v at any given time t can be approximated as follows:

$$\mathrm{SOC}_{vt} = \mathrm{SOC}_{v(t-1)} - \epsilon_{vt} + \left(\eta \cdot P_{vt}^{\mathrm{EV}+} - \frac{1}{\eta} \cdot P_{vt}^{\mathrm{EV}-}\right) \frac{T_s}{E_v}. \tag{1.1}$$

In the above expression, ϵ_{vt} represents the self-discharge of vehicle v at any given time t; η denotes the charging or discharging efficiency of the battery, with a limit of $0 \leq \eta \leq 1$. T_s refers to the sampling time in hours, and E_v represents the nominal battery energy capacity in kWh. The self-discharge of the battery can be neglected in the case of a Li-ion battery, as it is typically small.

Although Li-ion batteries have some disadvantages for certain grid services [25], they are considered the most reliable technology in present times, offering a wide range of grid services compared to other battery technologies. An EV battery pack is categorized by its nominal capacity. With aging, irreversible chemical processes reduce the energy capacity of the battery pack, which also increases the battery cell resistance. According to ENGIE, bidirectional vehicle-to-everything (V2X) integration has no impact on battery aging, as concluded after one year of intensive testing in a laboratory [68].

In Eq. (1.1), the charging (in the case of unidirectional controlled or V1G) and discharging (in the case of bidirectional or V2G) powers are denoted by $P_{vt}^{\mathrm{EV}+}$ and $P_{vt}^{\mathrm{EV}-}$, respectively. For example, in a smart charging problem, the charging and discharging powers are non-negative variables in an optimization problem and are mutually exclusive in nature, as an EV charger can either charge or discharge an EV at a given time.

Ignoring the self-discharge, and considering SOC_{v0} as the initial state-of-charge for unidirectional charging (i.e., $P_{vt}^{\mathrm{EV}} \geq 0$), Eq. (1.1) can be simplified as follows:

$$\mathrm{SOC}_{vt} = \mathrm{SOC}_{v0} + \frac{T_s}{E_v} \sum_{\tau=0}^{t-1} \left(\eta \cdot P_{v\tau}^{\mathrm{EV}}\right) \qquad \text{for all } t \text{ and } v, \tag{1.2}$$

The model in (1.2), as well as (1.1) assumes constant battery voltage and efficiency: it is commonly adopted in the literature because it is linear in the recharging power (e.g. [5]), leading to tractable mathematical formulations. To formulate the scheduling problem, the model (1.2) has been used in Chapter 2.

1.4.2 Optimal power flow

Optimization algorithms are useful for solving problems associated with smart grids. An extensive literature review on optimization algorithms has been reported in [69]. The "optimal power flow" (OPF) tool is mainly used by system operators to solve various problems related to grid operations, such as scheduling, planning, and security assessment. OPF is particularly popular for addressing the variability of renewable generation. It allows for the incorporation of different flexibilities in the problem, enabling system operators to study multi-period problems and compute optimal set

points for controllable variables (such as energy storage, flexible demand, etc.)[70]. OPF represents an optimization problem where the goal is to maximize or minimize a cost or objective function while subject to different constraints that ensure a balance between power production and consumption. Since OPF is useful for grid operators, they can consider various operational limits and constraints (such as upper or lower bounds of measured quantities) for devices connected to the distribution or transmission grid.

Optimal power flow can be of both AC and DC types. In AC optimal power flow, the optimization algorithms consider the full AC power flow equations, whereas DC optimal power flow refers to the approximations applied to the original non-linear AC power flow equations [70]. The underlying assumptions for DC load flow are as follows: (a) bus voltage magnitude, i.e., $V_{mag} = 1$ p.u. at nominal value, and (b) small angular differences in bus voltage. These assumptions are valid for lightly loaded grids. DC OPF is widely used in electricity market clearing algorithms in transmission grids due to its linear characteristics, which ensure tractability for very large-scale problems and guarantee convergence to a global optimum [71].

The traditional approach to power flow study in a given network involves computing the nodal active and reactive power flow. The AC power flow equations are nonlinear, as the power depends on the square of the voltage magnitude. When these nonlinear equations are included as constraints in an optimization problem, the problem becomes non-convex and high-dimensional. As a result, solving it can be computationally intensive or even difficult, as there is no guarantee that the solver will find a global minimum. To address the non-linear power flow equations, various methods have been reported in the existing literature, including forward/backward sweep, NR method [72, 73], z-bus matrix construction method [74], loop impedance method [75, 76], and fast-decoupled load-flow method [77, 78]. Consider a function $f(x)$ and a line joining any two points (a and b) on $f(x)$. The function $f(x)$ is considered convex based on the following definition:

$$f\left(\frac{a}{2}+\frac{b}{2}\right) \leq \frac{1}{2}\cdot f\left(a\right)+\frac{1}{2}\cdot f\left(b\right), \tag{1.3}$$

or, in other words, if the set of all function values between two points lies on the line or below it [79]. If a problem is convex, it may not precisely represent the original problem, but it is still possible to identify an optimal solution. For convex functions, by following slope algorithms (e.g., gradient descent method), it is possible to find the absolute minimum or maximum of the function. However, for a non-convex function, following the gradient does not guarantee finding an absolute minimum or maximum. Heuristic methods (e.g., particle swarm optimization [80], artificial bee colony [81, 82], differential evolution [83], hybrid tabu search particle swarm optimization [84] algorithms) can be useful for this purpose. As reported in [85], although heuristics provide a real representation of the original problem, the use of random search techniques in heuristic algorithms results in long computation times compared to convex relaxation algorithms. Convex relaxation provides an exact solution, and an optimal solution is guaranteed.

In the previous years, a lot of work has been done to convert AC-OPF into a convex formulation.

By defining a convex function around the non-convex function, one can solve a convex optimization problem and achieve the goal of finding the global optimum. If the obtained optimum is feasible for the original problem, then it is considered the optimal solution. On the other hand, if the global optimum lies outside the feasible space, several methods can be applied to identify a feasible solution as close as possible to the global optimum [71]. The most common convex relaxation algorithms for power flow equations are quadratically constrained quadratic programs (QCQPs), as reported in [86, 87]. Both convex relaxations, Semi-Definite Program (SDP) and Second-Order Cone Program (SOCP), fall under QCQP algorithms and can be exact under certain conditions [88–91]. However, in the case of high renewable generation, these relaxations can be inexact due to elevated line losses [92]. In the literature, to solve the optimal scheduling problem in a power grid consisting of DERs and controllable loads (e.g., EVs), deterministic [93, 94], stochastic [95, 96], and hybrid [97, 98] approaches have been considered. Stochastic approaches can be used in OPF algorithms to capture the uncertainties of consumer and generation profiles (e.g., PV and wind production). These strategies include scenario trees [95, 99] or statistical parameters of the stochastic variables [100, 101]. As mentioned before, although heuristics are advantageous for exact network representation, for the optimal scheduling of DERs in multi-node distribution grids, quadratic programs (QPs) perform significantly better in terms of computational time to find the optimal solution [70]. An alternative to convex relaxations is to linearize the load flow equations around a working point. This approach is known as the computation of sensitivity coefficients (SCs). In this thesis, sensitivity coefficients (SCs) have been used to avoid the non-linearity of AC power flow equations. The linearized voltage and current models are presented in the next section.

1.4.3 The power grid model

We consider a power distribution grid (as shown in Figure 1.8) that interfaces with loads (e.g., commercial, residential, and industrial), potentially distributed generation, and EV charging infrastructures installed at multiple grid nodes. Distribution grids, both LV and MV, are designed to accommodate specified levels of power demand. Exceeding these demand levels may result in violations of the operational requirements of the distribution grids. Distribution grid operators must ensure that voltage levels remain within statutory limits, line currents stay below cable ampacities, and power flow at the substation remains within the transformer ratings.

The nodes of the power network are referred to with the index $n = 1, \ldots, N$, where N is the total number of grid nodes. We use the index $t = 1, \ldots, T$ to denote the discretized time intervals, where T represents the total number of samples. The time horizon $(1, \ldots, T)$ also corresponds to the recharging horizon for the EVs located at the specified grid nodes. The active and reactive power nodal injections at node n and time interval t can be written as follows:

$$P_{tn}^{\text{node}} = P_{tn}^{\text{net}} + P_{tn}^{(\text{EV nodal})} \tag{1.4a}$$

$$Q_{tn}^{\text{node}} = Q_{tn}^{\text{net}} + Q_{tn}^{(\text{EV nodal})} \tag{1.4b}$$

where P_{tn}^{net} is the net demand (i.e., power demand, P_{tn}^{demand} minus local renewable generation) and $P_{tn}^{(\text{EV nodal})}$ is the total nodal power demand due to charging of EVs connected at that node.

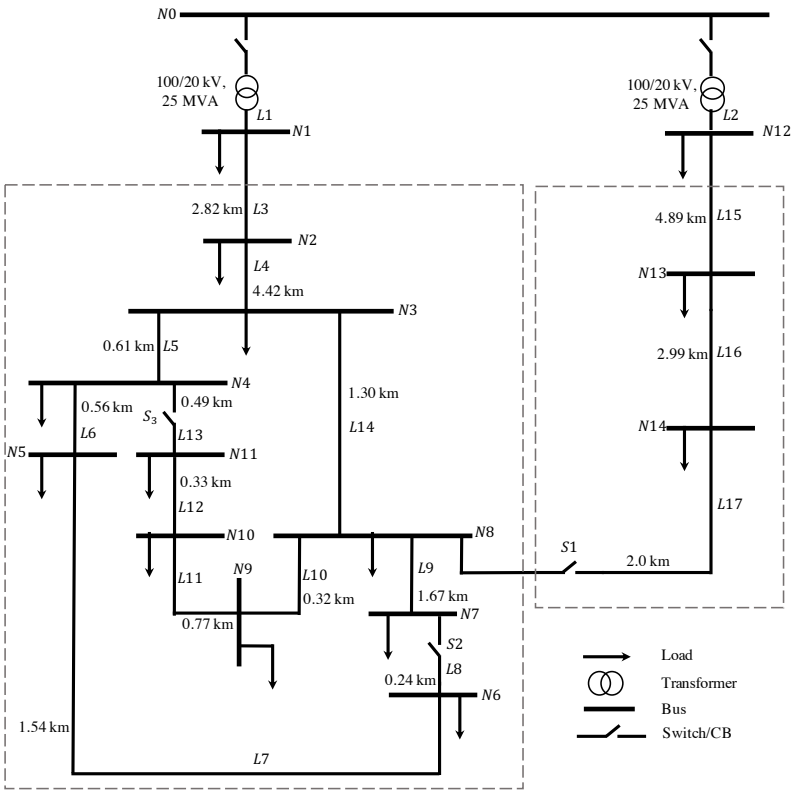

Figure 1.8: Topology of the CIGRE European MV distribution network benchmark for residential system [6].

In Eq. (1.4a) the first term is generally an input of the problem (as it depends on demand and generations), whereas the latter depends on the charging policy of EVs. To formulate the scheduling problems (see Chapter 2) and planning problems (see Chapter 3) one can consider nodal injection of EVs at all nodes as optimization variables. Similar to Eq. (1.4a), the reactive power at each node can be modelled as in Eq. (1.4b) as the sum of the reactive power injections due to net demand and EV charging.

The voltage levels at the grid nodes and the current values in the lines (i.e., voltage magnitudes and line current magnitudes) depend on the grid topology, cable parameters, voltage of the slack bus, and nodal injections. They can be modeled using load flow equations, which we generically denote as functions f_n (for the voltage magnitudes) and h_l (for line current magnitudes). Let v_{tn} and i_{tl} be the voltage magnitude at node n and current magnitude in line l, respectively, during time interval t. Taking into account the dependencies on the EVs' charging demand $(\boldsymbol{P}_t^{(\text{EV nodal})}, \boldsymbol{Q}_t^{(\text{EV nodal})})$ and charging locations $(\boldsymbol{b}_n)$, we denote the load flow equations as follows:

$$v_{tn}\left(\boldsymbol{P}_t^{(\text{EV nodal})}, \boldsymbol{Q}_t^{(\text{EV nodal})}, \boldsymbol{b}_n\right) = f_n\left(P_1(\cdot), \ldots, P_N(\cdot), Q_1(\cdot), \ldots, Q_N(\cdot), v_0, Y\right) \tag{1.5a}$$

$$i_{tl}\left(\boldsymbol{P}_t^{(\text{EV nodal})}, \boldsymbol{Q}_t^{(\text{EV nodal})}, \boldsymbol{b}_n\right) = h_l\left(P_1(\cdot), \ldots, P_N(\cdot), Q_1(\cdot), \ldots, Q_N(\cdot), v_0, Y\right), \tag{1.5b}$$

Similarly, the complex power absorbed at the single grid connection point (GCP) can be expressed

as:

$$S_t\left(\boldsymbol{P}_t^{(\text{EV nodal})}, \boldsymbol{Q}_t^{(\text{EV nodal})}, \boldsymbol{b}_n\right) = g\left(P_1(\cdot), \ldots, P_N(\cdot), Q_1(\cdot), \ldots, Q_N(\cdot), v_0, Y\right), \tag{1.5c}$$

where Y is the admittance matrix of the grid (constructed using the grid topology information and cable parameters), and v_0 is the voltage at the slack bus. Functions $f_1, \ldots, f_N$, $h_1, \ldots, h_L$, and g are nonlinear, and their inclusion in optimization problems leads to non-convexities and low tractability, as discussed earlier.

Sensitivity is defined as the ratio of a dependent variable to small changes in an independent or controllable variable [102]. Sensitivity coefficients (SCs) are commonly computed for both transmission and distribution networks. There are three traditional methods for computing SCs. The first method uses the Gauss-Seidel (GS) formulation, where power flow is performed for a balanced network considering a small deviation of a single control variable, such as nodal active or reactive power injections [103]. The second method involves the Newton-Raphson (NR) formulation of the load flow. The third method is derived from circuit theory, where Tellegen's theorem is applied in power networks, and the concept of an adjoint network is used [104–106]. In [107], a method to compute SCs based on the GS formulation, similar to [103], is proposed. This method is applicable to both multi-phase and unbalanced distribution networks. It is also valid for a generic number of slack buses. This approach has been adopted for the linearized power flow models considered in this thesis. To compute the current SCs, the assumption is made that the lines of the network have π models. To compute the voltage SCs, the assumption is made that during the perturbation of voltage independent nodal power injections, there is no change in the power set point for loads and generators. This way, SCs consider the response of the network in terms of both active and reactive power variations. By using the concept presented in [107], the voltage and current deviations can be locally linearized to formulate a convex optimization problem, as follows:

$$\Delta v_{tn} = A_{Pt} \cdot \Delta P_n(t) + A_{Qt} \cdot \Delta Q_n(t) + A_{nt} \cdot \Delta n_n(t) \tag{1.6a}$$

$$\Delta i_{tl} = B_{Pt} \cdot \Delta P_n(t) + B_{Qt} \cdot \Delta Q_n(t) + B_{nt} \cdot \Delta n_n(t) \tag{1.6b}$$

In Eq. (1.6a), A_{Pt} and A_{Qt} are the vectors of voltage sensitivity coefficients (SCs) with respect to active and reactive power, respectively. A_{nt} represents the vector of voltage SCs with respect to transformer's tap positions. $\Delta P_n(t)$, $\Delta Q_n(t)$, and $\Delta n_n(t)$ denote the adjustments in nodal active power, reactive power, and on-load tap changer (OLTC), respectively. Similarly, in Eq. (1.6b), B_{Pt}, B_{Qt}, and B_{nt} are the vectors of current sensitivity coefficients.

1.4.4 Conclusions

In conclusion, the state-of-the-art analysis has provided valuable insights into the modeling of EVs into power grids. The study of battery charging models has revealed the potential of treating charging and discharging powers as optimization variables, enabling the formulation of various EV charging strategies. Furthermore, the exploration of OPF techniques has emphasized the crucial role of optimization algorithms in addressing operational challenges faced by grid operators. Additionally, the comprehensive power grid modeling has enhanced our understanding of the operational

requirements of distribution grids. The utilization of convex optimization problems, leveraging SCs, has been validated as an effective approach in attaining the global optimum within distribution grids. These findings collectively lay a solid foundation for identifying the research questions and scientific objectives of the Thesis, which will be discussed further.

1.5 Research questions and scientific objectives

Thesis tackles two main problems: scheduling the charge of electric vehicles and planning their charging infrastructure accounting for the constraints of the existing power distribution grid. In the context of the scheduling problem, the research questions are as follows:

- Question 1: For large penetration of electric vehicles in a distribution grid, how different charging algorithms (uncoordinated, V1G, V1G with reactive power support from the chargers, V2G, and V2G with reactive power support from the chargers) for EVs can be accommodated under a common settings so that their performances can be compared in terms of their impact on distribution grids and meeting charging demands?

- Question 2: How to formulate the OPF based charge scheduling problem for the above charging policies so that information of EVs can be integrated along with the grid information?

- Question 3: What are the roles of constraints related to different electric vehicles charging policies?

Therefore, the first scientific objective is to develop a unified algorithmic framework based on an optimal power flow (OPF) problem with the aims of comparing different EV charging ploicies while respecting the operational constraints of distribution grids and satisfying their driving demand. Another objective of the thesis is to develop a method that provides Distribution System Operators (DSOs) with a flexible framework to evaluate, compare, and select from various EV charging strategies, by conveniently inserting or removing specific sets of constraints in the formulation, thereby enabling an effective analysis of their impact on distribution grids and the ability to meet charging demands.

In order to develop optimization techniques to site and size charging infrastructure for large penetration of traditional EVs in a distribution grid while respecting the operational distribution grid constraints and satisfying the charging demand of the EVs, the following research questions have been identified:

- Question 4: How can chargers for EVs be cost-optimally located and sized at different distribution grid nodes, taking into account the technical constraints of the grid, various charger typologies, the requirements for charging infrastructure, and scenarios involving drivers' flexibility to plug and unplug their EVs?

- Question 5: What are the impacts of different charger types, flexibility of EV owners in terms of capital investment?

- Question 6: How do different battery sizes (16 kWh and 60 kWh) and planning horizon influence the planning options for charger installation?
- Question 7: What is the impact of vehicle-to-grid technology on the optimal planning problem?
- Question 8: If planning objective is changed, would this lead to a substantially different charging infrastructure or whether similar configurations of EV charging infrastructures would be suitable to accommodate different objectives (e.g. minimize the capital investment while optimizing the renewable self-consumption)?

All of the above questions are of interest for urban planners or policymakers to identify if an existing charging infrastructure will soon become obsolete if planning objectives change over time. To answer these questions, the first scientific objectives of this dissertation is to develop a mathematical formulation that can incorporate various charger types, flexibility models of EV owners and V2G technology into one the optimization formulation with an objective to cost-optimally determine the location, size and type (fast, slow, multi-port chargers, single-port chargers) of EV chargers while considering power distribution grid constraints. Here, the scientific objective is to model multi-port charging infrastructures and evaluate their role as the primary autonomous automation layer, aiming to enhance flexibility in the conventional process of EV charging. This represents a introductory step toward the development of more sophisticated planning algorithms for autonomous driving of EVs, explaining the relevance of the doctoral thesis for the EVA project. Modifying non-convex constraints in the planning formulation our objective is to derive a mixed-integer linear program that can be efficiently solved with off-the-shelf software libraries while addressing the computational challenges. Our further objective is to explore problem approximations to enhance tractability when considering more extensive input information (e.g. 5 days optimization horizons) and large number of optimization variables.

Finally, in this dissertation the objective is to develop a methodology for validating the results obtained from solving the optimal planning problem in the context of electric vehicle (EV) charging scheduling. Here the aim is to evaluate the significance of optimal placement for EV charging systems and its impact on the performance of scheduling algorithm and overall charge levels of the EVs population. Therefore, the following research question has been identified:

- Question 9: What will be the effect of strategically allocating chargers based on the results of the optimal planning problem on EVs' SOC levels and efficiency of the charging process, compared to the scenario where chargers are uniformly distributed across medium-voltage (MV) grid nodes?

1.6 Thesis outline and contributions

The thesis concerns the impact of recharging needs of electric vehicles (for both planning and scheduling formulations) on distribution grids. The thesis is organized in five chapters including introduction and conclusion. The main results of the work have been communicated in peer reviewed articles and conference papers.

Journal papers:

- **Publication A**: Biswarup Mukherjee, Fabrizio Sossan. Optimal Planning of Single-Port and Multi-Port Charging Stations for Electric Vehicles in Medium Voltage Distribution Networks. IEEE Transactions on Smart Grid, 2022, pp.1-13. (DOI:10.1109/TSG.2022.3204150). (hal-03779746)
- **Publication B**: Biswarup Mukherjee, Fabrizio Sossan. Optimized Planning of Chargers for Electric Vehicles in Distribution Grids Including PV Self-consumption and Cooperative Vehicle Owners. Energy Conversion and Economics, 2023, 4(1), (DOI:10.1049/enc2.12080). (hal-03998742)

Peer-reviewed conference papers:

- **Publication C**: Biswarup Mukherjee, Georges Kariniotakis, and Fabrizio Sossan. "Smart Charging, Vehicle-to-Grid, and Reactive Power Support from Electric Vehicles in Distribution Grids: A Performance Comparison." 2021 IEEE PES Innovative Smart Grid Technologies Europe (ISGT Europe). IEEE, 2021.
- **Publication D**: Biswarup Mukherjee, Georges Kariniotakis, and Fabrizio Sossan. "Scheduling the Charge of Electric Vehicles Including Reactive Power Support: Application to a Medium-Voltage Grid." (2021): 1534-1538.

Technical reports:

- Fabrizio Sossan, Biswarup Mukherjee. Planning of EV charging infrastructure in distribution grids: a comparison of options. [Technical Report] Mines ParisTech - PSL University. 2022, pp.1-18. ⟨hal-03759268⟩
- Fabrizio Sossan, Charitha Buddhika Heendeniya, Biswarup Mukherjee, Vasco Medici. Smart Charging of Electric Vehicles: an Autonomous Driving Perspective. [Technical Report] MINES ParisTech - Université PSL; SUPSI. 2022, pp.1-26. ⟨hal-03756809⟩

Thesis outline and contributions of the individual chapters are summarized below.

In Section 1.2, a comprehensive literature review is presented, focusing on the challenges associated with recharging electric vehicles from the power grid. This review encompasses various aspects, including existing EV charging standards, strategies, control architectures, and planning for traditional EV charging stations. Moving on to Section 1.3, the distinctions between traditional EVs and autonomous EVs (AEVs) are explained, along with an exploration of the potential integration impacts arising from their grid-based charging. Subsequently, in Section 1.4, the state-of-the-art approaches are discussed, specifically addressing the modeling of EVs' charging requirements from the power grid. This section provides an overview of the latest advancements in this field, offering insights into the current research and developments.

In **Chapter 2**, various EV charging strategies, such as uncoordinated charging, smart charging, and vehicle-to-grid (V2G) with reactive power support from EVs, have been modeled based on existing literature. These charging strategies are implemented within a unified algorithmic framework. The framework is designed with a common configuration, enabling the resolution of scheduling problems for a large population of EVs and comparing their performances. The scheduling problems are derived from a baseline convex optimization problem that takes into account the linearized grid constraints, including voltage magnitude, line ampacities, and other relevant factors [107]. The performance of these charging algorithms is compared, and the impact on the CIGRE MV distribution grid resulting from the scheduling of EVs is analyzed. This chapter incorporates content from Publications C and D.

In **Chapter 3**, a planning formulation for EV charging infrastructure is developed. The planning of the EV charging infrastructure in power distribution grids is developed as an economic cost minimization problem. The objective is to minimize capital investments required to set up the EV charging infrastructure at specific distribution grid nodes. This task can be of interest to urban planners or grid operators. This chapter makes a significant contribution to the state of the art by quantitatively investigating the sensitivity of the EV charging infrastructure to various optimization objectives. This includes considering battery packs of two different capacities (16 kWh and 60 kWh) and incorporating PV self-consumption modeling. Furthermore, the formulation is extended to incorporate smart charging and V2G features for EV charging. Additionally, different flexibility scenarios for EV owners are modeled in this chapter. The planning problem is formulated as a mixed-integer linear program (MILP), where nonlinear grid constraints are approximated using linearized grid models. The results obtained from the planning problem are compared for both single-port chargers (SPCs) and multi-port chargers (MPCs), considering proposed flexibility models for different optimization horizons in the CIGRE MV distribution grid. This chapter includes the findings and contributions from Publications A and B, providing valuable insights into the planning of EV charging infrastructure.

In **Chapter 4**, the contributions from the previous two chapters are consolidated, and a method is developed to validate the planning formulation. This method utilizes the results obtained from **Chapter 3** to solve a scheduling problem.

Finally, **Chapter 5** concludes the thesis, summarizing the main results. At the end of this chapter, a preview of future work is presented.

Chapter 2

The scheduling problem for EVs

Résumé en Français

À partir de la littérature existante, ce chapitre présente la modélisation de la charge non coordonnée, de la charge intelligente, de la charge V2G avec le soutien de la puissance réactive des chargeurs de VE. Afin de disposer d'un cadre commun pour toutes les différentes stratégies de charge, ce chapitre propose un cadre algorithmique unifié qui permet de formuler le problème de programmation des VE comme un problème d'optimisation convexe avec des contraintes de réseau linéarisées. Les performances de ces algorithmes de charge sont comparées pour une large population de VE traditionnels en tenant compte de leur présence à différents nœuds du réseau de distribution MV de CIGRE. En outre, ce chapitre introduit le concept de formulation du problème de programmation pour les VEA. Les résultats de deux articles distincts, Publication C et Publication D, sont inclus dans ce chapitre.

Summary

From the existing literature, this chapter presents the modeling of uncoordinated charging, smart charging, V2G charging with reactive power support from EV chargers. To have a common setting for all different charging strategies, this chapter proposes a unified algorithmic framework that allows the formulation of the scheduling problem of EVs as a convex optimization problem with linearized grid constraints. The performance of these charging algorithms is compared for a large population of traditional EVs considering their presence at different nodes of the CIGRE MV distribution grid. Furthermore, this chapter introduces the concept of formulating the scheduling problem for AEVs. The results of two separate papers Publication C and Publication D are included in this chapter.

2.1 Introduction

This chapter of the thesis focuses on the approaches to solving the scheduling problem of EV charging and formulating them. In general, scheduling is a procedure required for operating the electric power system. For example, TSOs use schedulers to determine the power that power plants should produce

while respecting the grid constraints prior to real-time operations. In the case of EVs, a scheduler can be used to compute the recharging trajectories of EVs subject to grid constraints in the context of a smart charging procedure. Solving a scheduling problem for EV smart charging algorithms is not new and has been addressed in the existing literature. In [108], the scheduling problem of on-the-move EVs has been addressed in a transportation network based on a graphical game approach with the objective of minimizing the charging latency of EVs, considering their driving time to EV charging stations and waiting-and-charging time. Authors in [109, 110] have considered distributed and hierarchical computing approaches to achieve computational efficiency without considering the grid model and constraints.

According to [111–113], EVs can provide and consume reactive power at any SOC level without impacting the life cycle of the batteries. It is reported in [114] that the frequent charging and discharging of EVs can cause unnecessary damage to the batteries. This work also claims that with the bidirectional charging capability of EV chargers, it is possible to avoid the grid shock caused by large-scale EV penetration [114]. Two different frameworks for coordinated charging of EVs with reactive power support have been proposed in [27]. Here, one framework supports solving the optimal power flow model at the grid level by DSOs, obtaining different EV-related information (e.g., socket rating, SOC, etc.) from the EV aggregators. Based on the optimal power flow solution, upper bounds on active power consumption and reactive power injection at each aggregated node on the feeder are generated by the DSOs. The same bounds from DSOs are then used to solve the optimal EV scheduling problem at the aggregation level, ensuring feasible grid operations. The other coordinated framework involves solving the optimal scheduling problem at the aggregation level first, and optimal EV charging profiles from each node are sent to the grid control centre to solve OPF with the objective of minimizing the deviation of EVs' charging schedule through load shifting and load curtailment. In [115], the scheduler optimizes the energy flow from the power grid to the battery of the EV, while in the case of V2G, the scheduler tries to optimize the bidirectional power flows (i.e., from the grid to the EV battery and from the EV battery to the grid) subject to multiple constraints.

In light of the existing methods, the main contribution of this chapter is to present the methodology and formulation of EV charging algorithms under a common setting, accounting for the distribution grid's operational constraints, to enable a comparison among them. The optimization problems in this chapter are formulated as convex optimization problems. Detailed methodology, formulation, and case studies of the scheduling problem are presented next.

2.2 Methodology

This section presents the optimal power flow-based methodology for formulating the scheduling problems for the following EV charging policies: (a) uncoordinated charging, (b) grid-aware coordinated or V1G, (c) grid-aware coordinated charging with reactive power support from the chargers, (d) grid-aware coordinated bidirectional charging or V2G, (e) V2G with reactive power support

from the chargers.

The recharging solutions considered in the scheduling problem are shown in Fig. 2.1. The integrated framework is useful for DSOs as it allows for formulating the scheduling problems at the grid level with information on EVs for different charging policies. Compared to uncoordinated charging (shown in the green box), V1G or smart charging strategy (shown in the grey box) can be formulated by leveraging an optimal power flow where the power flow is unidirectional (from the grid to EVs). Constraints for reactive power capability can be associated on top of the V1G algorithm, considering the case when EVs can inject or absorb reactive power through the EV charger with unidirectional charging feature (shown in the blue box). With the bidirectional capability of the EV charger, grid-aware coordinated bidirectional charging or V2G can be formulated (shown in the yellow box). Finally, by incorporating the bidirectional capability and the reactive power constraints from the EV chargers, V2G with reactive power support can be formulated (shown in the light orange box). In this case, it is considered that EVs can inject or absorb reactive power while charging and discharging. The inclusion of bidirectional capability and the reactive power constraints of EV chargers increases the number of optimization variables for the scheduling problem. When a large number of EVs are considered in a distribution grid, the formulation of the problem remains unaltered; however, the change in the number of EVs affects the number of variables of the problem.

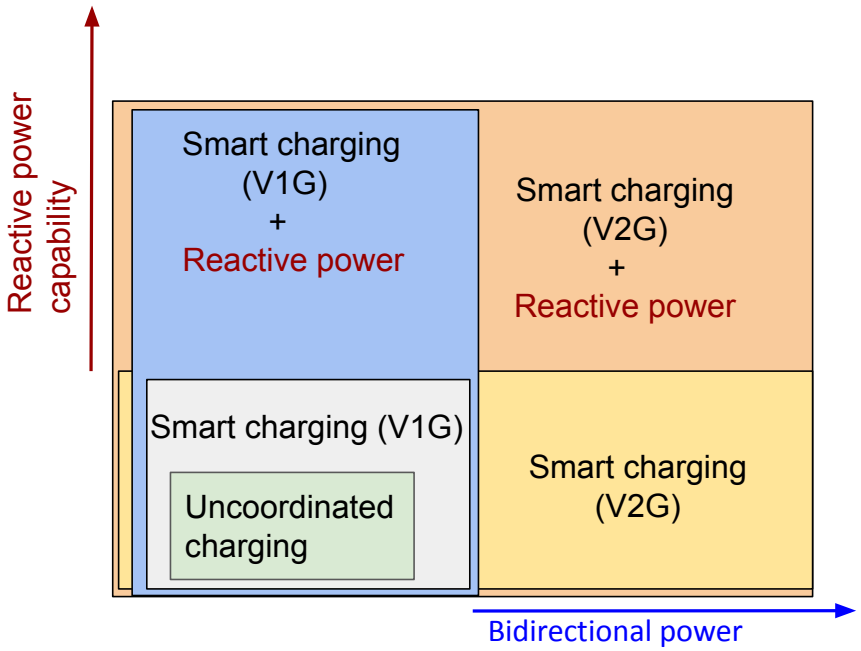

Figure 2.1: Scheme to formulate EV charging strategies.

Figure 2.2 presents the main components for formulating the optimal power flow-based scheduling problem. The scheduling problem is a decision-making problem where the EV information is coupled with the grid information. In this thesis, traditional EVs have been explored, and their

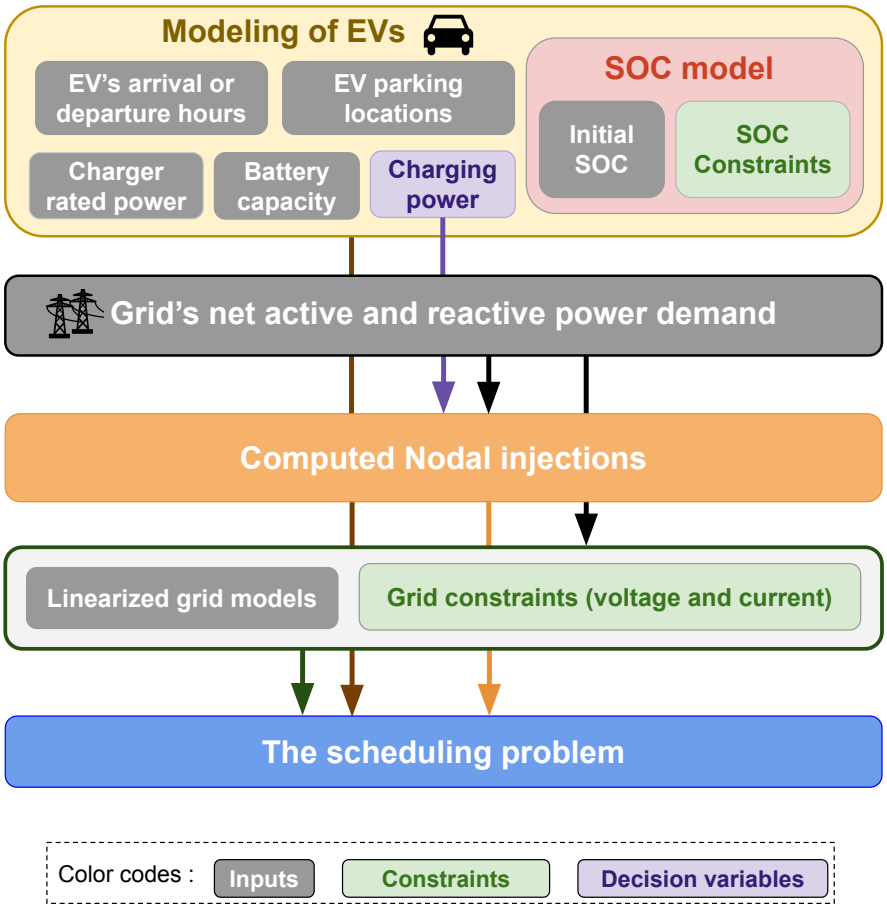

Figure 2.2: The main elements used to formulate the scheduling problem using OPF.

locations are considered fixed based on their parking locations, which serve as inputs for the problem. Other inputs for modeling EVs include the energy capacity of EV batteries, rated power of the EV charger, initial SOC (i.e., SOC of EVs upon arrival at respective grid nodes), and their arrival and departure information. Depending on the charging policies, the EV charging powers serve as decision variables for formulating the decision-making problem (shown by the light purple box). The different components for modeling the EVs are shown within the yellow box in Figure 2.2. The nodal injections can be computed (as shown by the light orange box) using both grid information (grid's nodal demand) and the charging demand of EVs located at multiple grid nodes, as discussed in section 1.4.3. To solve this decision-making problem (as shown by the blue box), an optimal power flow with linearized grid models based on the literature [19] has been used. The linearized grid models serve as inputs, while nodal voltage magnitudes and line current bounds serve as constraints for the problem. The optimal power flow follows a common baseline structure, where the constraints can be adapted to represent different charging strategies, as mentioned earlier in this section. By employing different policies, we investigate how different constraints can be embedded and enforced in the decision-making problem for EV charging. The formulation of different charging

policies is presented in the next section.

2.3 Formulation of EVs charging algorithms

2.3.1 Modelling the charging of EVs

We consider total V number of vehicles with index $v = 1, \ldots, V$ are charging from the MV distribution grid. The charging power of a vehicle v is limited by the kVA rated power of the converter, denoted by $\overline{S}_v^{\text{EV}}$. Assuming the capability of the charger is independent from the voltage of the AC grid and of the DC bus, the apparent power limit of the charger for all t and v can be expressed as:

$$\left(P_{vt}^{\text{EV}}\right)^2 + \left(Q_{vt}^{\text{EV}}\right)^2 \leq \left(\overline{S}_v^{\text{EV}}\right)^2. \tag{2.1}$$

The above expression characterizes the ideal "capability curve" of a power converter and the same can be implemented in the EV chargers. In Eq. (2.1), Q_{vt}^{EV} and P_{vt}^{EV} represent the reactive power and the active power respectively while a vehicle v charges at time t.

Unidirectional and Bidirectional controlled charging

As mentioned in the previous chapter for unidirectional controlled charging (V1G), the power flows from the grid to the EVs (i.e., the recharging power) for all t and v can be expressed as $P_{vt}^{\text{EV}} \geq 0$. But, in case of bidirectional controlled charging process (V2G) the positive charging power (a real variable) can be splitted into two new non-negative variables as below:

$$P_{vt}^{\text{EV}} = P_{vt}^{\text{EV}+} - P_{vt}^{\text{EV}-}, \qquad \forall v, t. \tag{2.2}$$

The Eq. (2.2) preserves the linearity of the non-ideal-efficiency SOC model, as discussed in section 1.4.1. These non-negative variables in the above expression are mutually exclusive as an EV charger can either charge or discharge the EV at the same time.

With operators $[\cdot]^+$ and $[\cdot]^-$ denoting respectively the positive and negative part of the argument of EV charging power P_{vt}^{EV}, the state-of-charge of EV v (as derived from Eq. 1.2 in Chapter 1) can be modelled as the following function:

$$\text{SOC}_{vt} = \text{SOC}_{v0} + \sum_{\tau=0}^{t-1} \left(\eta \left[P_{v\tau}^{\text{EV}}\right]^+ - \frac{1}{\eta} \left[P_{v\tau}^{\text{EV}}\right]^- \right) \frac{T_s}{E_v}, \quad \text{for all } t \text{ and } v. \tag{2.3}$$

In Eq. (2.3), SOC_{v0} is the SOC at arrival. This SOC expression is non-linear as it involves the arguments of EVs' charging power and determines non-convexity in the OPF formulation. Splitting the charging power into two non-negative (mutually exclusive) variables as in (2.2), the linear SOC model reads as:

$$\text{SOC}_{vt} = \text{SOC}_{v0} + \sum_{\tau=0}^{t-1} \left(\eta P_{v\tau}^{\text{EV}+} - \frac{1}{\eta} P_{v\tau}^{\text{EV-}} \right) \frac{T_s}{E_v}, \quad \text{for all } t \text{ and } v. \tag{2.4}$$

2.3.2 Nodal injections due to EVs charging demand and grid model

The link between the nodal injections of EVs, $P_{tn}^{(\text{EV nodal})}, Q_{tn}^{(\text{EV nodal})}$ in (1.4), and the charging of the single vehicles P_{vt}^{EV} is given by the locations where the EVs charge. The charging location of EV v is encoded in the sequence of binary inputs $b_{1v}, b_{2v}, \ldots, b_{Nv}$, that contain one 1 in the node where the EV charges, and N-1 0's (i.e. where the EV does not charge) at all other nodes.

This way, the nodal EV injections can be expressed as:

$$P_{tn}^{(\text{EV nodal})} = \sum_{v=1}^{V} b_{nv} \cdot P_{vt}^{\text{EV}} \tag{2.5}$$

$$Q_{tn}^{(\text{EV nodal})} = \sum_{v=1}^{V} b_{nv} \cdot Q_{vt}^{\text{EV}}, \tag{2.6}$$

for all n and t. The binary inputs b_{nv} thus represent a matrix of size $N \times V$ and can be interpreted as the map reporting the recharging locations of all EVs in the power grid. Because the grid voltage is constrained in a narrow band, we use the approximation that nodal power injections are voltage-independent.

The dependency between grid quantities (nodal voltage magnitudes v_{tn}, line current magnitudes i_{tl}, and apparent power flow at the substation transformer S_{t0}) and the nodal injections are discussed in section 1.4.3. In a distribution grid, the operational grid quantities should be within prescribed limits. In other words, the nodal voltage magnitudes should remain within limits $(\underline{v}, \overline{v})$, currents in the lines must remain below the lines' ampacities $\overline{i}_l$. Also the power flow at the substation transformer should be less than its rating $\overline{S}_0$. These constraints reads as:

$$\underline{v} \leq v_{tn} \leq \overline{v} \qquad \forall t \text{ and } n \tag{2.7a}$$

$$|i_{tl}| \leq \overline{i}_l \qquad \forall t \text{ and } l \tag{2.7b}$$

$$S_{t0} \leq \overline{S}_0 \qquad \forall t. \tag{2.7c}$$

The following section presents how the above constraints can be embedded to model different EV charging policies.

2.3.3 Modeling different recharging strategies

Uncoordinated charging

This section presents the formulation of the decision-making problem due to uncoordinated charging of EVs. In the case of uncoordinated charging process, all EVs charge with the objective of minimizing their respective recharging time at the grid nodes, independent of the state of the grid and other EVs. Based on this requirement, we can formulate a decision-making problem where the EVs' charging power is determined such that all vehicles reach their respective target state-of-charge level, $\text{SOC}_v^\star$, as quickly as possible. In this case, the chargers, modeled with (2.1), only supply active

power since not only is reactive power not conducive to recharging the vehicles, but it would also limit the capability of the charger. The decision-making problem can be written as follows:

$$\underset{P_{11}^{\mathrm{EV}},\dots,P_{VT}^{\mathrm{EV}}\in\mathbb{R}_+}{\arg\min} \left\{ \sum_{t=1}^{T}\sum_{v=1}^{V} (\mathrm{SOC}_{vt} - \mathrm{SOC}_v^*)^2 \right\} \tag{2.8a}$$

subject to the following constraints:

$$\mathrm{SOC}_{vt} = \mathrm{SOC}_{v(t-1)} + \eta \frac{T_S}{E_v} P_{vt}^{\mathrm{EV}} \qquad \text{for all } t \text{ and } v \tag{2.8b}$$

$$0 \le \mathrm{SOC}_{vt} \le 100\%, \qquad \text{for all } t \text{ and } v \tag{2.8c}$$

$$0 \le P_{vt}^{\mathrm{EV}} \le \overline{S}_v^{\mathrm{EV}} \qquad \text{for all } t \text{ and } v. \tag{2.8d}$$

The uncoordinated charging problem is separable, because it has no coupling constraints. In other words, solving this problem (2.8) is equivalent to solving V independent optimization problems (one per vehicle) with local information only. The uncoordinated charging problem is thus used in this thesis as benchmark scenario to evaluate the impact of EVs' charging on grid constraints.

Smart charging

In the case of smart charging, the charging process is scheduled in such a way that the EVs' charging demand does not cause violations of the grid constraints. Let quantities $\underline{v}$ and $\overline{v}$ denote the admissible voltage magnitude, $\bar{i}_l$ denote the line ampacity, and $\overline{S}_0^2$ denote the power flow at the substation transformer. Grid constraints are modeled in problem (2.9) using the linearized grid models discussed in 1.4.3. The scheduling problem can be formulated as follows

$$\underset{P_{11}^{\mathrm{EV}},\dots,P_{VT}^{\mathrm{EV}}\in\mathbb{R}_+}{\arg\min} \left\{ \sum_{t=1}^{T}\sum_{v=1}^{V} (\mathrm{SOC}_{vt} - \mathrm{SOC}_v^*)^2 \right\} \tag{2.9a}$$

subject to the following constraints:

$$\text{SOC model and constraints (2.8b), (2.8c)} \qquad \text{for all } t \text{ and } v \tag{2.9b}$$

$$0 \le P_{vt}^{\mathrm{EV}} \le \overline{S}_v^{\mathrm{EV}} \qquad \text{for all } t \text{ and } v \tag{2.9c}$$

$$\text{Nodal injections (1.4a), (1.4b), and (2.5)} \qquad \text{for all } t \text{ and } n \tag{2.9d}$$

$$\text{Linearized grid models (1.5)} \qquad \text{for all } t,\ n \text{ and } l \tag{2.9e}$$

$$\underline{v} \le v_{tn} \le \overline{v} \qquad \text{for all } t \text{ and } n \tag{2.9f}$$

$$|i_{tl}| \le \bar{i}_l \qquad \text{for all } t \text{ and } l \tag{2.9g}$$

$$P_{t0}^2 + Q_{t0}^2 \le \overline{S}_0^2 \qquad \text{for all } t. \tag{2.9h}$$

Compared to (2.8), problem (2.9) features coupling constraints, given by the grid model, which requires the information on all nodal injections. This formulation requires gathering all the vehicles' information and the grid in a single (centralized) optimization problem. Centralized formulations of this kind can be used to derive signals to incentive or disincentivize the charge of EVs and achieve a form of indirect control (e.g., [30]).

Smart charging with reactive power support

We extend problem (2.9) by allowing chargers to inject/absorb reactive power with the objective of controlling the nodal voltages of the grid[1]. The decision variables, are in a vector with dimension of $2 \times V \times T$ denoted by:

$$\boldsymbol{x} = \left[P_{11}^{\mathrm{EV}}, \ldots, P_{VT}^{\mathrm{EV}}, Q_{11}^{\mathrm{EV}}, \ldots, Q_{VT}^{\mathrm{EV}}\right]. \tag{2.10}$$

The decision-making problem for both EV chargers' active and reactive power can be formulated as:

$$\arg\min_{\boldsymbol{x}} \left\{ \sum_{t=1}^{T} \sum_{v=1}^{V} \left(\mathrm{SOC}_{vt} - \mathrm{SOC}_{v}^{*}\right)^2 \right\} \tag{2.11a}$$

subject to the following constraints:

$$\text{SOC model and constraints (2.8b), (2.8c)} \qquad \text{for all } t \text{ and } v \tag{2.11b}$$

$$\left(P_{vt}^{\mathrm{EV}}\right)^2 + \left(Q_{vt}^{\mathrm{EV}}\right)^2 \leq \left(\overline{S}_{v}^{\mathrm{EV}}\right)^2 \qquad \text{for all } t \text{ and } v \tag{2.11c}$$

$$P_{vt}^{(\mathrm{EV})} \geq 0 \qquad \text{for all } t \text{ and } v \tag{2.11d}$$

$$\text{Nodal injections (1.4a), (1.4b), (2.5), and (2.6),} \qquad \text{for all } t \text{ and } n \tag{2.11e}$$

$$\text{Linear grid models (1.5)} \qquad \text{for all } t,\ n \text{ and } l \tag{2.11f}$$

$$\overline{v} \leq v_{tn} \leq \underline{v}, \qquad \text{for all } t \text{ and } n \tag{2.11g}$$

$$|i_{tl}| \leq \overline{i}_{l}, \qquad \text{for all } t \text{ and } l \tag{2.11h}$$

$$P_{t0}^2 + Q_{t0}^2 \leq \overline{S}_{0}^2 \qquad \text{for all } t. \tag{2.11i}$$

Vehicle-to-grid problem

In the vehicle-to-grid (V2G) problem EVs are allowed to discharge if this is conducive to alleviate the grid constraints. To formulate the V2G problem we consider charging power, discharging power, and the reactive power as decision variables. Although both the discharging power and the reactive power do not contribute to recharge the EVs directly (indeed, reactive power does not appear in (2.3)), their contribution might be useful to alleviate network congestions, ultimately allowing other EVs to recharge and improving the global charging time across the population.

In this case, the decision variables are:

$$\boldsymbol{w} = \left[P_{11}^{\mathrm{EV}+}, \ldots, P_{VT}^{\mathrm{EV}+}, P_{11}^{\mathrm{EV}-}, \ldots, P_{VT}^{\mathrm{EV}-}\right] \tag{2.12}$$

$$\boldsymbol{y} = \left[Q_{11}^{\mathrm{EV}}, \ldots, Q_{VT}^{\mathrm{EV}}\right]. \tag{2.13}$$

The decision-making problem for both EV chargers' active and reactive power is:

$$\arg\min_{\boldsymbol{w},\boldsymbol{y}} \left\{ \sum_{t=1}^{T} \sum_{v=1}^{V} \left(\mathrm{SOC}_{vt} - \mathrm{SOC}_{v}^{*}\right)^2 + k \sum_{t=1}^{T} \sum_{v=1}^{V} \left(P_{vt}^{\mathrm{EV}+} + P_{vt}^{\mathrm{EV}-}\right) \right\} \tag{2.14a}$$

[1]Where the reactance of the lines' longitudinal components may be dominant over the resistance, reactive power control can be an effective way to provide voltage regulation

subject to the following constraints:

$$\text{SOC model and constraints (2.8b), (2.8c)} \qquad \text{for all } t \text{ and } v \qquad (2.14b)$$

$$\left(P_{vt}^{\text{EV+}} - P_{vt}^{\text{EV-}}\right)^2 + \left(Q_{vt}^{\text{EV}}\right)^2 \leq \left(\overline{S}_v^{\text{EV}}\right)^2 \qquad \text{for all } t \text{ and } v \qquad (2.14c)$$

$$\text{Nodal injections (2.5), (2.6), (2.2),(1.4a), (1.4b)} \qquad \text{for all } t,\ n \text{ and } v \qquad (2.14d)$$

$$\text{Linear grid models (1.5a)-(1.5b)} \qquad \text{for all } t,\ n \text{ and } l \qquad (2.14e)$$

$$\overline{v} \leq v_{tn} \leq \underline{v}, \qquad \text{for all } t \text{ and } n \qquad (2.14f)$$

$$|i_{tl}| \leq \bar{i}_l, \qquad \text{for all } t \text{ and } l \qquad (2.14g)$$

$$P_{t0}^2 + Q_{t0}^2 \leq \overline{S}_0^2 \qquad \text{for all } t. \qquad (2.14h)$$

The problem (2.14) refers to the V2G scheduling problem with reactive power support. The reactive power support can be excluded either by forcing $\boldsymbol{y}$ to zero with equality constraints or by removing the associated decision variables from the problem and constraints. In the cost function (2.14a), we introduce a second term, weighted by the coefficient k, which aims to promote mutually exclusive charging and discharging power. As the second term of the cost function corresponds to the SOC's model relaxation and does not have a specific physical meaning, k should be small to not significantly alter the original cost function. The impact of k on the algorithm performance and on the original problem objective is small, as presented under the results section.

2.4 Case study and Results

2.4.1 Power grid and EVs

This dissertation considers the CIGRE benchmark European version of the MV grid from [6] as the case study. The topology of the grid is shown in Fig.1.8 (refer to the previous chapter for details). According to [6], LV grids are connected to different grid nodes of the CIGRE MV grid, which are modeled in terms of their aggregated contributions. It is assumed that there are no violations of grid constraints in each LV grid. The MV grid is modeled with a single-phase equivalent, assuming a balanced grid with transposed conductors. The per unit active power demand at each node used to model nodal injections is shown in Fig.2.3, and it can be observed that the demand peaks during the evening hours. The nodal apparent power, power factors, and the number of parked EVs at each node of the CIGRE MV grid are reported in Table 2.1. The reactive power demand is modeled as the product of the active power and the tangent of the arc-cosine of the power factor in Table 2.1. The statutory voltage levels of the MV grid are $1 \pm 3\%$ per unit values. Line ampacities are determined based on the conductor diameter. To compute sensitivity coefficients for the linear grid models, nominal active and reactive nodal injections are required for the linearization. We use the same nodal power injections as the demand (P_{nt}^{demand} and Q_{nt}^{demand} in (1.4)) from the CIGRE specifications for this purpose. At this stage PV injections at the grid nodes are not considered[2].

[2]It is worth noting that PV generation could be accounted by altering the net demand (input of the problem), thus detracting no value from the general applicability of the formulation.

The input information related to EVs charging at multiple grid nodes will be discussed in the next paragraph.

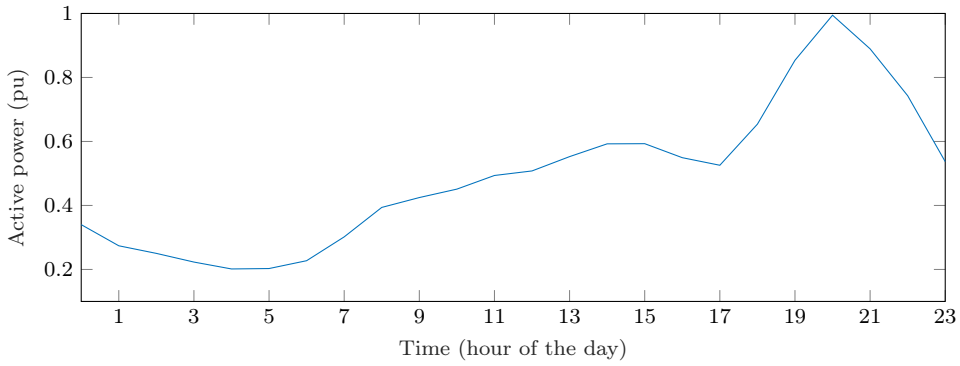

Figure 2.3: Profile of the net active power demand from CIGRE specifications[6].

Table 2.1: Nodal nominal demand per node and number of EVs

Node	**Apparent Power** [kVA]	**Power factor**	**Number of EVs**
1	15'300	0.98	0
3	285	0.97	68
4	445	0.97	106
5	750	0.97	178
6	565	0.97	134
8	605	0.97	144
10	490	0.97	116
11	340	0.97	81
12	15'300	0.98	0
14	215	0.97	51

In [114], 200 EVs have been considered in a 33-node distribution grid that hosts 5 EV charging stations, where EVs are allocated according to the peak load of the grid nodes assuming that the charging stations can meet the charging demands of EVs. For a 5 MVA MV residential grid, a total of 2,340 EVs have been considered in [116], implying a case with intense loading due to the recharging of EVs in an the grid. In [64], a total of 98 EVs have been considered for an LV distribution grid, where the EVs are allocated to respective grid nodes considering the nodal power. A similar approach has been considered to study the scheduling algorithms in this dissertation to accommodate EVs in the MV grid nodes. As reported in [5], the number of EVs per household can range between 0-3, with an average number of 1.1 (see Table 2.2). Additionally, the work in [117] considers an average of 1.3 EVs per household. In this thesis, for the CIGRE MV (1 MVA base) residential grid, nearly 1.4 EVs per household and a total of 878 EVs have been considered (estimated by dividing the nominal nodal power by an estimated single-phase household contractual power of 6 kVA), which is in line with existing literature. In Table 2.1, nodes 1 and 12 are less

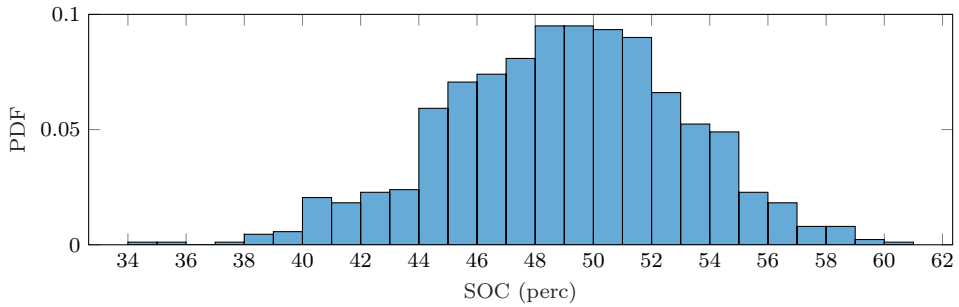

Figure 2.4: Distribution of EVs' initial state-of-charge used in the case

critical for grid constraint violations as they are located near the upper grid's connection point, and thus they have been excluded from considering EV charging stations. This also reduces the number of variables in the scheduling problem.

Similar to [118, 119], the departure times and initial SOCs of EVs are sampled using the following distributions: Weibull (scale 7.67, shape 21.83) and Gaussian (mean 0.49, standard deviation 0.04) distributions, respectively, as shown in Fig. 2.4. The energy capacity of the EV batteries, the chargers' rated power, efficiency, and power factor are assumed to be constant across their population and are 16 kWh, 3.6 kVA, 0.9, and 1, respectively. It is considered that the target SOC levels are uniform across the population of EVs and assumed to be 100%.

Table 2.2: Number of vehicles per household [5].

Number of EVs	0	1	2	≥ 3
% of households	18.21	53.65	24.75	3.39

In this dissertation, both simultaneous and distributed arrival of EVs has been considered. The principles of charging for these different cases are summarized below:

- **Simultaneous arrivals**: This scenario assumes that all EVs are available to be recharged together at 16:00 at different grid nodes with an initial SOC (see Fig. 2.4) derived from the Gaussian distribution discussed earlier. They recharge at the rated power of the charger over the optimization horizon.
- **Distributed arrivals**: This scenario considers that the arrival hours of EVs are desynchronized over time. Their arrival times are sampled using the generalized extreme value inverse distribution function with the following values: shape (-0.06), scale (0.85), location (17.3), from the Test-an-EV experiment [118, 119]. If the arrival hours fall within the optimization hours, the EVs recharge at the rated power of the EV charger. If their arrival hours are beyond the optimization hours, they do not participate in the charging process.

For both of the above scenarios, comparative studies have been performed to explore their impact on the grid due to uncoordinated charging of EVs, as discussed in the following sections.

2.4.2 Optimization results

For the scheduling problems presented under section 2.3.3, the results of five cases are compared in this section. The five cases are as follows: (A) uncoordinated charging - for both simultaneous and distributed arrival of EVs; (B) smart charging - without reactive power support; (C) smart charging with reactive power support; (D) V2G without reactive power support; (E) V2G with reactive power support.

We consider a sampling time of 1 hour and set the scheduling horizon from 16:00 to 7:00 of the next day. The power flow at the HV/MV substation transformer is not considered in the case study. The scheduling problems are implemented in MATLAB and solved using Gurobi on an Intel processor. Under these settings the optimization problems take nearly an hour to converge.

The voltage profiles

Fig. 2.5 shows the nodal voltage magnitudes due to `uncoordinated charging` of EVs for both simultaneous and distributed arrival of the EVs (as described in 2.4.1). The green shades denote the quantile of the voltage magnitude across the nodes. It is observed that, in both cases the voltage magnitudes fall below the lower bound as the uncoordinated charging process does not take into account the grid constraints.

It is observed from Fig. 2.5a that between 16 h and 17 h voltage limits are violated, whereas in Fig. 2.5b between 16 h and 17 h, voltage limits are respected. This is expected as distributed arrivals of EVs induces a natural smoothing of the total charging demand because EVs arrive at different hours which "desynchronize" their charging process. From Fig. 2.5b it is also seen that during the evening hours, voltage limit violations are more severe (as compared to Fig. 2.5a) because the EV charging demand overlaps with the peak hours of conventional demand of the CIGRE MV grid as reported in [6].

Fig. 2.6a shows the voltage levels due to coordinated or smart charging of EVs; while Fig. 2.7a shows the voltage levels due to V2G charging of EVs. For both these cases, the effect of reactive power support from the EV chargers have been analyzed and are shown in Fig. 2.6b Fig. 2.7b. As seen, in case of coordinated and V2G charging of EVs the voltage magnitudes are respected as the grid constraints are implemented in the scheduling problem. The differences in magnitudes between these plots are prominent due to handling differently the active and reactive powers by the chargers over the optimization horizon.

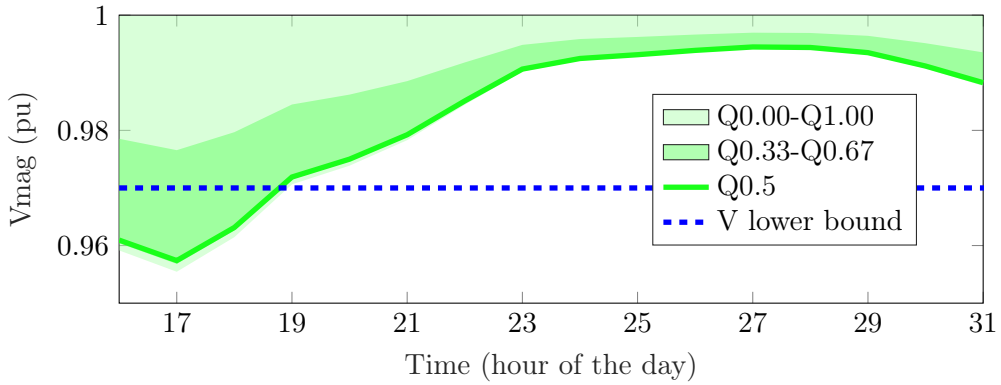

(a) with arrival time at 16h for all vehicles

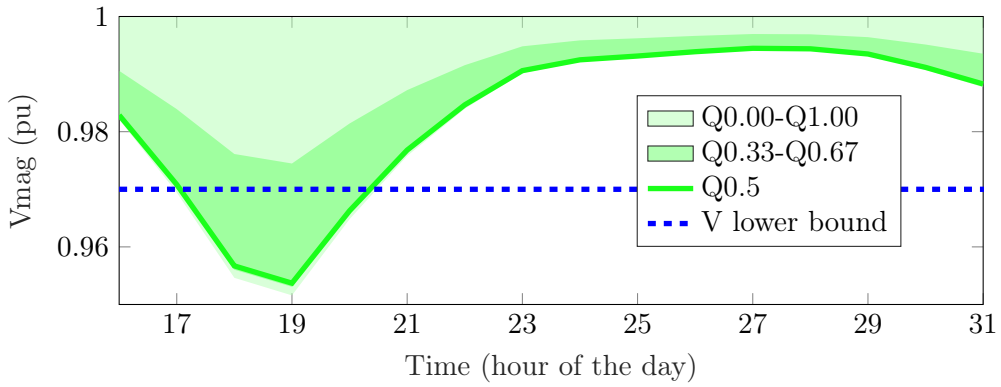

(b) with distributed arrival of vehicles

Figure 2.5: Nodal voltage magnitudes over time due to uncoordinated charging. The shaded bands denote different quantile intervals across the nodes. Voltage bounds are within 1 ± 3% pu values. The dashed lines indicate the lower voltage limit.

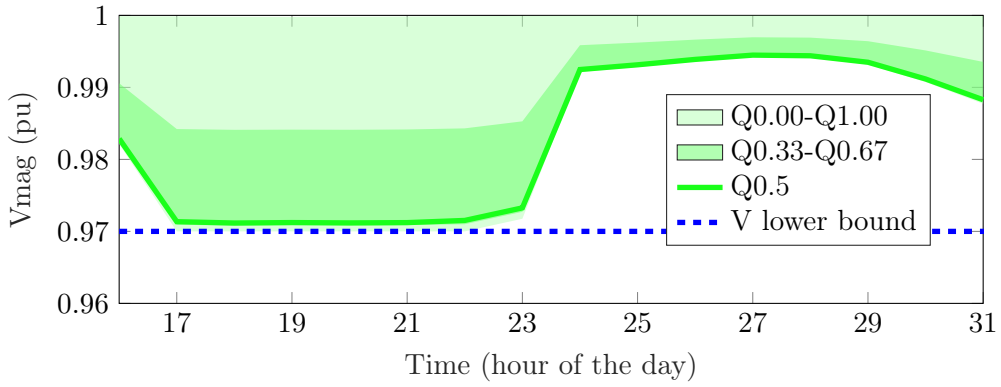

(a) Smart charging without reactive power support.

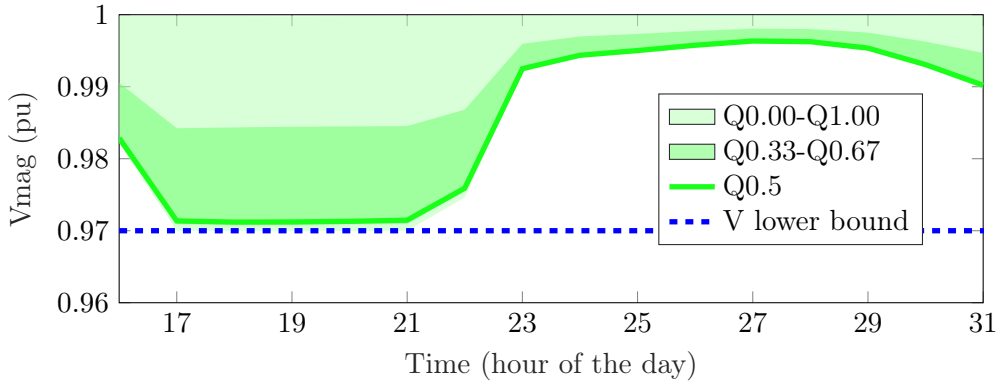

(b) Smart charging with reactive power support.

Figure 2.6: Nodal voltage magnitudes over time and with distributed arrival of vehicles due to coordinated charging policies. The shaded bands denote different quantile intervals across the nodes. Voltage bounds are within $1 \pm 3\%$ pu values. The dashed lines indicate the lower voltage limit.

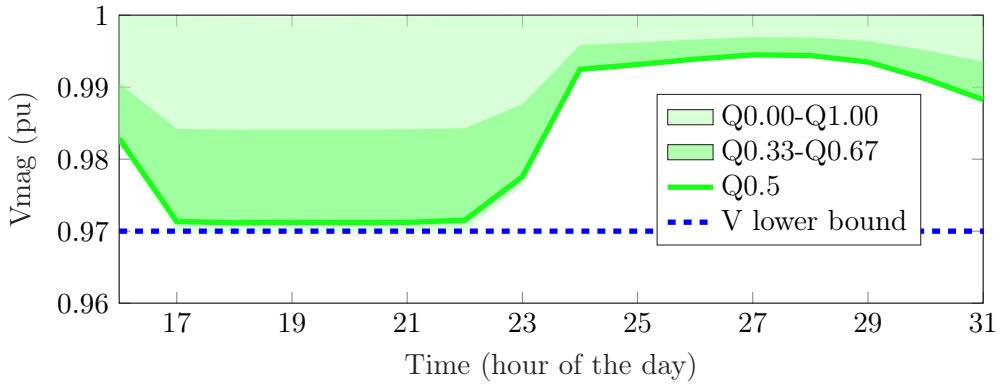

(a) V2G without reactive power support

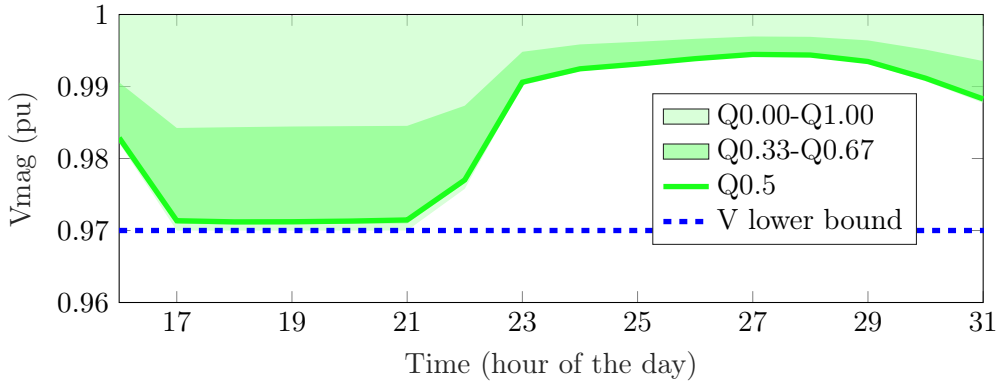

(b) V2G with reactive power support.

Figure 2.7: Nodal voltage magnitudes over time and with distributed arrival of vehicles due to V2G charging policies. The shaded bands denote different quantile intervals across the nodes. Voltage bounds are within $1 \pm 3\%$ pu values. The dashed lines indicate the lower voltage limit.

Impact on line currents

For all five charging policies, the per unit currents over time are plotted in Fig. 2.8. Although the uncoordinated charging process of EVs does not consider current constraints, it is observed that the line current limits are not violated. Furthermore, it is observed that in the case of smart charging and V2G, the current constraints are respected without significant impacts due to the charging process of 878 EVs. Similar results are observed in the case of smart charging and V2G with reactive power support from the chargers.

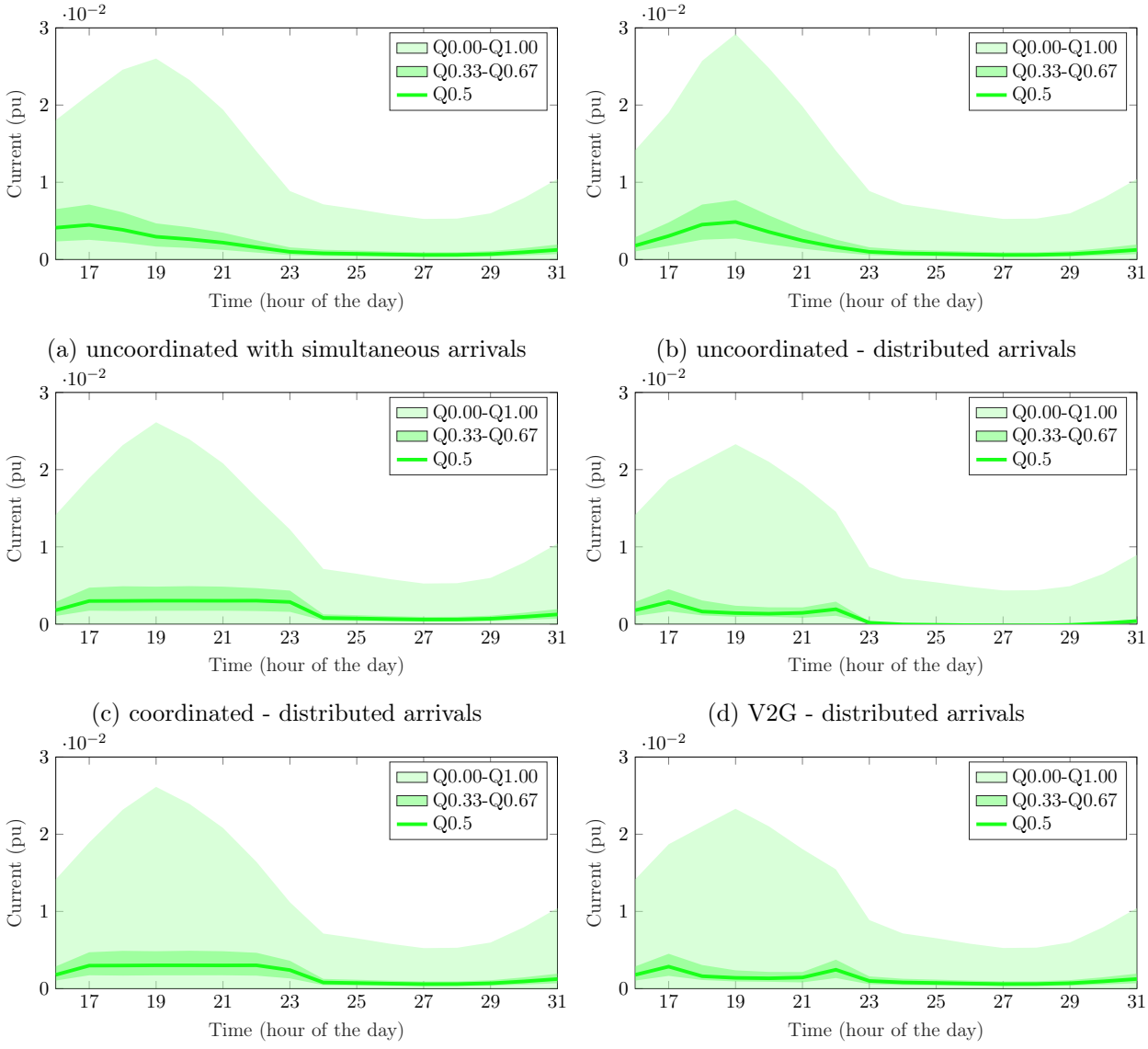

(a) uncoordinated with simultaneous arrivals

(b) uncoordinated - distributed arrivals

(c) coordinated - distributed arrivals

(d) V2G - distributed arrivals

(e) coordinated - distributed arrivals

(f) V2G - distributed arrivals

Figure 2.8: Line currents over time due to different charging policies. The shaded bands denote different quantile intervals across the nodes. Current bounds are within 1 pu values.

Impact of modeling reactive power support

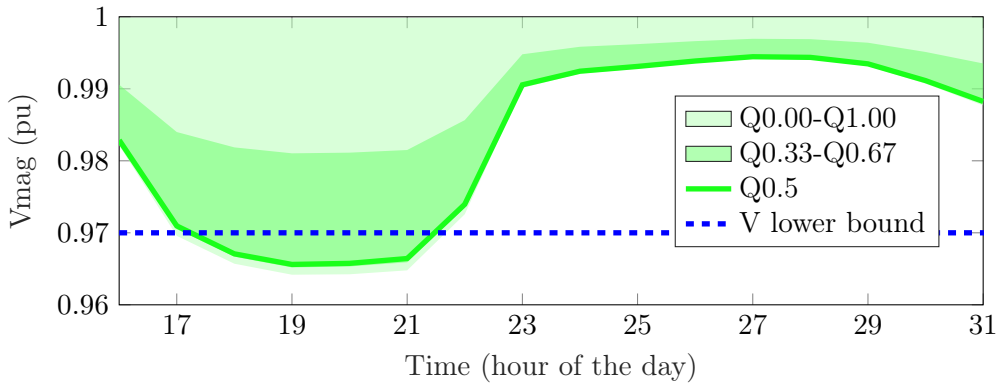

(a) Case: smart charging with reactive power support.

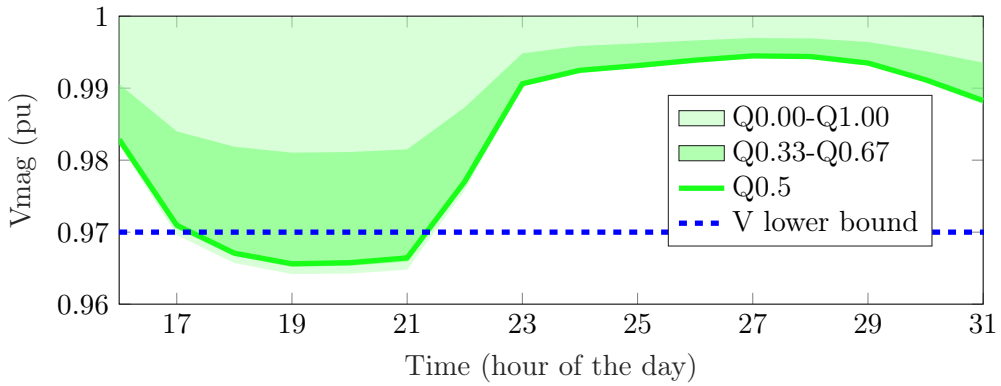

(b) Case: V2G charging with reactive power support.

Figure 2.9: Voltage magnitude computed by assuming the same active power demand but reactive power contribution from the EVs forced to zero. Voltage bounds are within $1 \pm 3\%$ pu values. The dashed blue lines are the lower voltage limit.

This section exhibits the notion of modeling reactive power support from the EV chargers on the grid performance, validated by solution obtained from the scheduling problem as discussed in the previous section. Fig. 2.9 shows the voltage magnitudes obtained from a (linearized) load flow but with the reactive power contributions from the chargers when forced to zero for the two following cases: smart charging and V2G charging.

Both the cases, Fig. 2.9a and Fig. 2.9b feature the same active power demand (as in smart charging with reactive power support); interestingly it is observed that voltage constraints are violated for both the cases when reactive power is forced to zero, implying reactive power for both the cases are fundamental to improve voltage levels in the MV feeders. The same results and conclusions have been found by changing the target SOC levels to lower values (90% and 80%).

Impact on the recharging speed of EVs

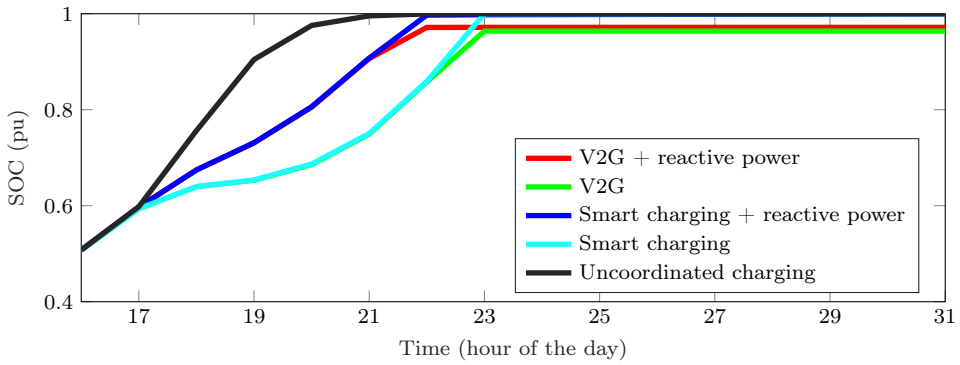

Figure 2.10: Average SOC across the EVs population for different charging policies.

Over the optimization horizon the mean SOC across the EV population is plotted in Fig. 2.10. As observed from the black line, in case of uncoordinated charging the targeted SOC is achieved in quickest recharging time; however, this is achieved at the price of violating grid constraints as shown earlier (see Fig. 2.5b). This solution is thus not viable in practical grid applications. In case of smart charging (cyan trace) and V2G (green trace) it is seen that the targeted SOC is achieved in slowest recharging time. This denotes that, though the voltage limits are respected by the V2G charging policy, it does not conduce to improve overall system performance. A difference between the steady-state average SOC values are observed after 23 h between the smart charging and V2G policy; this is due to the modelling relaxation of the SOC. In particular, due to the modified cost function for the V2G problem in (2.14), there is a trade off between the cost associated to EVs' charging power and cost associated towards achieving the target SOC that determines the steady-state SOC error. The same steady-state SOC error is observed between the smart charging and V2G with reactive power support (blue and red traces respectively). These errors can be reduced by decreasing the value of k in the cost function of (2.14a).

For a fine comparison of the recharging speed we proceed as follows. For any optimization problem, evaluation of the cost function provides an immediate interpretation of the performance of the scheduler over the optimization horizon. Based on it, the metric in 2.15 is computed for all the schedulers and performance is reported in Table 2.3. It is observed that for uncoordinated charging the metric achieves the lowest value (21.4714). V1G and V2G achieve nearly the same value; with reactive power support V1G and V2G achieve nearly the same value.

$$\text{Metric} = \sum_{t=1}^{T} \sum_{v=1}^{V} (SOC_{tv} - SOC_v^*)^2 \tag{2.15}$$

Thus, it can be seen from Fig. 2.10 that the best-performing schedulers are smart charging and V2G with reactive power support that eventually allow more EVs to recharge over the optimization horizon; however, in this case V2G does not help to minimize the charging times.

Table 2.3: Metric performances for different policies. 'Q' is the reactive power support.

Recharging policies	V1G	V1G with Q	V2G	V2G with Q
Metric values	27.7098	24.0421	27.8987	24.1896

2.5 Solving scheduling problem for AEVs

Charging location of AEVs

This section briefly discusses how the former scheduler can be extended to autonomous EVs or AEVs. To formulate the scheduling problem, in section 2.3.2, the nodal injections due to traditional EVs have been presented where it is said that the charging location of an EV is known and encoded as input for the problem with a set of binary inputs. In case of AEVs, they are no longer an input for the scheduling problem as autonomous EVs can pick independently a charging station to accelerate their recharging process and reduce the impact of charging on the grid.

For AEVs, b_{nv} (as in section 2.3.2) no longer represent the binary inputs (as they no longer represent fixed parking spots of EVs), but the binary variables with $b_{nv} \in \{0, 1\}$ are now optimization variables of the decision making problem. Thus the scheduling problem for AEVs becomes a MIP (mixed integer programing) problem that determines the charging spots for AEVs. Also in this case we need to ensures that each vehicle is charging at one location maximum. This requirement is modelled by enforcing an additional constraint, also known as the non-multilocation constraint that reads as:

$$\sum_{n=1}^{N} b_{nv} \leq 1. \tag{2.16}$$

Modeling nodal injections for AEVs

To compute the nodal injection for AEVs, similar set of equations as in traditional EVs in section 2.3.2 can be written with b_{nv}.

At each node of the grid the active and reactive power demand can be modelled as the sum of the net demand[3] and the aggregated charging demand of all the AEVs charging from a node. With b_{nv} as optimization variables, the nodal injection model (1.4a) at a grid node n and at time t can be updated as:

$$P_{tn}^{\text{node}}\left(P_{t1}, ..., P_{tV}, b_{n1}, ..., b_{nV}\right) = P_{tn}^{\text{net}} + \sum_{v=1}^{V} b_{nv} P_{vt}^{(\text{EV})}. \tag{2.17}$$

The net demand P_{tn}^{net} is an input of the problem as it is in case of traditional EVs. The charging demand from an EV v is contributed to the nodal injection by the decision making problem when

[3]Net demand is the conventional power demand minus distributed generations

the binary variable b_{nv} is activated. Following expressions collect all the variables from (2.17) in the vectors when the scheduling problem is solved for AEVs:

$$\boldsymbol{\lambda} = \left[P_{11}^{(\mathrm{EV})}, \ldots, P_{VT}^{(\mathrm{EV})}\right] \tag{2.18}$$

$$\boldsymbol{b}_n = \left[b_{n1}, \ldots, b_{nV}\right]. \tag{2.19}$$

In Eq. (2.17) the second term comprises products between decision variables (as collected in Eq. (2.18) and Eq. (2.19)), thus introduces a bi-linear formulation. To linearize this expression the McCormick's relaxation [120] can be used. Analyzing the impact of AEVs on the MV or LV distribution grid is beyond the scope of this dissertation. The notion presented above for AEVs has been explored within the context of the EVA project as a contribution towards the following conference publication.

> F. Sossan, B. Mukherjee and Z. Hu, "Impact of the Charging Demand of Electric Vehicles on Distribution Grids: a Comparison Between Autonomous and Non-Autonomous Driving," 2020 Fifteenth International Conference on Ecological Vehicles and Renewable Energies (EVER), 2020, pp. 1-6, doi: 10.1109/EVER48776.2020.9243122.

2.6 Conclusions

This chapter presents the formulation of different charging strategies for traditional EVs based on the existing state-of-the-art. In the modeling context, the following charging policies have been considered: uncoordinated charging, smart charging, V2G with and without reactive power support from the EV chargers. The problem formulation of all the schedulers is derived from a common (convex) optimization framework accounting for (linearized) power grid constraints (nodal voltage magnitudes, line currents etc.), charging/discharging efficiency, and 4-quadrant (and 2-quadrant unidirectional) chargers, that allow an efficient comparison among the charging policies. The applicability of this contribution is envisaged in the context of an urban planner or DSO willing to compare the performance of different charging strategies. The scheduling problems (2.8) and (2.9) feature linearized models and constraints. When the cost function is formulated linearly, these problems can be effectively solved as linear programming (LP) models. When the constraints (2.11c) and (2.14c) accounting for the capability of EV chargers are included in the problem formulations (2.11) and (2.14), respectively, due to their second-order cone characteristics, the scheduling problems can be solved as convex nonlinear programming (NLP) problems. Nodal apparent power limits, which are quadratic in nature for the apparatus at the substation, were not taken into account as constraints in the scheduling problems discussed in this chapter. However, in the next chapter, these constraints have been included in the optimization problem, and it will be demonstrated how they can be approximated as linearized constraints.

Finally, this chapter presents the key findings from comparing the performance of different EV charging strategies on the residential MV grid in the presence of a large population of EVs. It

is observed that in the case of uncoordinated charging of 878 EVs at different nodes of the European CIGRE MV grid, the grid's voltage constraints are violated during the afternoon/evening periods. In this context, smart charging proves to be effective in reducing congestion during the afternoon/evening periods. From the scheduling problem (2.14), it is evident that the V2G feature is never activated. However, the reactive power support from the EV chargers is valuable in reducing voltage congestion, enabling more EVs to charge and shortening the overall charging time to achieve a target SOC. When considering the charging of AEVs in the power grid, as presented in section 2.5, the problems for different charging policies can be formulated under a common framework, as proposed in this thesis. However, this imposes a computational burden due to the increased number of variables (mainly due to the variables 2.19) in the optimization problem.

Chapter 3

Planning of EV charging stations in MV grid

Résumé en Français

L'objectif de la planification de l'infrastructure de charge dans un réseau de distribution d'électricité MV est de situer et de dimensionner les chargeurs de VE à différents nœuds du réseau, en tenant compte des contraintes techniques du réseau, des multiples typologies de chargeurs (rapides, lents, chargeurs à ports multiples, chargeurs à port unique) et des scénarios impliquant la flexibilité des conducteurs à brancher et à débrancher leurs VE. La méthode proposée dans ce chapitre vise d'abord à minimiser l'investissement en capital de l'infrastructure de charge et, ensuite, à minimiser conjointement l'investissement en capital tout en maximisant l'autoconsommation photovoltaïque. Le problème de planification optimale a été formulé comme une optimisation économique basée sur un programme linéaire mixte (MILP). La méthodologie présentée utilise l'approche du flux de puissance optimal (OPF) et peut être intéressante pour les opérateurs de systèmes de distribution intégrés (DSO) et les urbanistes. L'étude de cas synthétique présentée dans ce chapitre analyse les impacts des infrastructures de recharge à port multiple et à port unique, y compris les modèles de flexibilité des conducteurs. Les résultats de deux documents distincts, la publication A et la publication B, sont inclus dans ce chapitre.

Summary

The objective of planning the charging infrastructure in an MV power distribution grid is to site and size EV chargers at different grid nodes, accounting for the technical constraints of the grid, multiple charger typologies (fast, slow, multi-port chargers, single-port chargers), and scenarios involving drivers' flexibility to plug and unplug their EVs. The method proposed in this chapter aims to first minimize the capital investment of the charging infrastructure and secondly, to jointly minimize the capital investment while maximizing PV self-consumption. The optimal planning problem has been formulated as an economic optimization based on a mixed-integer linear program (MILP). The presented methodology utilizes the optimal power flow (OPF) approach and can be of interest

to integrated distribution system operators (DSOs) and urban planners. The synthetic case study presented in this chapter analyzes the impacts of both multi-port and single-port charging infrastructures, including models of drivers' flexibility. The results from two separate papers, Publication A and Publication B, are included in this chapter.

3.1 Introduction

While Enedis in France is planning to accommodate charging stations at the location of street lamps[1] along the road, many other companies are also planning to set up charging infrastructures for EVs. According to [121], in a power distribution network, the EV charging system connected to the street lamps does not require any additional work, except for the installation of an electricity meter and its long-term operation. An EV owner primarily considers home charging (using a slow charger) [121, 122]. When home charging is unavailable, people consider charging at public places or the workplace. At the workplace, charging stations are set up either for employees using personal electric vehicles or for companies' electric fleets [121]. In 1.2.5, the primary motivation behind the development of an extended EV charging infrastructure and the literature review on existing methods to address the problem of charging infrastructure planning have been explored.

In light of the current state-of-the-art, the main contribution of this chapter is to formulate the optimization problem with the objective of siting and sizing EV chargers in a distribution grid while accounting for grid constraints, multiple charger typologies such as fast and slow chargers, as well as single-port chargers (SPCs) and multi-port chargers (MPCs). The proposed method in this chapter also models EV owners' flexibility in plugging and unplugging their EVs to and from public charging stations. This last consideration is reasonable to achieve better utilization of the charging columns, which eventually impacts the deployment of chargers throughout the distribution grid. This chapter also presents a quantitative investigation into the sensitivity of the EV charging infrastructure to different optimization objectives, including photovoltaic (PV) self-consumption. The widely advocated PV self-consumption paradigm from the literature has been considered herein to reduce grid congestion and grid losses. With the integration of local renewable generation (e.g., PV power) into the existing distribution grid, the recharging process of EVs can benefit from direct recharging using these local renewable sources. The proposed method in this chapter enables the direct utilization of PV power to recharge EVs and promotes the integration of more PV power into existing distribution grids. This integration helps to reduce grid congestion while satisfying the charging demand of EVs.

This chapter delves into the question of whether different planning objectives would result in significantly distinct charging infrastructures or if similar infrastructure configurations can be adapted to accommodate various objectives. This inquiry is particularly relevant for integrated distribution system operators (DSOs), urban planners, and policymakers who must anticipate potential obsolescence of charging infrastructure as objectives evolve over time. To address this question, we propose

[1]The number of streetlights in France is approximately ten million units [121].

an adaptable mathematical optimization model that facilitates this analysis. The planning formulation presented here, takes the form of a constrained economic optimization problem, employing a mixed-integer linear program (MILP) approach that can be efficiently solved with off-the-shelf optimization libraries.

3.1.1 Modeling principles and optimization problem

Figure 3.1 presents all the modeling elements required to formulate the optimal planning problem. In Fig. 3.1, at the top, the black box computes the SOC evolution in time of all EVs as a function of the EVs' driving demand (as presented by the yellow box). For EVs to remain in a functional condition and satisfy the driving requirements by the EV owners, their SOCs should be within the physical ranges (e.g., between 10% and 100%, or any other configurable limit).

The planning problem computes the EVs' recharging decision or when to recharge them (as shown by the red box) over the optimization horizon, and this depends upon the following constraints: charge an EV while it is plugged into a charger (first blue box from the top). This is possible only when an EV is parked (this information is available from the input variables p_{nvt}, as discussed in the next section). The plugged-in state of an EV does not only depend on its parking state, but also on i) availability of a charger and ii) availability of an EV owner to unplug a charged EV and plug in an EV that needs to be recharged. For example, it is unlikely that an EV is plugged into a charger in the early morning hours as its owner might sleep: this flexibility of the owner is specifically modeled with a dedicated set of constraints, as explained later in section 3.3.2.

Some additional set of constraints related to the operational limits of the grid are shown by the green box to ensure the charging an EV do not violate them. The parking location of the EVs establishes the link between the EVs' recharging demand and the power demand at respective grid nodes, allowing to model nodal power injections.

After the charging schedules for all the EVs are determined (grey boxes, related to cost function model), the information is then processed to estimate the number of charging infrastructures at different locations of the grid to satisfy the recharging demand. The objective function of the problem minimizes the total cost of the infrastructure based on the total number of charging infrastructures. As denoted by the last blue boxes (for SPCs or MPCs) are the additional set of constraints to model whether SPC or MPC infrastructures are allowed in the optimization problem. The whole problem of Fig. 3.1 is formulated as a MILP program, allowing for a compact formulation of all constraints and economic optimization. The methodology to formulate the planning problem is presented next. The economical cost minimization problem of charger deployment is solved with and without PV self-consumption modeling.

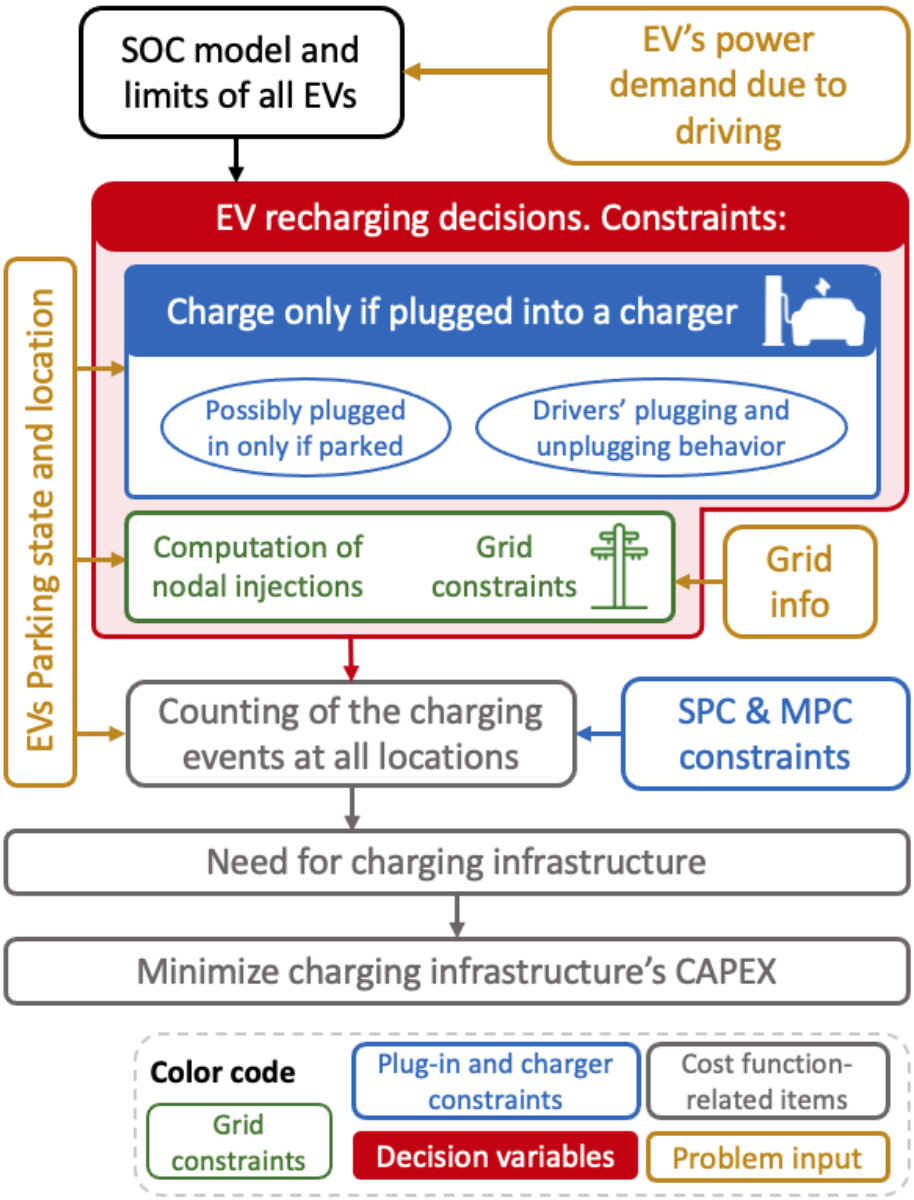

Figure 3.1: The main elements used in the planning problem.

3.2 Methodology

3.2.1 Input information to the problem

It is assumed that the parking locations of the EVs over the time at the distribution grid nodes are known; this information has been considered as an input of the planning problem. We encode EVs'

parking locations in the following input binary parameters:

$$p_{nvt} = \begin{cases} 1, & \text{if EV } v \text{ is connected to node } n \text{ at time } t \\ 0, & \text{otherwise.} \end{cases} \tag{3.1}$$

The subscript "*nvt*", as well as other subscripts introduced in this thesis, denotes quantities for grid node n and vehicle v at time interval t, and not the product among these indexes. It is illustrative to mention that because a vehicle can be parked at one node only at a given time, the following holds:

$$\sum_{n=1}^{N} p_{nvt} \leq 1 \qquad \forall t \text{ and } v. \tag{3.2}$$

We denote the energy storage capacity of the EVs by E_v and the discharging power of EV batteries by $p_{vt}^{\text{EV-}}$. The discharging power depends primarily on the driving/transportation demand, but also on other factors, such as driving style and regenerative breaking, auxiliaries' consumption (e.g., [123]), battery self-discharge, and battery state in general. Because this discharging power is an input quantity, the method proposed herein is independent from the specific way it is computed. For example, it can be computed by way of transport simulations (e.g., [124]), or estimated from experimental measurements or statistics (e.g., [22, 119, 125]).

3.2.2 Modeling connection and charging state

To define whether the EV is plugged into a fast or a slow charger, for each vehicle v and time interval t, we define the binary variables f_{vt}^{plugged} and s_{vt}^{plugged} respectively. As an EV cannot be connected to a fast and slow charger simultaneously, it holds that f_{vt}^{plugged} and s_{vt}^{plugged} cannot be active at the same time; moreover, as an EV can be plugged only when parked, f_{vt}^{plugged} and s_{vt}^{plugged} can remain active only if at least one p_{nvt} among all nodes remain active. These two requirements can be formalized in the following inequality constraint:

$$f_{vt}^{\text{plugged}} + s_{vt}^{\text{plugged}} \leq \sum_{n=1}^{N} p_{nvt} \qquad \forall t \text{ and } v. \tag{3.3}$$

We consider two additional binary variables per vehicle and time interval, denoted by $f_{vt}^{\text{charge}}, s_{vt}^{\text{charge}}$, indicate whether a vehicle v is charging from a fast or a slow charger at time t. As EVs can charge only when plugged into a charger[2], it holds that:

$$f_{vt}^{\text{charge}} \leq f_{vt}^{\text{plugged}} \qquad \forall t \text{ and } v \tag{3.4a}$$

$$s_{vt}^{\text{charge}} \leq s_{vt}^{\text{plugged}} \qquad \forall t \text{ and } v \tag{3.4b}$$

Thus, the quantities $f_{vt}^{\text{plugged}}, s_{vt}^{\text{plugged}}, f_{vt}^{\text{charge}}, s_{vt}^{\text{charge}}$ are the variables of the optimization problem; based on these variables, the charging power of the EVs, as well as the needs for fast and slow chargers are determined, as explained next.

[2]Indeed, being connected to a charger does not necessarily imply that an EV is recharging.

Extension to V2G

This paragraph presents how the above formulation can be extended to model vehicle-to-grid (V2G) support from the EVs with bidirectional chargers. For brevity, this is demonstrated for slow chargers only. For fast chargers, similar expressions can be derived by replacing the corresponding variables.

Similarly to the binary variable s_{vt}^{charge} that denotes if an EV is recharging or not, a new binary variable, $s_{vt}^{\text{discharge}}$, is introduced that indicates whether an EV is discharging. Because an EV can either be charged or discharged at the same time, and can be discharged only when plugged, the following two constraints must hold:

$$s_{vt}^{\text{discharge}} + s_{vt}^{\text{charge}} \leq 1, \qquad \forall t \text{ and } v \tag{3.5}$$

$$s_{vt}^{\text{discharge}} \leq s_{vt}^{\text{plugged}}, \qquad \forall t \text{ and } v. \tag{3.6}$$

3.2.3 Modeling of EV charging power

With the above definitions in place, the charging power of a vehicle v and time t is:

$$p_{vt}^{\text{EV+}} = f_{vt}^{\text{charge}} \cdot \bar{F} \cdot \cos\phi_F + s_{vt}^{\text{charge}} \cdot \bar{S} \cdot \cos\phi_S, \tag{3.7a}$$

where input parameters $\bar{F}$ and $\cos\phi_F$ are the kVA rating and power factor of the fast charger, respectively, and similarly $\bar{S}$ and $\cos\phi_S$ for the slow charger. The reactive power associated to this charging demand is:

$$q_{vt}^{\text{EV+}} = f_{vt}^{\text{charge}} \cdot \bar{F} \cdot \sin\phi_F + s_{vt}^{\text{charge}} \cdot \bar{S} \cdot \sin\phi_S. \tag{3.7b}$$

It is worth highlighting that, here, chargers are assumed to operate in an on-off manner, meaning that the recharging power cannot be modulated in intensity. However, the recharging power of all chargers can be modulated over time, ultimately achieving power intensity modulation at the aggregated level and enabling grid congestion management. Modulation of the charging power at the level of the single charging station is illustrated in the next paragraph.

Case of smart charging

In the case of smart charging, the output power of an EV charger can be modulated. For brevity, this section presents the formulation for slow chargers only. For fast chargers, similar expressions can be derived by replacing the corresponding variables.Assuming the charger works at a constant power factor (regardless of its power output), the previous models in (3.7) can be modified as:

$$0 \leq p_{vt}^{\text{EV+}} \leq s_{vt}^{\text{charge}} \cdot \bar{S} \cdot \cos\phi \qquad \forall t \text{ and } v, \tag{3.8a}$$

$$q_{vt}^{\text{EV+}} = p_{vt}^{\text{EV+}} \cdot \tan\phi \qquad \forall t \text{ and } v. \tag{3.8b}$$

3.2.4 EVs' state-of-charge (SOC) model

The evolution of the vehicles' SOC depends on the charging power $p_{vt}^{\text{EV+}}$, given by (3.7a), and the discharging power $p_{vt}^{\text{EV-}}$, which is an input of the problem. The SOC of vehicle v at time t is modeled

as:

$$\mathrm{SOC}_v(t) = \mathrm{SOC}_v(0) + \frac{T_s}{E_v} \sum_{\tau=0}^{t-1} \left(\eta \cdot p_{v\tau}^{\mathrm{EV}+} - p_{v\tau}^{\mathrm{EV}-} \right), \tag{3.9}$$

where $\mathrm{SOC}_v(0)$ is the initial SOC (a problem decision variable, as it is discussed later), T_s the sampling time in hours, E_v the nominal energy capacity of the EV's battery (in kWh), and η is the charging efficiency. It is worth highlighting that since the discharging power is assumed estimated directly from the vehicles' SOCs, it is not weighted by the efficiency in (3.9).

Model (3.9) is linear in the charging power. This model, commonly adopted in the literature (e.g. [5]), assumes constant battery's voltage and efficiency. These assumptions, which trade-off accuracy for increased model tractability, can be considered acceptable in a planning problem with sparse temporal resolution (e.g., 1 hour). The vehicles' SOCs should be within a feasible range, denoted by $(\underline{\mathrm{SOC}}, \overline{\mathrm{SOC}})$. This constraint reads as:

$$\underline{\mathrm{SOC}} \leq \mathrm{SOC}_v(t) \leq \overline{\mathrm{SOC}}. \tag{3.10}$$

Extension to V2G

To model V2G support from the EVs with bidirectional chargers, the SOC model in (3.9) needs to account for the discharging power too. The updated model reads as:

$$\mathrm{SOC}_v(t) = \mathrm{SOC}_v(0) + \frac{T_s}{E_v} \sum_{\tau=0}^{t-1} \left(\eta p_{v\tau}^{\mathrm{EV}+} - p_{v\tau}^{\mathrm{EV}-} - \frac{1}{\eta} p_{v\tau}^{\mathrm{V2G}} \right) \quad \forall v \tag{3.11}$$

In 3.11, for slow chargers only V2G power can be expressed as:

$$p_{vt}^{\mathrm{V2G}} = s_{vt}^{\mathrm{discharge}} \cdot \bar{S} \cdot \cos\phi_S. \tag{3.12}$$

3.2.5 Identifying the need for charging infrastructure

This section describes how we can identify the number of chargers and their locations in a distribution grid based on the modeling information introduced above. Based on the number of chargers, the capital investment of the charging infrastructure can be computed. In this Thesis, modeling of both single-port chargers (SPCs) and multi-port chargers (MPCs) have been considered in the planning context to evaluate the techno-economic benefits of each other, or a combination of both. The distinction between these two charger typologies is that SPCs have a plug for each charging column, whereas MPCs have a centralized AC/DC power conversion stage and multiple ports to enable the connection of multiple EVs.

Modeling the single-port chargers

Single-port chargers feature an equal number of plugs and chargers (see Fig. 3.2). The following explanation refers to fast chargers; for slow chargers, the principles are identical and not repeated.

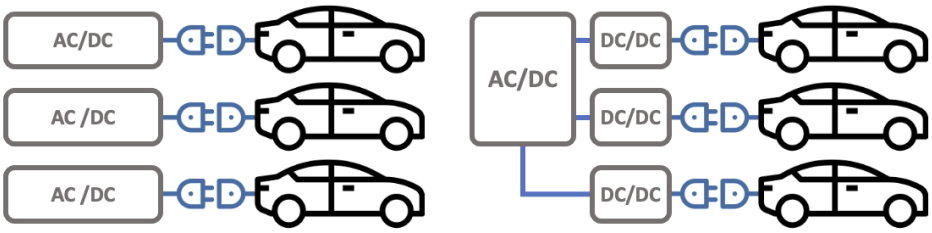

Figure 3.2: Single-port chargers (SPCs) on the left, and multi-port chargers (MPCs) on the right.

The modeling principle used to determine the number of chargers to install involves evaluating the maximum number of EVs connected to a charger at a given grid node and time interval (this information is given by the variables f_{vt}^{plugged} and s_{vt}^{plugged} explained in section 3.2.2). For instance, if at node 2, a maximum of 10 vehicles are simultaneously plugged into a charger throughout the planning horizon, then 10 chargers will be required to meet the demand at this node. This modeling principle is now formalized.

The number of fast chargers in use at a specific grid node can be evaluated by coupling the information in f_{vt}^{plugged} (telling whether an EV is plugged into a charger) and p_{nvt} (the EV parking location). More specifically, the number of fast chargers in use at time interval t at node n is the sum over all vehicles of the product between p_{nvt} and f_{vt}^{plugged}. The maximum value over time of this expression is the required number of fast chargers to be installed at node n, denoted by F_n^{chargers}. Formally, it is:

$$F_n^{\text{chargers}} = \max_t \left\{ \sum_{v=1}^{V} p_{nvt} \cdot f_{vt}^{\text{plugged}} \right\}, \qquad n = 1, \ldots, N. \tag{3.13a}$$

Because SPC chargers have one plug per charger by design, the number of available plugs must match the number of chargers. Say F_n^{plugs} is the number of plugs, then the following equality constraint must hold:

$$F_n^{\text{plugs}} = F_n^{\text{chargers}}. \tag{3.13b}$$

For slow chargers, similar expressions hold:

$$S_n^{\text{chargers}} = \max_t \left\{ \sum_{v=1}^{V} p_{nvt} \cdot s_{vt}^{\text{plugged}} \right\}, \qquad n = 1, \ldots, N \tag{3.13c}$$

$$S_n^{\text{plugs}} = S_n^{\text{chargers}}. \tag{3.13d}$$

where S_n^{chargers} and S_n^{plugs} are the number of chargers and of plugs, respectively.

Modeling the multi-port chargers

Differently than a SPC, a single MPC can have multiple plugs. The numbers of plugs and chargers now follow from different models, as explained hereafter.

The number of fast chargers is calculated considering the variables f_{vt}^{charge}, which tell, for a given time t, how many vehicles are recharging at the same time, so providing information on the rated power required to meet the realized recharging demand. Following the same principle discussed above for SPCs, coupling this information with p_{nvt} enables to locate this power demand in the grid. Formally, the number of fast and slow MPCs is:

$$F_n^{\text{chargers}} = \max_t \left\{ \sum_{v=1}^{V} p_{nvt} \cdot f_{vt}^{\text{charge}} \right\}, \qquad n = 1, \dots, N \tag{3.14a}$$

$$S_n^{\text{chargers}} = \max_t \left\{ \sum_{v=1}^{V} p_{nvt} \cdot s_{vt}^{\text{charge}} \right\}, \qquad n = 1, \dots, N. \tag{3.14b}$$

The number of plugs for, e.g., fast chargers is instead calculated considering the variables f_{vt}^{plugged}, which provide the information of how many vehicles are connected to a charger at the same time. Formally, the numbers of plugs for fast and slow chargers are:

$$F_n^{\text{plugs}} = \max_t \left\{ \sum_{v=1}^{V} p_{nvt} \cdot f_{vt}^{\text{plugged}} \right\}, \qquad n = 1, \dots, N \tag{3.14c}$$

$$S_n^{\text{plugs}} = \max_t \left\{ \sum_{v=1}^{V} p_{nvt} \cdot s_{vt}^{\text{plugged}} \right\}, \qquad n = 1, \dots, N. \tag{3.14d}$$

It is worth to highlight that the planning problem for MPCs is a generalization of the one of SPCs. This is because, if the solution of the MPCs' problem is such that $f_{vt}^{\text{charge}} = f_{vt}^{\text{plugged}}$ and $s_{vt}^{\text{charge}} = s_{vt}^{\text{plugged}}$ for all v and t, then formulations in (3.14) and (3.13) are the same and the two problems would have the same solution.

Investment costs for the charging infrastructures

Based on the required numbers of plugs and chargers, we can estimate the capital cost of the EV charging infrastructure. The total investment cost is denoted by $J(\cdot)$, where notation $(\cdot)$ refers to the dependency of J on the problem decision variables f_{vt}^{plugged}, s_{vt}^{plugged}, f_{vt}^{charge}, and s_{vt}^{charge}, which is not explicitly reported for compactness. It reads as:

$$J(\cdot) = J_{plugs}^{F} + J_{chargers}^{F} + J_{plugs}^{S} + J_{chargers}^{S} \tag{3.15a}$$

where J^F_{plugs}, $J^F_{chargers}$ are the cost of fast-charging plugs and stations, and J^S_{plugs} and $J^S_{chargers}$ are the cost of slow-charging plugs and stations. The components of (3.15a) are as follows:

$$J^F_{plugs} = \sum_{n=1}^{N} F_n^{\text{plugs}} \cdot \text{cost}^F_{plugs} \tag{3.15b}$$

$$J^S_{plugs} = \sum_{n=1}^{N} S_n^{\text{plugs}} \cdot \text{cost}^S_{plugs} \tag{3.15c}$$

$$J^F_{chargers} = \sum_{n=1}^{N} F_n^{\text{chargers}} \cdot \text{cost}^F_{chargers} \tag{3.15d}$$

$$J^S_{chargers} = \sum_{n=1}^{N} S_n^{\text{chargers}} \cdot \text{cost}^S_{chargers} \tag{3.15e}$$

where $\text{cost}^F_{plugs}, \text{cost}^F_{chargers}, \text{cost}^S_{plugs}, \text{cost}^S_{chargers}$ are the unitary cost of plugs and chargers for fast and slow charging.

3.2.6 Nodal injections due to EVs charging demand and grid model

The nodal injections of EVs, $P^{(\text{EV nodal})}_{tn}, Q^{(\text{EV nodal})}_{tn}$ connected to node n in (1.4), can be computed by coupling the information on the charging power of the individual EVs ($p^{\text{EV}+}_{vt}$ and $q^{\text{EV}+}_{vt}$) in (3.7), with their parking location, p_{nvt}. Formally, they read as:

$$P^{(\text{EV nodal})}_{tn} = \sum_{v=1}^{V} p_{nvt} \cdot p^{\text{EV}+}_{vt} \qquad \forall t \text{ and } n \tag{3.16a}$$

$$Q^{(\text{EV nodal})}_{tn} = \sum_{v=1}^{V} p_{nvt} \cdot q^{\text{EV}+}_{vt} \qquad \forall t \text{ and } n. \tag{3.16b}$$

If the local PV generation is taken into account at any node, the active power injection in Eq (1.4a) can be expressed as follows:

$$P^{\text{node}}_{tn} = P^{\text{demand}}_{tn} - P^{\text{PV}}_{tn} + P^{(\text{EV nodal})}_{tn}, \tag{3.17}$$

where P^{PV}_{tn} represents the PV generation (taken with a negative sign because it is generation). PV plants are assumed to operate at a unit power factor, so the reactive power contribution of PV plants is not required to appear in Equation (1.4b).

Since the grid voltage is constrained within a narrow band, we make the approximation that nodal power injections are independent of voltage. The dependency between grid quantities (nodal voltage magnitudes v_{tn}, line current magnitudes i_{tl}, and apparent power flow at the substation transformer S_{t0}) and the nodal injections is discussed in Section 1.4.3. When planning the charging infrastructures in a distribution grid, it is crucial to ensure that the operational grid quantities remain within

prescribed limits. Therefore, the following operational grid constraints can be considered:

$$\underline{v} \leq v_{tn} \leq \overline{v} \qquad \forall t \text{ and } n \tag{3.18a}$$

$$|i_{tl}| \leq \bar{i}_l \qquad \forall t \text{ and } l \tag{3.18b}$$

$$S_{t0} \leq \overline{S}_0 \qquad \forall t. \tag{3.18c}$$

where, $\underline{v}, \overline{v}$ respectively define lower and upper limits nodal voltage magnitudes; upper limits of lines' ampacity $\bar{i}_l$; rating of power flow at the substation transformer $\overline{S}_0$.

In addition to these constraints, to solve the optimal planning problem we need to consider that the nodal injections remain below the apparent power limit of the node, S_n (i.e., the rated power of the MV/LV transformer):

$$\left(P_{tn}^{\text{node}}\right)^2 + \left(Q_{tn}^{\text{node}}\right)^2 \leq (S_n)^2. \tag{3.18d}$$

The constraint (3.18d) is useful in the case of apparatus with apparent power limitations connected at the nodes, such as nodes hosting substation step-down transformers. Later in 3.2.8 it is explained how this constraint can be approximated to solve the optimal planning problem.

Extension to V2G

To model V2G support from the EVs with bidirectional chargers, the nodal injections model (1.4a) can be modified to include the contribution of V2G. This reads as:

$$P_{tn}^{\text{node}} = \sum_{v \in \mathcal{V}} p_{nvt} \cdot \left(p_{vt}^{\text{EV+}} - p_{vt}^{\text{V2G}}\right) + P_{tn}^{\text{net}}. \tag{3.19}$$

3.2.7 The optimal planning problem

Planning without PV self-consumption

In this section we propose the methodology of planning the EV recharging infrastructure without consideration of local PV generation. The problem here consists of the following binary variables:

$$\boldsymbol{x} = [f_{11}^{\text{charge}}, \ldots, f_{VT}^{\text{charge}}, f_{11}^{\text{plugged}}, \ldots, f_{VT}^{\text{plugged}}] \tag{3.20}$$

$$\boldsymbol{y} = [s_{11}^{\text{charge}}, \ldots, s_{VT}^{\text{charge}}\, s_{11}^{\text{plugged}}, \ldots, s_{VT}^{\text{plugged}}] \tag{3.21}$$

that minimize the capital investment for the EV charging infrastructure while respecting the grid constraints.

To ensure that the problem solution does not depend on the initial SOC values in (3.9), we choose to designate them as problem variables, denoted by:

$$\boldsymbol{z} = [\text{SOC}_1(0), \ldots, \text{SOC}_V(0)] \in \mathbb{R}^V. \tag{3.22}$$

Besides, the final SOC should be larger than or equal to the initial one to avoid benefiting from the initial energy stock:

$$\text{SOC}_v(T) \geq \text{SOC}_v(0), \qquad \text{for all } v. \tag{3.23}$$

In this way, the planning problem accounts for the charging demand of the vehicles, regardless of their specific initial conditions. The planning problem is formulated as a constrained economic optimization. Its formulation reads as:

$$\min_{\boldsymbol{x},\boldsymbol{y}\in\{0,1\}^{V\times T},\boldsymbol{z}\in\mathbb{R}^{V}} \{J(\cdot)\} \tag{3.24a}$$

subject to the following constraints:

Plugged-in only if parked constraints (3.3)	$\forall t$ and v	(3.24b)
Charge only if plugged-in constraints (3.4)	$\forall t$ and v	(3.24c)
EV charging power (3.7)	$\forall t$ and v	(3.24d)
SOC model and constraints (3.9), (3.10), (3.23)	$\forall t$ and v	(3.24e)
Nodal injection models (3.16) and (1.4)	$\forall t$ and n	(3.24f)
Linear grid models (1.5) and constraints (3.18)		(3.24g)
Chargers and plugs number model:		
(3.13) for SPCs, or (3.14) for MPCs		(3.24h)

Planning with PV self-consumption

In this section, we propose a methodology for jointly planning the EV recharging infrastructure while maximizing the PV self-consumption of EVs. One potential solution to reduce grid congestion and improve the carbon footprint of the recharging process is to utilize electricity generated from local Photovoltaic (PV) sources to recharge EVs. This approach, known as PV self-consumption, has been extensively discussed in the literature as a means to integrate more PV electricity into distribution grids [35, 36].

PV self-consumption of EVs at the power grid nodes can be promoted by incentivizing EVs to consume more power during time intervals when there is local PV production and vice-versa. This is modeled by minimizing the following objective function:

$$J^{\mathrm{PV}} = \sum_{n=1}^{N}\sum_{t=1}^{T} \frac{1}{P_{tn}^{\mathrm{PV}} + \epsilon} P_{tn}^{(\text{EV nodal})}, \tag{3.25}$$

where, t is the index of the time interval with total number of intervals T and n is the index of the distribution grid nodes with total N nodes. P_{tn}^{PV} represents the PV generation at node n at time t, which is an input of the optimization problem. The coefficient ϵ is a small quantity and it is added to avoid dividing EV nodal injections ($P_{tn}^{(\text{EV nodal})}$) by zero when there is no PV generation at time t. In case of planning with PV self-consumption we extend the cost function in (3.15a) as below:

$$J^{\mathrm{total}} = J(\cdot) + k \cdot J^{\mathrm{PV}} \tag{3.26}$$

where, k is an input coefficient. The value of k determines how one wants to weight one or the other term. Thus, with the new cost (3.26) charging infrastructure planning is performed by jointly minimizing the total investment (J^{total}) while maximizing the PV self-consumption subject to several constraints.

The problem formulation consists of minimizing the cost function in (3.15a) over the decision variables $\boldsymbol{y}$ and $\boldsymbol{z}$:

$$\min_{\boldsymbol{y}\in\{0,1\}^{V\times T},\boldsymbol{z}\in\mathbb{R}^{V}} \left\{J(\cdot) + k \cdot J^{\text{PV}}\right\} \tag{3.27a}$$

subject to the following constraints:

Plugged-in only if parked constraints (3.3)	$\forall t$ and v	(3.27b)
Charge only if plugged-in constraints (3.4)	$\forall t$ and v	(3.27c)
EV charging power (3.7)	$\forall t$ and v	(3.27d)
SOC model and constraints (3.9), (3.10), (3.23)	$\forall t$ and v	(3.27e)
Nodal injection models (3.16), (3.17), (1.4b)	$\forall t$ and n	(3.27f)
Linear grid models (1.5) and constraints (3.18)		(3.27g)
Chargers and plugs number model:		
(3.13) for SPCs, or (3.14) for MPCs.		(3.27h)

In this thesis, the optimization problem (3.27) with PV self-consumption is specifically solved for single-port slow chargers. Therefore, the constraint for the number of chargers and plugs (3.27h) needs to be updated with (3.13c). The decision to intentionally deactivate the deployment of fast chargers is based on the optimization results, as discussed in the next section (3.5.1), while solving 3.24. Since the fast chargers were never activated or required, this consideration is reasonable. It should also be noted that deactivating the number of fast chargers effectively reduces the number of binary variables in 3.27.

Joint minimization of investment and operational costs with time-of-use electricity tariffs

To jointly minimize the investment and operational costs considering a time-of-use electricity tariff, the optimization problem (3.24) can be updated by incorporating the following cost function:

$$J^{\text{total}} = J(\cdot) + \alpha \cdot \sum_{n=1}^{N}\sum_{t=1}^{T} P_{nt}^{\text{EV}} \cdot c_t \tag{3.28}$$

where c_t is a time-of-use electricity tariff at time t (assumed the same across the all grid) and the coefficient α. The discount rate is here neglected because it is not of primary interest in the results comparison. The coefficient:

$$\alpha = \frac{\text{Service-life of chargers}}{\text{Optimization horizon}} \tag{3.29}$$

is a scale factor to make the two costs comparable in the considered optimization horizon.

3.2.8 Problem properties and approximations

Problems (3.24) and (3.27) are nonlinear due to the set maximum in (3.13)-(3.14), the point-wise maximum in (3.32d) (a new constraint, explained in the next section), and the quadratic expression in (3.18d). Suitable reformulations or approximations of these constraints are now discussed to render the problem linear. The set maximum, here denoted by $\bar{v} = \max\{v_t, t = 1, \ldots, T\}$ for convenience, is replaced by T linear inequalities $\bar{v} \geq v_t$ for all t. As the problem (3.24) entails *minimizing* expressions of the same kind as $\bar{v}$, this reformulation holds as exact. The point-wise maximum, $a^+ = \max(a, 0)$, is replaced by 2 inequalities, $a^+ \geq a$ and $a^+ \geq 0$ and can be used to replace convex constraints in the form of $\max(a, 0) \leq \bar{a}$ with linear ones [79].

Finally, the apparent power constraint in (3.18d), now denoted by $P^2 + Q^2 \leq S^2$ for simplicity, is approximated by replacing the reactive power with an upper bound $\overline{Q} = S \cdot \overline{\sin}\phi$; since $Q \leq \overline{Q}$, it follows that:

$$P^2 + Q^2 \leq P^2 + \overline{Q}^2 \leq S^2 \tag{3.30a}$$

$$P^2 \leq S^2 - \overline{Q}^2 = S^2 - S^2 \cdot \overline{\sin}^2\phi = S^2 \underline{\cos}^2\phi \tag{3.30b}$$

$$P \geq -S \cdot \underline{\cos}\phi \quad \text{and} \quad P \leq S \cdot \underline{\cos}\phi. \tag{3.30c}$$

In summary, while solving the problems in (3.24) and (3.27), the original quadratic constraint is replaced by two linear inequalities as in (3.30c), with $\underline{\cos}\phi$ as a lower-bound estimate of the load power factor of the nodal injection at node n. We thus have the following linear expression[3]:

$$-\bar{S}_n \cdot \underline{\cos}\phi_n \leq P_{tn}^{\text{node}} \leq \bar{S}_n \cdot \underline{\cos}\phi_n. \tag{3.31}$$

With this equivalent formulations and approximation, it is possible to write the optimization problem as a mixed integer linear program (MILP) that introduces better computational performance than the original one.

3.3 Modeling EV connection and disconnection preferences of EV owners

As stated, the variables f_{vt}^{plugged} and s_{vt}^{plugged} (indicating whether an EV is plugged into a charger) can only be active when an EV is parked. However, there is more. Because plugging an EV into a charging column is an operation performed by the EV owner (or driver), their availability to plug and unplug an EV should also be modeled. For example, a person driving home in the evening and using a public charging column might prefer to plug their EV at the arrival rather than queuing for a charger to become available. To model this preference, we introduce additional constraints on f_{vt}^{plugged} and s_{vt}^{plugged} to capture two scenarios of EV owners' flexibility for plugging and unplugging their EVs. To explain these constraints, we refer to the case study analyzed in this thesis, which is a home-work commute where EVs are used in the morning, parked in the central part of the day, used again in the afternoon, and finally parked overnight (as encoded in the input parameters p_{nvt}). The constraints to model EV owners' flexibility are discussed in the rest of this section.

[3] Piecewise linearization could also be considered in this context.[126]

3.3.1 Modeling connection to and disconnection from chargers

Before describing the EV owners' flexibility scenarios, the models of connection-to-a-charger and disconnection-from-a-charger events are explained. For fast chargers, let binary variables c^f_{vt}, d^f_{vt} denote the events when EV v is connected to and disconnected from a charger, respectively, and similarly for slow chargers, with variables c^s_{vt} and d^s_{vt}. In these variables, the logical state "1" denotes a connection or a disconnection event, and 0 no event. Connections and disconnections are modeled by detecting rising and falling edges of f^{plugged}_{vt} and s^{plugged}_{vt} (Fig. 3.3). Formally, this is as (with max as the point-wise maximum):

$$c^f_{vt} = \max\left(f^{\text{plugged}}_{vt} - f^{\text{plugged}}_{v(t-1)}, 0\right) \qquad \forall t \text{ and } v \qquad (3.32a)$$

$$d^f_{vt} = \max\left(f^{\text{plugged}}_{v(t-1)} - f^{\text{plugged}}_{vt}, 0\right) \qquad \forall t \text{ and } v \qquad (3.32b)$$

$$c^s_{vt} = \max\left(s^{\text{plugged}}_{vt} - s^{\text{plugged}}_{v(t-1)}, 0\right) \qquad \forall t \text{ and } v \qquad (3.32c)$$

$$d^s_{vt} = \max\left(s^{\text{plugged}}_{v(t-1)} - s^{\text{plugged}}_{vt}, 0\right) \qquad \forall t \text{ and } v. \qquad (3.32d)$$

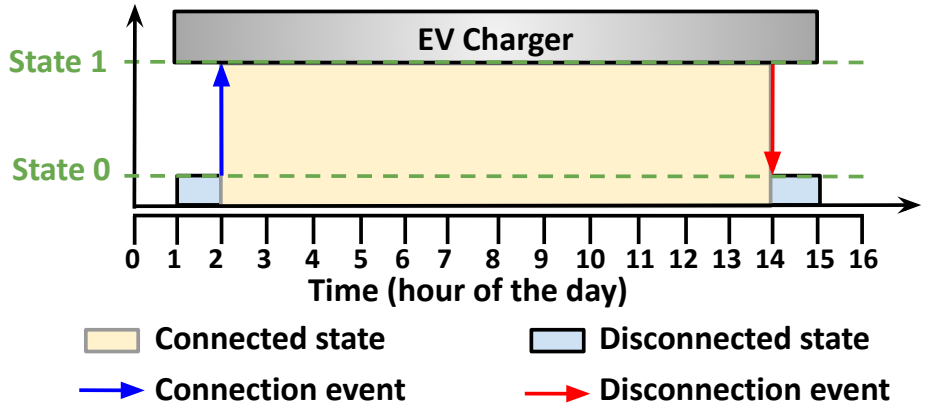

Figure 3.3: Example of the connection-state variable (f^{plugged}_{vt} or s^{plugged}_{vt}) and connection and disconnection events (blue and red arrows), corresponding to the raising and falling edges of the plugging state, respectively.

3.3.2 EV owners' (drivers) flexibility scenarios

Let the time interval $(\tau^{(1)}_v, \tau^{(2)}_v)$ denote the overnight parking stay, and $(\tau^{(3)}_v, \tau^{(4)}_v)$ the parking stay during the central hours of the day for vehicle v. The two EV owners' flexibility scenarios are as follows.

Scenario A (forgetful EV owners): *In both parking intervals, drivers plug their EVs to a charger only at the arrival time, and unplug them only at the departure time.* In other words, drivers let their vehicles plugged into a charger whenever their EVs is parked. Formally, this is implemented by enforcing no connection outside the initial parking time interval (for both fast and slow chargers)

$$c_{vt}^{f} \leq 0 \qquad \text{for all } t \text{ except } t = \tau_v^{(1)} \text{ and } t = \tau_v^{(3)} \tag{3.33a}$$
$$c_{vt}^{s} \leq 0 \qquad \text{for all } t \text{ except } t = \tau_v^{(1)} \text{ and } t = \tau_v^{(3)}, \tag{3.33b}$$

and no disconnection outside the final parking time interval

$$d_{vt}^{f} \leq 0 \qquad \text{for all } t \text{ except } t = \tau_v^{(2)} \text{ and } t = \tau_v^{(4)} \tag{3.33c}$$
$$d_{vt}^{s} \leq 0 \qquad \text{for all } t \text{ except } t = \tau_v^{(2)} \text{ and } t = \tau_v^{(4)}. \tag{3.33d}$$

Scenario B (cooperative EV owners): *For overnight parking, drivers plug their EVs to a charger only at the arrival time; when parking in the central part of the day, drivers allow one disconnection.* In the central part of the day, drivers allow one disconnection to give to others the possibility of using that charging spot. This is implemented by enforcing no connection outside the initial parking time for the overnight time interval

$$c_{vt}^{f} \leq 0 \qquad \text{for all } t \text{ except } t = \tau_v^{(1)} \tag{3.34a}$$
$$c_{vt}^{s} \leq 0 \qquad \text{for all } t \text{ except } t = \tau_v^{(1)}, \tag{3.34b}$$

and up to one disconnection in the central parking hours

$$\sum_{t=\tau_3}^{\tau_4} d_{vt}^{f} \leq 1, \tag{3.34c}$$
$$\sum_{t=\tau_3}^{\tau_4} d_{vt}^{s} \leq 1. \tag{3.34d}$$

3.3.3 Implementing flexibility scenarios

Scenarios are implemented by adding either (3.33) or (3.34) to the optimization problems (3.24) and (3.27). A comparative analysis of these 2 scenarios is performed in the results section to evaluate the impact of EV owners' flexibility on the problem solution and charging infrastructure.

3.4 Case study

This section presents the case study adopted to exemplify the operations of the proposed optimal planning method. The case study presented here is reasonably guessed to reproduce a real possible scenario. The input information used for the case study can be modified or tuned according to the specific situation to model, on the basis of, for example, information from the distribution grid operator and urban planner.

3.4.1 The distribution grid

The European version of the 14-bus CIGRE benchmark grid [6] for medium voltage (MV) systems has been considered herein for the case study. The description and topology of the grid is the same as presented in section 2.4.1. The sensitivity coefficients for the linearized grid model are computed once for the nominal demand profiles, similarly, as done in the Chapter 2, one could compute successive linearizations to improve the linear estimates.

To solve the planning problem, a home-work commute of EV owners has been considered, where the parking and charging locations of EVs correspond to different nodes of the 14-bus MV grid. As mentioned before, EVs are utilized by their owners in the morning and remain parked during the central hours of the day. In the afternoon, they are used again and parked overnight at the origin node. In Fig. 3.4, the residential nodes are indicated as the purple nodes, where EVs are parked overnight i.e. "Cluster 1", whereas the destination nodes are the green nodes i.e. "Cluster 2" (see Table 3.1).

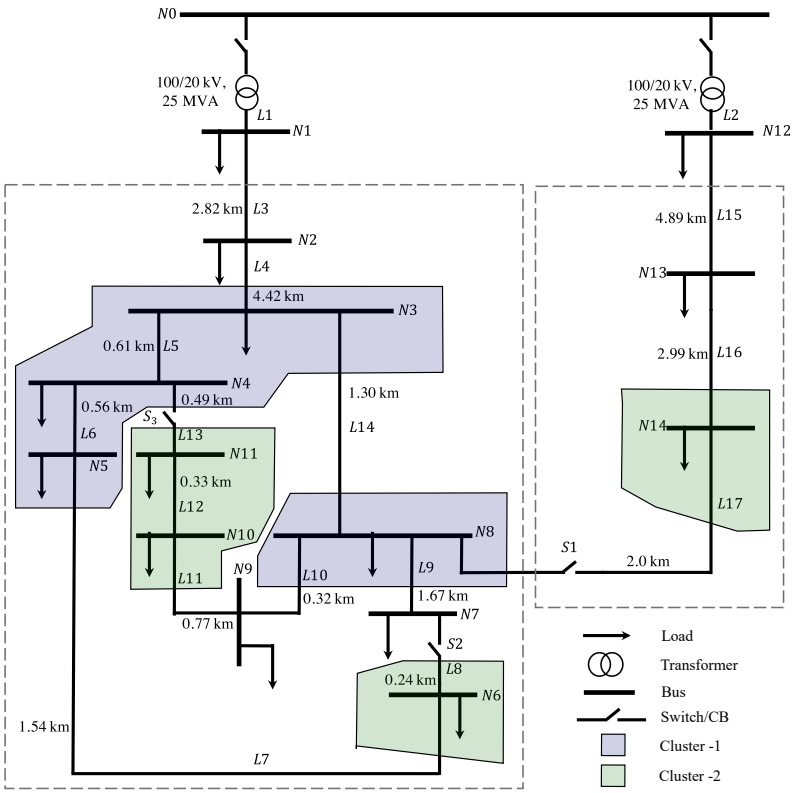

Figure 3.4: Topology of the CIGRE European MV distribution network benchmark for residential system with two Clusters [6, 7].

Demand and PV generation

The nodal demand, P_{nt}^{demand} and Q_{nt}^{demand} in (1.4), is simulated considering the 1-day long load coincidence factor described in [6], rescaled for the kVA nominal power of the nodes and then split

into the active and reactive components with the nominal power factor of the nodes. Table 3.1 reports the PV generation capacity installed at the various nodes of the grid. A total of 400 kWp of PV generation is installed in the network and connected to nodes 6, 10, and 11, corresponding to nodes where EVs are parked during the daytime. PV generation is simulated with first-principles models starting from irradiance time series as described in [127], considering clear-sky conditions and PV panels with tilt and azimuth optimized to guarantee the largest yield over the year.

Table 3.1: Nodal nominal demand and power factors

Node	Apparent Power [kVA]	Power factor	Cluster	PV Gen [kW]
3	285	0.97	1	0
4	445	0.97	1	0
5	750	0.97	1	0
6	565	0.97	2	150
8	605	0.97	1	0
10	490	0.97	2	200
11	340	0.97	2	50
14	215	0.97	2	0

Nodal electricity tariff

The time-of-use retail electricity tariff is approximated with the day-ahead electricity prices obtained from [128] and shown in Fig. 3.5 for 24 hours. This 1-day-long profile is replicated 5 times to obtain the profile of the 5-day-long optimization horizon adopted in the optimization.

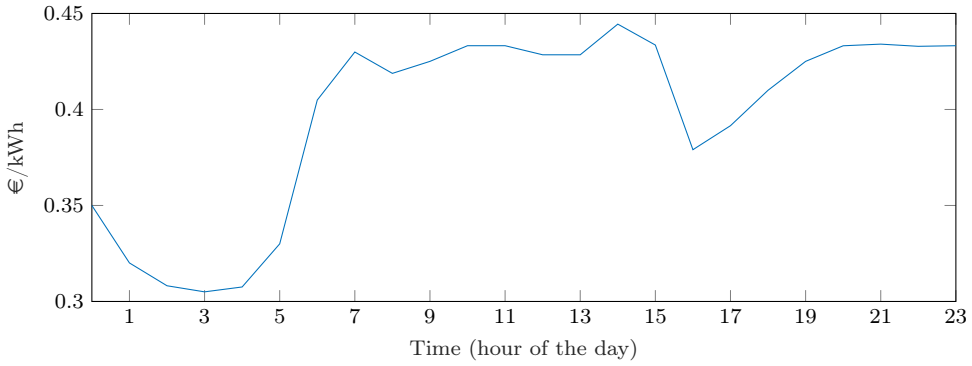

Figure 3.5: Cost of the electricity in the month of July in France.

3.4.2 Number of EVs and driving demand

Total 878 EVs have been considered herein[4]. The number of EVs parked during the night and central hours are shown in Fig. 3.6a and 3.6b, respectively. The EVs' morning departures and arrivals are sampled from uniform distributions with values between hours 5-8 and 8-11, respectively; evening departures and arrivals are sampled from uniform distributions with values between hours 14-18 and 17-21. Based on this information, variables p_{nvt} (input for the problem) are built. The origin and destination nodes of the EVs are assigned randomly and uniformly to all nodes hosting EVs. To generate p_{nvt} other methods can be used, including using real data.

The duration of the daytime parking intervals of the EVs could impact the results of the planning problem and PV self-consumption. In particular, longer daytime parking hours would allow charging more EVs in the central part of the day, coinciding with PV generation. In order to evaluate the sensitivity of the results to the duration of the daytime parking intervals, two scenarios are considered:

- **Base case parking stay**: EVs are parked between 8 AM and 4 PM.
- **Extended parking stay**: EVs are parked between 5 AM and 8 PM.

The total energy demand for driving is estimated using data from [119]. The discharging power $p_{vt}^{\text{EV-}}$, necessary to model the SOC evolution in (3.9), is a positive constant quantity when a vehicle drives, and zero when the vehicle is parked. The discharging power is such that its total energy demand amounts to the quantity estimated above.

To illustrate the impact on the planning results, two different values for the EV battery's energy capacity are considered: 16 kWh and 60 kWh, under the same driving demand. The EVs' charging efficiency, η, is 0.95.

3.4.3 Chargers ratings and prices

We consider fast and slow chargers with kVA ratings of 20 kVA and 2.4 kVA, respectively, and power factors of 0.9. Their costs is 20'000€ and 1'500€, inspired from the existing technical literature [129–131] (although some price volatility might exist due to different regions, operators, and need for labor). The price of the charging plugs is assumed to be 15% of the price of a single-port charger.

3.4.4 Optimization horizon for the case study

The planning horizon refers to how many temporal samples are considered in the optimization problem, indicated by the parameter T. As the number of variables of the optimization problem increases linearly with T, and the complexity of the NP-hard MILP problem increases exponentially with the number of variables, it is necessary to limit the value of T to retain tractability of the problem. In

[4]This number is estimated by dividing the nominal nodal power by the single-phase household contractual power 6 kVA assuming nearly 1.4 EVs per household (see Chapter 2)

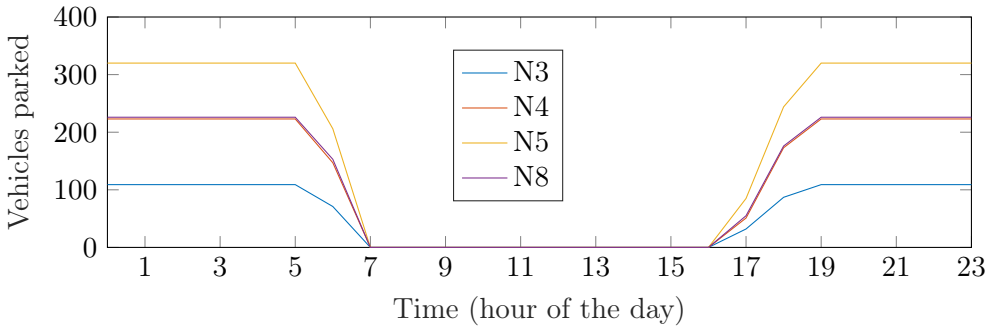

(a) Cluster 1

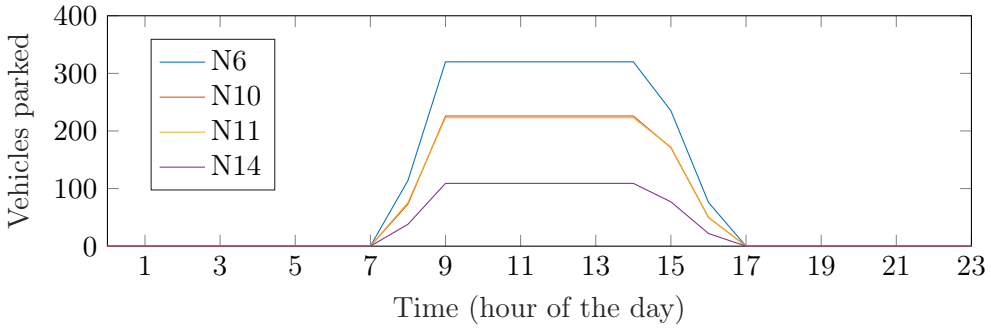

(b) Cluster 2

Figure 3.6: Number of EVs' parked at different grid nodes under two clusters during the day and night hours.

this thesis, T is set to 24 samples (i.e., 1 day with samples each hour) for the 16 kWh battery and to 120 (i.e., 5 days) for the 60 kWh battery, assuming that this interval represents a worst-case scenario of the driving demand or a pattern that regularly occurs throughout the charging infrastructure's service life. Future work will consider scenario reduction or decomposition methods to attain a tractable formulation of the optimization problem that decomposes the temporal dimension of the problem. A similar scalability issue will be encountered when extending to distribution grids with a more significant number of nodes, as this will require increasing the number of EVs involved in the problem. This aspect will be investigated in future works. The longer optimization horizon for larger batteries is because EVs with larger energy capacity can make multiple trips on a single charge and may not require daily charging, which can stagger the charging process and help avoid grid overloading. The 1-day demand profiles are replicated five times to obtain the input time series for the 5-day planning period.

3.5 Results and discussion

The results presented herein are first for the small-battery EVs, and next, the analysis is extended to the EVs with larger battery packs. The MILP problem was implemented in MATLAB and solved using Gurobi.

3.5.1 Planning without PV self-consumption

Results reported in this section do not consider PV productions at the grid nodes: 6, 10 and 11. For both 1 day and 5 days optimization horizons results are summarized below. First, the results are presented for the small-battery (16 kWh) EVs to illustrate some of the formulation's properties. The analysis is further extended to the EVs with larger batteries (60 kWh).

Results for one day horizon

The optimization problem with 1 day horizon for the small-battery (16 kWh) EVs was solved in about 90 minutes on an Intel i7 machine with a duality gap setting of 10%.

Fig. 3.7 is presented to illustrate the meaning of the variables s_{vt}^{plugged} and s_{vt}^{charge} for ten sample EVs in Scenario A and MPCs. The figure demonstrates that: (i) vehicles are mostly connected to the chargers, aligning with the definition of Scenario A where EVs are connected whenever parked, and (ii) the planning algorithm optimizes the charging of plugged EVs. This optimization ensures compliance with grid constraints, maintains the EVs' correct state of charge (SOC) throughout the day, and minimizes investment costs according to the problem's cost function. Therefore, we can infer that arbitraging the charge is beneficial to reducing the number of chargers, as explained hereafter.

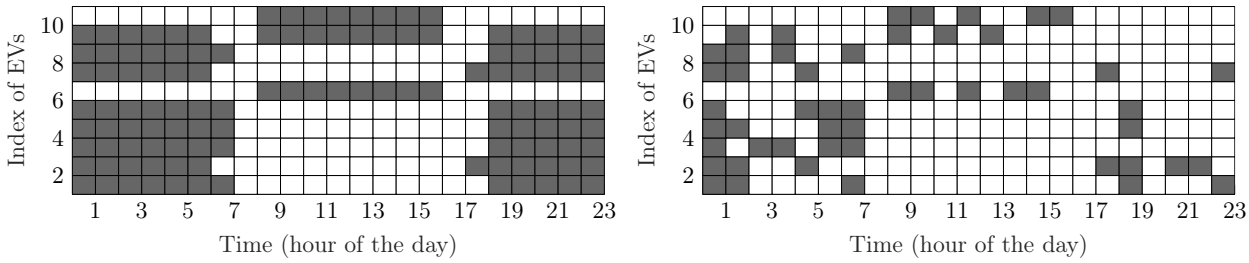

Figure 3.7: Variables s_{vt}^{plugged} (a) and s_{vt}^{charge} (b), showing the connection and charging state, respectively, for 10 sample EVs. Grey filling is 1, white filling is 0.

The number of required chargers and plugs for SPCs, MPCs, and the two driver's flexibility scenarios A and B are reported in Table 3.2 for 1 day horizon. For SPCs, the number of plugs is not indicated as it is the same as the number of chargers. Findings are as follows:

Finding 1. Fast chargers are not required; (cheaper) slow chargers are enough to satisfy the charging demand of EVs.

Finding 2. Moving from forgetful (Scenario A) to cooperative EV owners (Scenario B) attains smaller numbers of chargers and plugs for both SPCs and MPCs. This is because increasing the availability of the EV owners to plug/unplug their EVs leads to better utilization of the charging infrastructure, ultimately requiring fewer chargers to satisfy the same charging demand.

Finding 3. Implementing MPCs requires less chargers (and more plugs) than SPCs; because the MPCs problem is a generalization of the SPCs' and the problem aims at finding the economic

Table 3.2: Number of slow chargers and plugs (878 EVs, 16 kWh battery).

Node	Forgetful (Scenario A)			Cooperative (Scenario B)		
	MPCs		SPCs	MPCs		SPCs
	Chargers	Plugs	Chargers	Chargers	Plugs	Chargers
3	35	109	96	34	104	18
4	70	195	200	50	166	90
5	127	302	270	87	244	144
6	35	78	50	62	78	176
8	84	203	225	75	193	101
10	24	41	1	32	38	125
11	25	53	23	42	47	67
14	2	6	13	8	10	46
Cluster1	316	809	791	246	707	353
Cluster2	86	178	87	144	173	414
Total	402	987	878	390	880	767

minimum, we can infer that MPCs are conducive to lower infrastructure costs. Fig. 3.8 summarizes the cost achieved by the various cases for EVs with battery capacity 16kWh charging at different grid nodes during 1 day optimization horizon. It is observed that MPCs achieve higher cost savings than flexible drivers. Thus choosing MPCs over SPCs attains a cost reduction of 45% and 40% in Scenario A and B; whereas implementing flexible drivers (Scenario B) achieve a cost reduction of 13% and 5% for SPCs and MPCs, respectively. This implies that the technological solution (MPCs over SPCs) is able to achieve a better cost reduction than a change of consumer behavior.

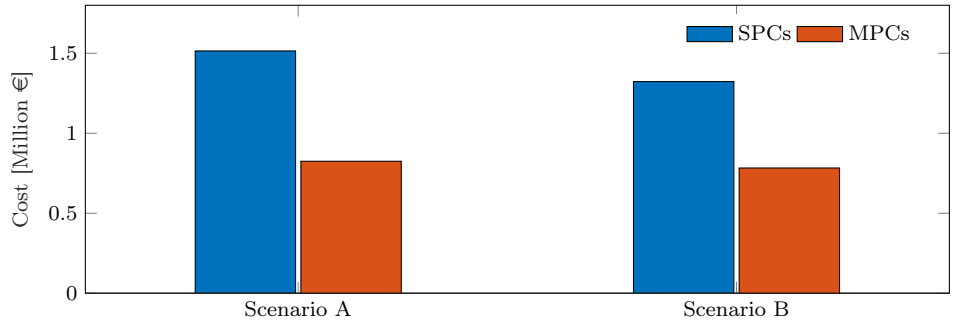

Figure 3.8: Cost of the four cases with 1 day horizon.

Finding 4. Different scenarios and charger typologies (MPCs/SPCs) lead to a different spatial distribution of the chargers. In almost all cases, more chargers are placed in Cluster 1, where vehicles are parked overnight. This is attributed to longer parking durations, which provide a greater opportunity for optimizing the charging process among a larger group of vehicles. Consequently, this leads to a more efficient utilization of the charging infrastructure.

Fig. 3.9 shows the distribution quantiles (in different shades of green) and median values (thick

green line) of the injections of active power (conventional demand plus EVs) across the nodes over time. Nodal injections are scaled by the rated power of each node, so that one per unit (denoted by the horizontal dashed lines) corresponds to the maximum power flow at that node. Nodal injections and power transformer limits in (3.18d) were found to be the active constraints of the planning problem. In all the cases, the nodal injections hit the limit value in the evening hours. This is due to the combination of the evening's conventional demand and the EVs' charging demand. With SPCs, the grid is mostly loaded in the day's central hours, whereas with MPCs, the grid is mostly loaded in the afternoon and evening hours. This denotes that MPCs tend to shift the charging demand from the central part of the day to the afternoon and evening hours.

V2G results

To evaluate whether V2G leads to lower development costs of the charging infrastructure, results are presented in this section for 1 day optimization horizon. For a fair comparison with the former case, the cost of V2G chargers is assumed to be the same as the one-directional chargers. Table 3.3 shows the number of V2G chargers and plugs obtained by solving the planning problem. Comparing tables 3.3 and 3.2, it can be seen that V2G achieves a slightly smaller number of total chargers, between 6% (Scenario A, MPCs) and 0.5% (Scenario B, SPCs).

Table 3.3: Number of slow chargers and plugs with V2G.

Forgetful (Scenario A)			Cooperative (Scenario B)		
MPCs		SPCs	MPCs		SPCs
Chargers	Plugs	Chargers	Chargers	Plugs	Chargers
370	884	878	370	855	763

Table 3.4: Total EV charging demand versus V2G injections.

	Forgetful (Scenario A)		Cooperative (Scenario B)	
	SPCs	MPCs	SPCs	MPCs
Charging demand (kWh)	16451	9380.9	9398.2	9335.5
Discharging demand (kWh)	1719.4	416.8	168.4	375.8

As the cost of the charging infrastructure is proportional to the number of chargers, the cost savings of V2G are also proportional. However, because the cost savings are comparable to the MIP gap setting adopted to solve the optimization problem (i.e., 10%), this gain is deemed as not specially significant. Table 3.4 shows the total charging and discharging energy of the EVs, calculated as $\sum_{v,t} p_{vt}^{\mathrm{EV}+}$ and $\sum_{v,t} p_{vt}^{\mathrm{V2G}}$, respectively. The total discharging demand is a small fraction of the total charging demand, between 2% and 10%, denoting limited use of V2G. Overall, we can conclude that using V2G leads to marginal improvements in this case study.

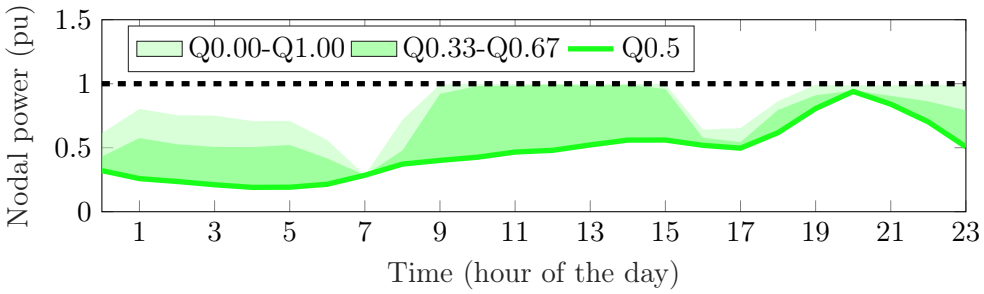

(a) Scenario A - SPC

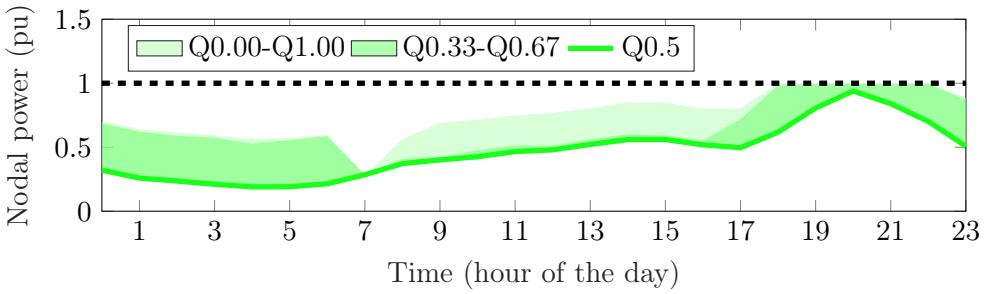

(b) Scenario A - MPC

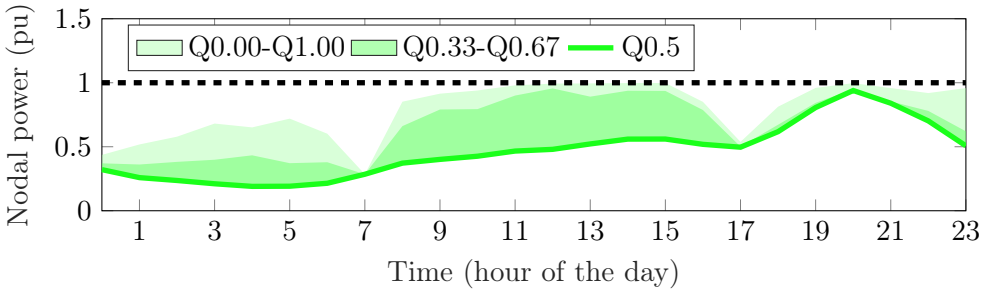

(c) Scenario B - SPC

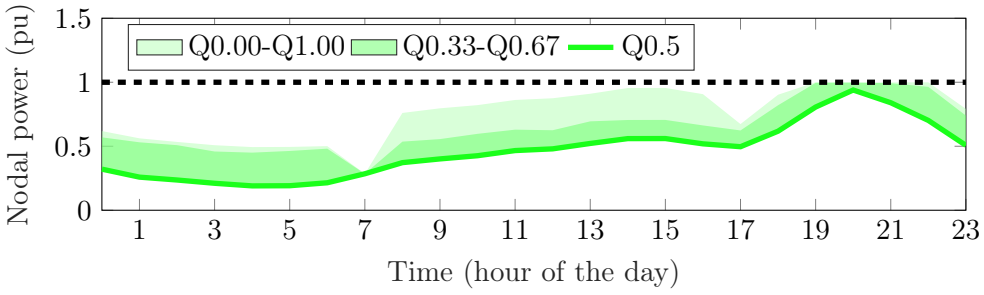

(d) Scenario B - MPC

Figure 3.9: Distribution quantiles and median values of the active power injections across the various nodes of the grid over time for the EVs with 16 kWh batteries.

Results for five days horizon

The optimization problem with 5 days horizon was solved with a duality gap of 15% to reduce the computation time. In these settings, the optimization problem was solved in around 5 hours. In

Table 3.5 the numbers are reported for 5 days optimization horizon.

Finding 5. It is observed that for both the scenarios and charging infrastructures, fast chargers are not required to be installed and slow chargers are enough to satisfy the charging demand of EVs.
Finding 6. In Table 3.5 it is observed that the number of installed chargers/plugs are the same for MPCs and SPCs, as it was in former case with smaller batteries of 16 kWh, where significant gap exists between these two numbers. This is because EVs with larger battery take longer to recharge, assuming the same charging power and initial state-of-charge. Due to longer recharging times and the fact that chargers tend to be in operation whenever an EV is plugged in, the feature of swapping among several EVs (thanks to MPCs or increased driver flexibility) falls unused, without leading to more optimal use of the charging infrastructure.
Finding 7. The number of chargers (or plugs) required for the 60 kWh EVs is smaller than for the 16 kWh EVs. This is because EVs with smaller batteries need to be recharged more often, possibly at different nodes, thus requiring the installation of more chargers. Instead, EVs with larger batteries and more driving autonomy can perform multiple travels on a single charge and stagger the recharging process.

Table 3.5: Number of slow chargers and plugs (878 EVs, 60 kWh battery).

Node	Forgetful (Scenario A)			Cooperative (Scenario B)		
	MPCs		SPCs	MPCs		SPCs
	Chargers	Plugs	Chargers	Chargers	Plugs	Chargers
3	57	57	57	58	59	57
4	110	110	110	110	118	110
5	188	188	187	190	190	188
6	117	117	118	115	115	117
8	124	124	125	132	132	130
10	65	65	64	57	57	59
11	76	76	76	76	76	76
14	20	20	20	19	19	20
Cluster1	479	479	479	490	499	485
Cluster2	278	278	278	267	267	272
Total	757	757	757	757	766	757

Fig. 3.10 summarizes the cost for 878 EVs with battery capacity 60kWh charging at different grid nodes over the 5 days optimization horizon. In this case we observe that the costs are nearly same for all four cases this refers that with 5 days horizon a technological solution will not be necessary with the change in driving behavior.

Finally, Fig. 3.11 shows the distribution quantiles of the nodal injections over the 5 days planning horizon. Compared to the case with smaller batteries which featured significant differences among

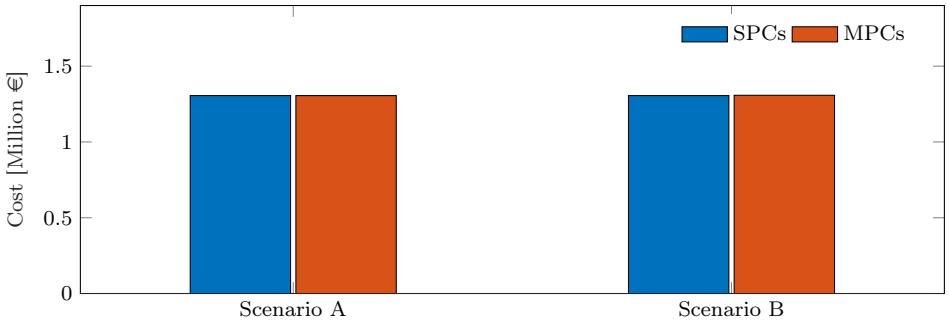

Figure 3.10: Cost of the four cases with 5 days horizon.

the nodal injections for different chargers and drivers' flexibility, nodal injections in the various cases are now similar.

3.5.2 Planning results with PV self-consumption

The planning results obtained by optimizing for PV self-consumption are illustrated and compared in this section for SPCs, considering only the slow chargers as the fast chargers were never required (as seen from the without PV self-consumption results presented in previous section). The optimization problems were solved with a MIP gap of 5% to decrease the computation time. Under this setting, it took nearly one hour to solve in a computer with an Intel Xeon processor.

At first the impact of different values of k in the cost function is illustrated; as a reminder from the previous sections, the coefficient k in (3.26) trades charging infrastructure costs for optimal planning problem when PV self-consumption is modeled.

In Fig. 3.12 the values of the two components of the planning problem's cost function in (3.26) is plotted for different values of k, forgetful/cooperative EV owners, and base case/extended parking intervals. The two cost components on the plot axis are the capital investments required for the resulting charging infrastructure (J^{chargers}) and the achieved PV self-consumption (J^{PV}). The lower values of J^{PV} denote improved PV self-consumption. Sub-figures are now discussed as follows. From Fig. 3.12(a) it is observed that, higher values of k attains lower values of J^{PV} (thus improving self consumption) but higher the infrastructure costs J^{chargers}. This trend, found also in the remaining plots of Fig. 3.12, is to be expected because larger values of k in the cost function (3.26) gives more weight to PV self-consumption, and less to decreasing infrastructure costs. Fig. 3.12(b) shows the evolution of the costs when introducing flexible drivers. Compared to Fig. 3.12(a), it can be seen that capital investment are marginally decreased, especially for $k > 0$. Fig. 3.12(c) shows the evolution of the costs with extended duration of the daytime parking intervals for forgetful EV owners. By comparing this figure against Fig. 3.12(a), it can be observed that that:

- Extending the daytime parking intervals leads to better PV self-consumption J^{PV}, as visible for $k = 0$.

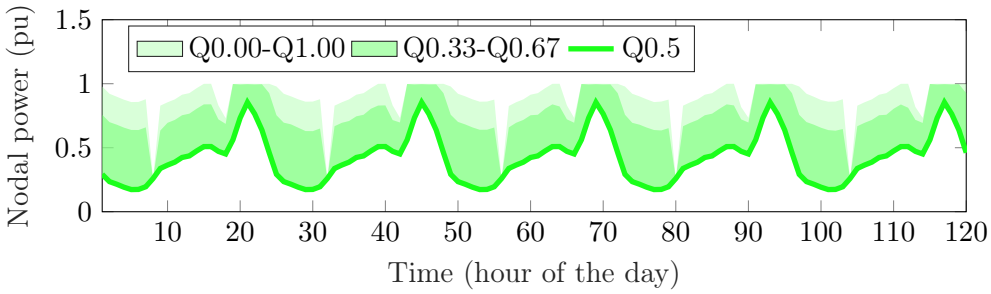

(a) Scenario A - SPC

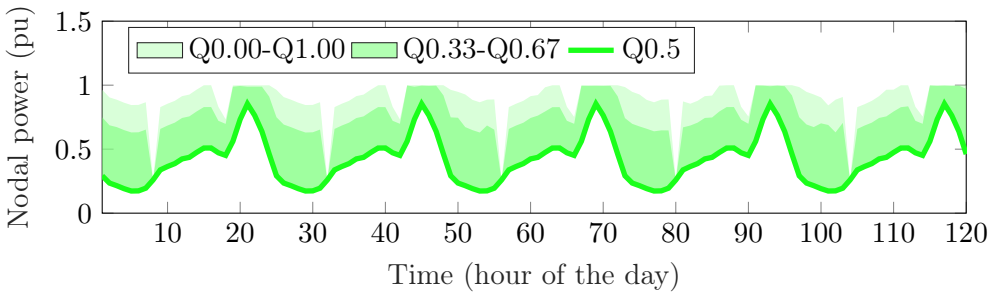

(b) Scenario A - MPC

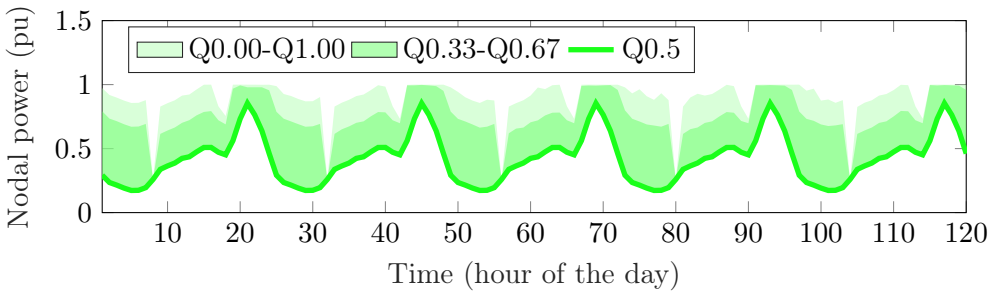

(c) Scenario B - SPC

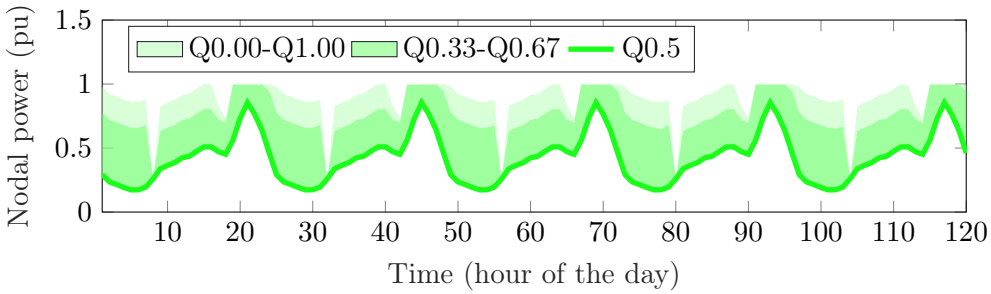

(d) Scenario B - MPC

Figure 3.11: Distribution quantiles and median values of the active power injections across the various nodes of the grid over time for the EVs with 60 kWh batteries.

- The value of the costs components in Fig. 3.12(c) is not as sensitive to variations of k values as in Fig. 3.12(a).

Finally, in Fig. 3.12(d) the evolution of the costs with extended duration of the daytime parking

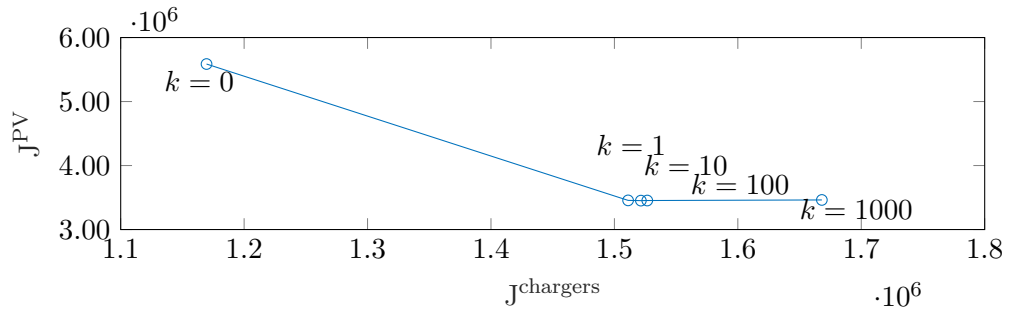

(a) Case 1

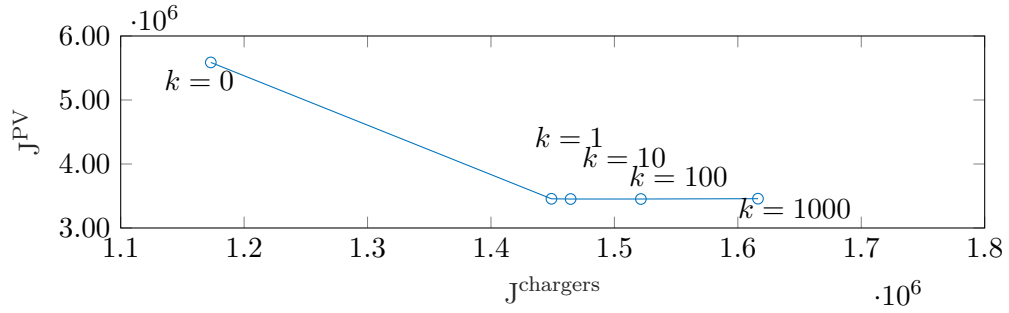

(b) Case 2

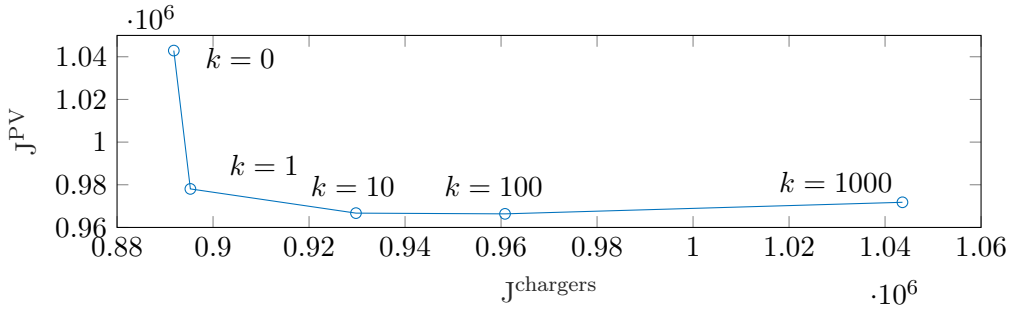

(c) Case 3

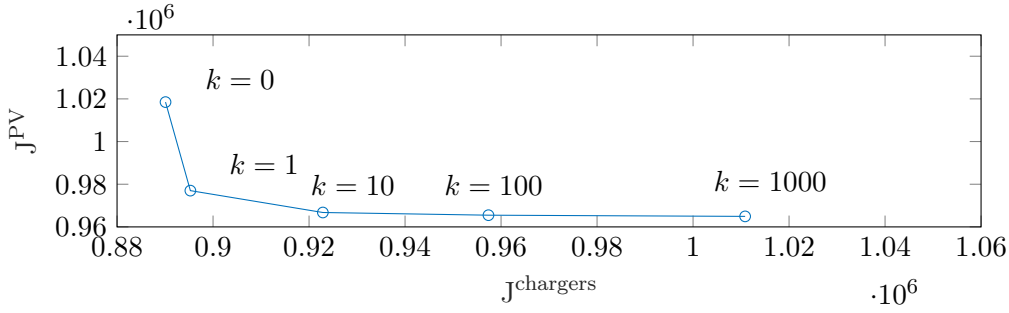

(d) Case 4

Figure 3.12: Change in PV self-consumption J^{PV} (lower values denote better PV self-consumption) with the cost of the recharging infrastructure J^{chargers}, for increasing values of k in different scenarios: (a) forgetful EV owners, (b) cooperative EV owners, (c) forgetful EV owners with extended daytime parking intervals, and (d) cooperative EV owners with extended daytime parking intervals.

intervals and *flexible* EV owners is shown. Compared to Fig. 3.12(b), it can be seen that increased flexibility of the EV owners leads to a (marginal) improvement of both the self-consumption and the infrastructure cost.

Table 3.6: Total number of chargers and distribution among clusters for different values of k, base case daytime parking intervals, and forgetful EV owners.

Node	k = 0	k = 1	k = 10	k = 100	k = 1000
3	55	68	69	72	80
4	109	92	102	99	117
5	187	134	141	160	144
6	121	216	220	225	220
8	123	63	57	44	60
10	69	217	219	219	219
11	77	118	117	118	118
14	22	29	33	27	33
Total	763	937	958	964	991
Cluster 1	62%	38%	39%	39%	40%
Cluster 2	38%	62%	61%	61%	60%

Table 3.7: Total number of chargers and distribution among clusters for different values of k, base case daytime parking intervals, and forgetful EV owners for modulated charging power.

Node	k = 0	k = 1	k = 10	k = 100	k = 1000
3	53	53	53	54	54
4	108	81	83	83	82
5	189	113	114	114	115
6	114	217	223	226	222
8	122	32	42	40	51
10	68	218	223	222	222
11	76	116	117	120	118
14	22	22	22	22	23
Total	752	852	877	881	887
Cluster 1	63%	33%	33%	33%	34%
Cluster 2	37%	67%	67%	67%	66%

Tables 3.6 and 3.7 report the total number of installed chargers with the base case daytime parking intervals, forgetful EV owners, and increasing values of k when the recharging power of the chargers is on-off and modulated (equations (3.7a) and (3.8a)), respectively. It can be seen that the number of chargers generally increases with larger values of k, inline with the former discussion. More interestingly, the two tables denote that the distribution of the chargers among clusters 1 and 2 changes between $k = 0$ and $k > 0$. In particular, with $k = 0$, chargers are mostly installed in Cluster

1 (where EVs are parked overnight), whereas with $k > 0$, chargers are mostly installed in Cluster 2 (where EVs are parked during the daytime). This denotes that promoting PV self-consumption from EVs requires developing a more pervasive charging infrastructure in those nodes where EVs are parked during the daytime.

Finally, it is also important to highlight that Tables 3.6 and 3.7 feature similar values and trends, denoting that on-off or continuous modulation does not make a significant difference. This can be explained by the fact that at the aggregated level, modulating on-off a large number of vehicles will still achieve efficient congestion management and that continuous modulation might not be required.

Table 3.8: Total number of chargers and distribution among clusters for different values of k, extended parking intervals, and forgetful EV owners.

Node	k = 0	k = 1	k = 10	k = 100	k = 1000
3	5	1	1	3	4
4	48	42	44	42	44
5	24	22	23	24	27
6	214	219	221	220	222
8	1	1	0	2	2
10	136	135	139	151	187
11	116	130	129	130	134
14	56	60	61	59	57
Total	600	610	618	631	677
Cluster 1	13%	11%	11%	11%	11%
Cluster 2	87%	89%	89%	89%	89%

Table 3.9: Total number of chargers and distribution among clusters for different values of k, extended parking intervals, and cooperative EV owners.

Node	k = 0	k = 1	k = 10	k = 100	k = 1000
3	2	5	5	5	5
4	49	42	42	42	42
5	24	22	24	24	23
6	214	218	220	220	220
8	2	2	1	2	2
10	135	134	139	148	187
11	115	129	129	129	129
14	59	56	56	56	56
Total	600	608	616	626	664
Cluster 1	13%	12%	12%	12%	11%
Cluster 2	87%	88%	88%	88%	89%

Table 3.8 and 3.9 show the total number of chargers and distribution between clusters 1 and 2 under the condition when the parking intervals are extended for both forgetful and cooperative EV owners, respectively, for increasing values of k. It can be seen that, in both these cases, the charging infrastructure is nearly entirely developed in Cluster 2, where EVs are parked for a longer duration during the daytime and where PV is available. Compared to the cases in Table 3.6 and 3.7, here it can also be observed that, for increasing values of k, first, it does not significantly impact the distribution of the chargers among the clusters, and second, it does not significantly impact the total number of required chargers to be installed. The fact that the properties of the charging infrastructure are similar for different values of k denotes that an EV charging infrastructure that is optimized for minimizing the investment cost is also capable of delivering "good performance" in terms of PV self-consumption.

3.5.3 Joint optimization of capital and operational costs

The planning results, obtained by jointly optimizing for capital and operational costs, are presented in this section.
Table 3.10 reports the number of chargers and their distributions for both normal and extended parking intervals and cooperative and forgetful EV owners. The following observations can be derived:

- For the normal parking interval, chargers are predominantly present in Cluster 1, similarly to the case $k = 0$ in the former tables. However, the number of chargers in this case is much higher than in the previous tables (approximately twice as much). This can be explained by the fact that the planning problem finds it beneficial to install more chargers in Cluster 1 (where EVs are parked overnight) in order to access lower electricity costs.
- For extended daytime parking intervals, where cars are parked longer in Cluster 2 and less in Cluster 1, chargers tend to be installed more in Cluster 2 than in Cluster 1. This is expected because installing chargers in Cluster 2 will enable access to lower electricity prices.

3.5.4 Comparison among all cases

This section compares all the aforementioned cases for SPCs. Fig. 3.13 compares the percentage of chargers installed in Cluster 1 versus the total number of chargers for all the considered cases (for PV self-consumption, only the case for $k = 100$ is considered). It can be seen that the difference between cooperative and forgetful drivers is negligible when the other features are the same. Thus, this factor does not affect the charging infrastructure requirements in this case study.

It can be observed from Fig. 3.13 that the case with extended parking intervals and PV self-consumption requires the smallest charging infrastructure, mostly developed away from Cluster 1 (i.e., in Cluster 2). The remaining cases feature a charging infrastructure that is more similar with respect to each other, so we can conclude that it is more robust against possible changes of the planning objective as it features a more similar distribution and a total number of chargers.

Table 3.10: Distribution of number of chargers for different parking intervals (878 EVs, 60 kWh battery, 5 days horizon, with service life factor).

Node	Normal interval		Extended interval	
	Forgetful	Cooperative	Forgetful	Cooperative
	chargers	chargers	chargers	chargers
3	107	107	47	47
4	168	168	109	109
5	243	243	185	185
6	215	215	215	215
8	196	196	153	153
10	205	205	196	196
11	103	103	115	115
14	48	48	62	62
Total	1285	1285	1082	1082
Cluster 1	56%	56%	46%	46%
Cluster 2	44%	44%	54%	54%

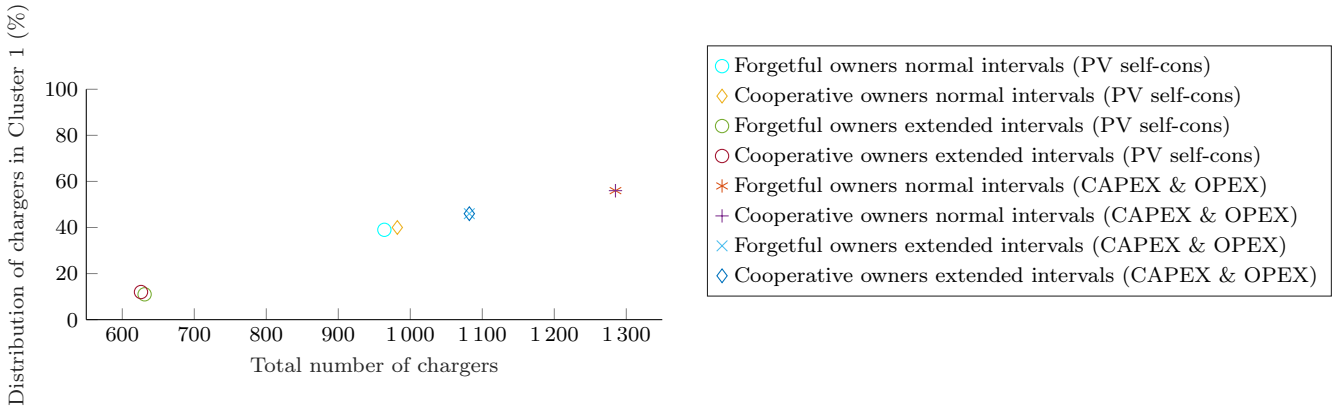

Figure 3.13: Distribution and number of chargers in Cluster 1 for two optimization problems. Data obtained for the optimization with PV self-consumption are plotted for $k = 100$.

3.6 Conclusions

A methodology is presented in this chapter for cost-optimally allocating EV chargers across the grid while considering the constraints of the power distribution grid, various charger types (slow, fast, single-port, and multi-port), and the vehicle-to-grid feature. The chapter also introduces flexibility modeling for EV owners to optimize the usage of the charging infrastructure. Additionally, the formulation is extended to minimize capital investments and maximize local PV self-consumption. By modifying nonlinear constraints, a mixed-integer linear formulation of the optimal planning problem is derived and efficiently solved using off-the-shelf software libraries.

The methodology is applied to a 14-bus MV network with 878 EVs, considering two battery sizes (16 kWh and 60 kWh). To ensure the tractability of the optimization problem, it is crucial to limit the number of temporal samples. As the number of variables in any optimization problem increases linearly with temporal samples, and the complexity of the MILP problem exponentially increases with the number of variables, careful consideration is required. For the case study, two sets of samples were utilized. Firstly, for the 16 kWh battery (i.e., a low-capacity EV battery), the optimization horizon was set to 24 samples, representing a 1-day horizon with hourly samples. Secondly, for the 60 kWh battery (i.e., a higher-capacity EV battery), the optimization horizon consisted of 120 samples, representing a 5-day horizon. The decision to opt for the longer time interval for larger battery EVs is based on the assumption that such EVs might not require a daily recharge. This choice is made under the consideration that this time interval either represents a worst-case scenario of the driving demand or a pattern that frequently occurs during the lifespan of the charging infrastructure.

The results indicate that multi-port chargers (MPCs) and cooperative EV owners contribute to reducing the required number of chargers for EVs with smaller batteries. However, for EVs with larger batteries, EV owners' flexibility and the use of MPCs result in similar planning options as forgetful EV owners and single-port chargers (SPCs). The case study demonstrates a preference for slow chargers over fast chargers. Sensitivity analysis demonstrates that shorter daytime parking intervals require more chargers to improve PV self-consumption, increasing infrastructure costs. Conversely, extending daytime parking hours reveals that a charging infrastructure at nodes where EVs are parked during the day is adequate to meet the total recharging demand, resulting in lower EV charging infrastructure costs and improved PV self-consumption.

The intermittent nature of PV generation will certainly introduce variations in the configuration of charger distribution, thereby influencing the planning results. Furthermore, minimizing nodal EV charging prices produces different outcomes, leading to higher costs for charger installation. As a future research direction, it is recommended to integrate all sources of uncertainty into a single optimization problem, aiming to develop a robust charging infrastructure capable of withstanding uncertainty. Additionally, future research should focus on formulating problem approximations to enhance tractability when incorporating more extensive input information. This research contributes to the advancement of efficient, cost-effective, and resilient EV charging infrastructure planning for distribution grids.

Chapter 4

Validation of Planning results by Scheduling problem

Résumé en Français

Ce chapitre vise à valider les résultats obtenus lors de la résolution du problème de planification optimale du chapitre 3. A cette fin, il propose une méthodologie pour formuler un problème d'ordonnancement qui utilise l'approche du flux de puissance optimal (OPF) et prend les résultats de la planification optimale comme données d'entrée pour résoudre le problème de prise de décision. Le problème de programmation est formulé sous la forme d'un programme mixte en nombres entiers (MIP). Le problème MIP est résolu en considérant que les VE se chargent à partir de chargeurs répartis de manière optimale et uniforme sur les nœuds du réseau MV. Dans le cas d'une infrastructure distribuée de manière optimale, le nombre de chargeurs à chaque nœud de la grille est connu tel qu'il est obtenu en résolvant le problème de planification optimale ; d'autre part, pour les chargeurs distribués de manière uniforme, le nombre total de chargeurs obtenu en résolvant le problème de planification optimale est réparti de manière égale entre les nœuds de la grille. En utilisant le réseau CIGRE MV pour l'étude de cas, nous montrons empiriquement que la population de VE atteint des niveaux de charge plus élevés dans le premier scénario que dans le second.

Summary

This chapter aims to validate the results obtained in solving the optimal planning problem of Chapter 3. For this purpose, this chapter proposes a methodology to formulate a scheduling problem that uses the optimal power flow (OPF) approach and takes the optimal planning results as input to solve the decision-making problem. The scheduling problem is formulated as a mixed-integer program (MIP). The MIP problem is solved by considering EVs charging from both optimally distributed and uniformly distributed chargers across MV grid nodes. In the case of optimally distributed infrastructure, the number of chargers at each grid node is known as it is obtained, solving the optimal planning problem; on the other hand, for uniformly distributed chargers, the total number of chargers obtained solving the optimal planning problem is equally distributed across the grid nodes. Using the CIGRE

MV grid for the case study, we empirically show that the EV population achieves higher charge levels in the first scenario than in the second one.

4.1 Introduction

To effectively accommodate the charging needs of EVs, DSOs must carefully plan the deployment of charging infrastructure across the grid to avoid overloading the system and causing violations of grid constraints on nodal voltage magnitudes and line currents.

In Chapter 3, we proposed a formulation for planning charging infrastructures in distribution grids accounting the technical constraints of the grid, multiple charger typologies and EV owner's flexibility scenarios to plug and unplug their EVs. To justify our proposed formulation, we must investigate whether the charger deployment configuration obtained from solving the planning problem in the previous chapter is sufficient for scheduling operations by DSOs, or whether a different configuration of chargers across the grid would be more ideal for meeting the charging demand of EVs while avoiding violations of grid constraints on nodal voltage magnitudes, line currents and nodal apparent power limits.

To this end, in this chapter, we will conduct case studies to evaluate the effectiveness of the optimized charger deployment configuration in meeting the charging demand of EVs and compare their performances with alternative deployment configurations. Through this investigation, we hope to justify our proposed formulation and provide insights into effective strategies for managing EV charging in distribution grids.

4.1.1 Modeling principles and optimization problem

In Figure 4.1, the salient components for formulating the optimal power flow-based scheduling problem to validate the planning results are presented. The results obtained from solving the optimal planning problem (indicated by the top yellow box) serve as inputs for the formulated scheduling problem, including the locations and number of EV chargers. The driving demand and parking locations of EVs over time, as discussed in Section 3.2.1, are reused for the scheduling problem. The light grey box represents the components for modeling EVs. The inputs include the energy capacity of EV batteries, rated power of the EV charger, and their initial SOC. The SOC evolution in time of all EVs is computed as a function of the EVs' driving demand. The charging policies determine the charging power of EVs, which serve as decision variables in the optimization problem (indicated by the light purple box). Therefore, constraints for the charging power can be enforced based on the selected policy. This chapter focuses only on the V1G policy for EVs. To solve the optimization problem, nodal injections are computed (as shown by the light orange box) using both grid information (net nodal active and reactive power demands, which are inputs for the optimization problem) and the charging demand of EVs parked at different grid nodes. Similar to previous chapters, the optimal power flow with linearized grid models from existing literature is

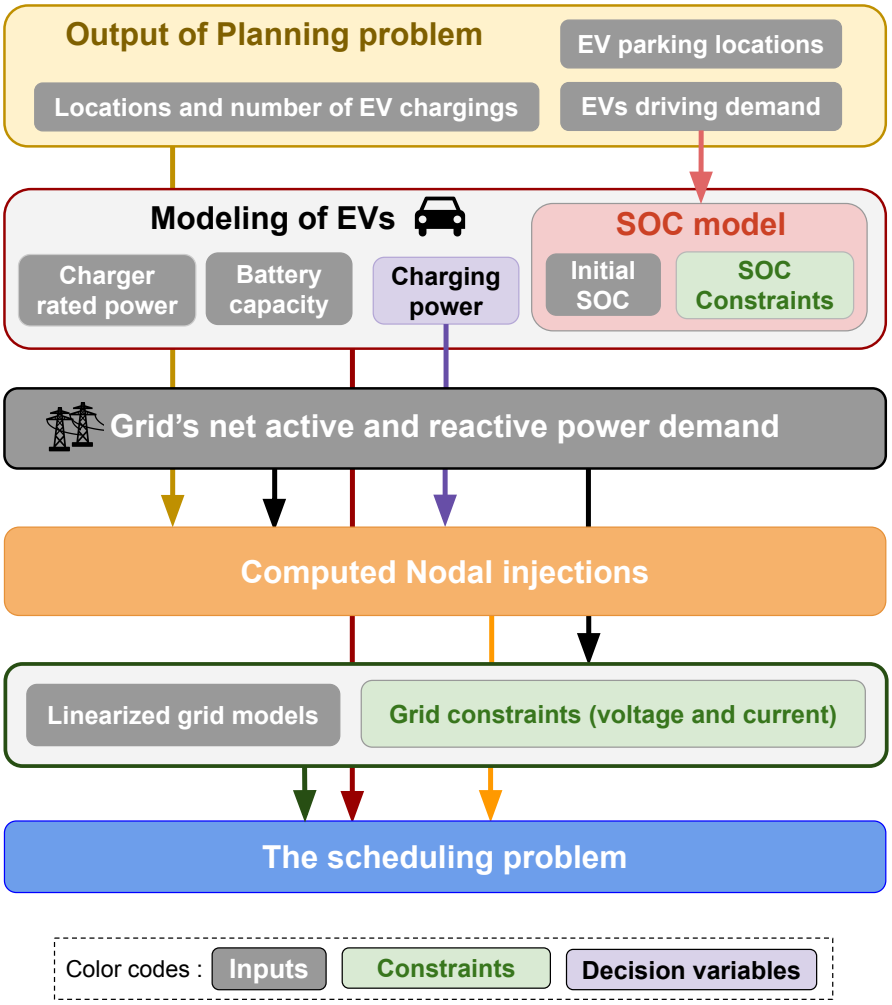

Figure 4.1: The main elements used to formulate the scheduling problem to validate planning results.

considered. The linearized grid models used to solve the optimal planning problem are the same as those used for solving the formulated scheduling problem, while nodal voltage magnitudes and line current bounds serve as constraints in the optimization problem. Finally, the scheduling problem can be solved, as shown by the blue box.

The key difference between the current scheduler and the one presented in Chapter 2 is that, here, the number of vehicles that can simultaneously charge should be less or equal than the available number of chargers. This constraint (described later in Eq. (4.5)) is the link between the optimal planning problem in Chapter 3 and the scheduling problem in Chapter 2.

4.2 Methodology

4.2.1 EVs' state-of-charge (SOC) model

For V1G policy, with an input initial state-of-charge $\mathrm{SOC}_v(0)$, the SOC of vehicle depends on the discharging power $p_{vt}^{\text{EV-}}$ and the charging power P_{vt}^{EV} (as discussed in the next section). The SOC of a vehicle v at time t is expressed as:

$$\mathrm{SOC}_v(t) = \mathrm{SOC}_v(0) + \frac{T_s}{E_v} \sum_{\tau=0}^{t-1} \left(\eta \cdot P_{v\tau}^{\text{EV}} - p_{v\tau}^{\text{EV}-} \right). \tag{4.1}$$

As discussed in previous chapter the discharging power $p_{vt}^{\text{EV-}}$, is estimated directly from the vehicles' SOCs and it is not weighted by the efficiency in (4.1). The discharging power computed while solving planning problem is now an input for the scheduling problem.

For EVs to remain in a functional condition and satisfy the driving requirements by the EV owners, the vehicles' SOCs should be within a feasible range, between 0 and 99% denoted by $(\underline{\mathrm{SOC}}, \overline{\mathrm{SOC}})$ respectively. Therefore, the SOC constraint reads as:

$$\underline{\mathrm{SOC}} \leq \mathrm{SOC}_v(t) \leq \overline{\mathrm{SOC}}. \tag{4.2}$$

4.2.2 Modeling the charging power and constraints

Assuming the EV chargers operate on and off during the scheduling process, the active (P_{tv}^{EV}) and reactive (Q_{tv}^{EV}) power demand of EVs can be modeled as a function of a binary variable p_{tv}^{charging}. Assuming the EV charger operating at a constant power factor $\cos\phi$ and kVA rating $\bar{S}$, the active and reactive power read as:

$$P_{vt}^{\text{EV}} = p_{vt}^{\text{charging}} \cdot \bar{S} \cdot \cos\phi, \qquad \forall t \text{ and } v \tag{4.3a}$$

$$Q_{vt}^{\text{EV}} = P_{vt}^{\text{EV}} \cdot \tan\phi, \qquad \forall t \text{ and } v \tag{4.3b}$$

The binary variable p_{vt}^{charging}, introduced in (4.4) is activated only if an EV v is charging at any time interval t and else it remains deactivated. In case of V1G, the EV charging power can be modulated. Hence, the capability of a EV charger to modulate its output power read as:

$$0 \leq P_{vt}^{\text{EV}} \leq p_{vt}^{\text{charging}} \cdot \bar{S} \cdot \cos\phi \qquad \forall t \text{ and } v \tag{4.4}$$

We now model the availability of chargers. In case the binary variable p_{vt}^{charging} is active, (i.e., the vehicle v charging at time t) the number chargers serving the EVs at any grid node n over time interval t should always be less or equal to the total number of installed chargers (S_n^*) at node n. S_n^* is the input for the scheduling problem and it can be either from the optimal planning problem of Chapter 3 or from uniform distribution of charging infrastructure. This constraint is expressed as::

$$\sum_{v} p_{vt}^{\text{charging}} \cdot p_{nvt} \leq S_n^* \qquad \forall t \text{ and } n \tag{4.5}$$

4.2.3 Nodal injections due to EVs' charging demand

Coupling the input binary parameters p_{nvt} with the charging powers of the individual EVs, nodal active ($P_{tn}^{(\text{EV nodal})}$) and reactive ($Q_{tn}^{(\text{EV nodal})}$) powers injected due to EVs' recharge at the grid nodes over time horizon can be computed as:

$$P_{tn}^{(\text{EV nodal})} = \sum_{v=1}^{V} p_{nvt} \cdot P_{vt}^{\text{EV}} \qquad \forall t \text{ and } n \tag{4.6a}$$

$$Q_{tn}^{(\text{EV nodal})} = \sum_{v=1}^{V} p_{nvt} \cdot Q_{vt}^{\text{EV}} \qquad \forall t \text{ and } n. \tag{4.6b}$$

in (4.6), P_{vt}^{EV} and Q_{vt}^{EV} are the active and reactive powers respectively as specified in (4.3), associated to this charging demand of a vehicle v and time t.

For the smart charging problem, the charging demand of EVs is scheduled in such a way that their charging process does not cause violations of the grid constraints on nodal voltage magnitudes, line currents. These operational grid constraints have been considered:

$$\underline{v} \leq v_{tn} \leq \overline{v} \qquad \forall t \text{ and } n \tag{4.7a}$$

$$|i_{tl}| \leq \bar{i}_l \qquad \forall t \text{ and } l \tag{4.7b}$$

where, $\underline{v}, \overline{v}$ respectively define lower and upper limits nodal voltage magnitudes; upper limits of lines' ampacity $\bar{i}_l$. In addition to these constraints, for smart charging problem it is considered that the nodal injections remain below the apparent power limit of the node, S_n:

$$\left(P_{tn}^{\text{node}}\right)^2 + \left(Q_{tn}^{\text{node}}\right)^2 \leq (S_n)^2. \tag{4.7c}$$

As mentioned previously, the constraint (4.7c) proves to be valuable when considering apparatus with apparent power limitations connected at specific grid nodes, such as MV/LV step-down transformers. In Section 4.2.5, we will delve into the explanation of how this constraint can be approximated to effectively address the optimal planning problem.

4.2.4 The scheduling problem

In this section, we present the formulation of the scheduling problem for validation. The objective of the scheduling problem is to minimize the recharging time of each individual EV at the grid nodes. This objective is independent of the state of the grid and other EVs. The problem involves the following decision variables which are vectors of $V \times T$ can be denoted by:

$$\boldsymbol{w} = \left[p_{11}^{\text{charging}}, \ldots, p_{VT}^{\text{charging}}\right] \tag{4.8}$$

$$\boldsymbol{x} = \left[P_{11}^{\text{EV}}, \ldots, P_{VT}^{\text{EV}}\right] \tag{4.9}$$

$$\boldsymbol{y} = \left[Q_{11}^{\text{EV}}, \ldots, Q_{VT}^{\text{EV}}\right] \tag{4.10}$$

Additionally, in order to prevent any advantage gained from the initial energy stock, it is crucial for the final state of charge (SOC) to be greater than or equal to the initial SOC. This is represented by the following constraint:

$$\mathrm{SOC}v(T) \geq \mathrm{SOC}v(0), \qquad \text{for all } v. \tag{4.11}$$

By imposing constraint (4.11), the formulation ensures that the charging demand of the vehicles is properly accounted for, regardless of their initial conditions.

Based on the requirement we can formulate a decision-making problem where the EVs' charging power is such that all vehicles reaches the respective target state-of-charge level, $\mathrm{SOC}_v^\star$ as fast as possible. Its formulation reads as:

$$\underset{\boldsymbol{w}\in\{0,1\}^{V\times T},\boldsymbol{x},\boldsymbol{y}\in\mathbb{R}_+}{\arg\min} \left\{ \sum_{t=1}^{T}\sum_{v=1}^{V} (\mathrm{SOC}_{vt} - \mathrm{SOC}_v^*)^2 \right\} \tag{4.12a}$$

subject to the following constraints:

SOC model and constraints (4.1), (4.2), (4.11)	$\forall t$ and v	(4.12b)
EV charging power and constraints (4.3), (4.4)	$\forall t$ and v	(4.12c)
Constraints for nodal chargers (4.5)	$\forall t$ and v	(4.12d)
Nodal injections (4.6) and (1.4)	$\forall t$ and n	(4.12e)
Linearized grid models (1.5a)-(1.5b)	$\forall t$, n and l	(4.12f)
Linear grid constraints (4.7a), (4.7b) and (4.7c).		(4.12g)

The constraint (4.7c) has been considered in the scheduling problem to limit the nodal injections below the apparent power limit of the node, S_n. These constraints are important for the apparatus with apparent power limitations connected at the nodes, such as nodes hosting substation step-down transformers.

4.2.5 Problem properties and approximations

The problem (4.12) is nonlinear (quadratic MIP) due to its objective function and the apparent power constraint in (4.7c). This quadratic constraint can be replaced by two linear inequalities as in (4.13), with $\underline{\cos}\phi$ as a lower-bound estimate of the load power factor of the nodal injection at node n. For the problem (4.12) we thus have the following linear expression:

$$-\bar{S}_n \cdot \underline{\cos}\phi_n \leq P_{nt}^{\mathrm{node}} \leq \bar{S}_n \cdot \underline{\cos}\phi_n. \tag{4.13}$$

By employing this equivalent approximation and implementing a linear cost function, the optimization problem (4.12) can be transformed into a mixed-integer linear program (MILP). This modification will significantly improve computational performance compared to the original formulation, enabling more efficient problem solving.

4.2.6 Optimization horizon for the case study

In MIP, the number of optimization variables increases with an increase in temporal samples. However, this growth depends on the specific formulation of the problem and how temporal aspects are integrated. The time complexity of solving MIP problems is typically exponential in the worst case, as MIP problems are generally NP-hard. Therefore, efficient solution techniques and algorithmic improvements are crucial for addressing the computational challenges associated with MIP problems, especially as problem size grows. In this chapter, the case study focuses on EVs with low-capacity batteries (specifically, 16 kWh) and considers a 24-sample configuration. This corresponds to a 1-day optimization horizon with samples taken at hourly intervals.

4.3 Case study and Results

4.3.1 Power grid and EVs

For the case study, the previously described 14-bus European CIGRE benchmark grid for medium voltage (MV) systems has been utilized. The outputs of the optimal planning problem serve as inputs for the scheduling problem. Therefore, in the case study, the optimization problem is solved for the same number of EVs as considered in the previous chapter, which is 878 EVs. The parking locations of the EVs at the distribution grid nodes over time are also identical to those used in the planning problem. This consistency ensures that the scheduling problem is based on the same set of EVs and their respective locations, enabling a meaningful comparison and analysis of the results. Finally, the scheduling problem is solved, considering a smart charging policy for EVs, under two different charging infrastructure scenarios as specified below:

- **Uniformly distributed chargers**: In this scenario, the total number of chargers obtained by solving the optimal planning problem is evenly distributed across all MV grid nodes.

- **Optimally distributed chargers**: In this scenario, chargers are distributed across MV grid nodes based on the results obtained from the optimal planning problem.

These two scenarios allow for a comparison of the scheduling outcomes and the evaluation of the performance of the charging infrastructure in each case. In the comparative analysis of the two scheduling problems with the aforementioned charging infrastructure, several assumptions are made. Firstly, it is assumed that all 878 EVs in the grid start charging from their specified locations with an initial state of charge (SOC) derived from a Gaussian distribution. The mean of the distribution is set at 0.49, and the standard deviation is 0.04. Additionally, the energy capacity of the EV batteries, the rated power of the chargers, their efficiency, and power factor are assumed to be constant across the entire EV population. Specifically, the battery energy capacity is set at 16 kWh, the charger's rated power is 3.6 kVA, the efficiency is 0.9, and the power factor is 1. Moreover, the target SOC levels for all EVs are assumed to be uniform, with a set value of 99%. These assumptions establish a standardized basis for comparing the scheduling problems and analyzing their respective outcomes.

4.3.2 Optimization results

For the scheduling problem 4.2.4 presented above, results are presented herein for both uniformly and optimally distributed charging infrastructure. For both cases the charging policy remains the smart charging with reactive power support from the EV chargers. The input information and the number of chargers used for the case was SPCs/Scenario A.

The scheduling problems are implemented in MATLAB and solved using Gurobi on an Intel machine with 15% duality gap. Under these settings the optimization problems take nearly two hours to converge.

Results: the impact of the spatial distribution of chargers on SOC profiles

Figure 4.2 shows the average SOC of the EV population over the 1-day optimization horizon in per- unit values. It can be seen that optimally distributed chargers achieve faster recharging times than uniformly distributed chargers, thus featuring better performance. Figure 4.3 shows the same comparison but for a second scheduler with a driving demand increased by 20%, resulting in an increase of the recharging demand of 20% (for the same level of attained SOC); this is done with the objective of analyzing the sensitivity of the performance of the charger distribution on the results. It can be seen that the optimal distribution of chargers still achieves faster recharging times than uniformly distributed chargers, as denoted by the steeper ramps.

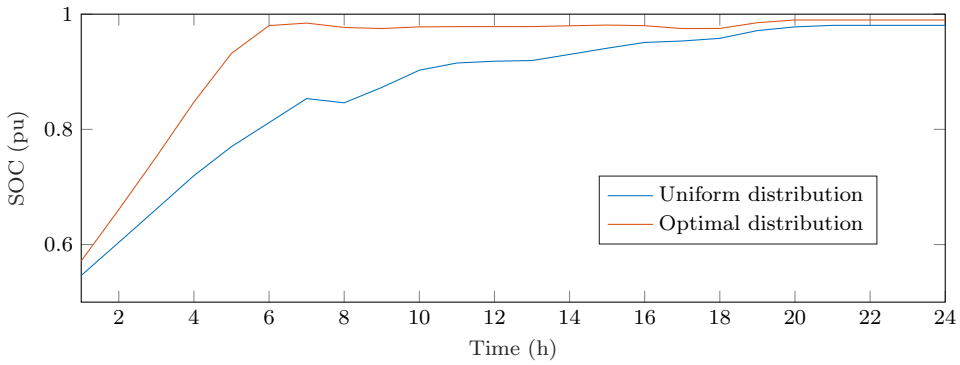

Figure 4.2: Comparison of mean SOC across the EVs population for different charging infrastructures for original discharging power of EVs.

Performance evaluation

The cost function serves as a crucial metric for assessing the performance of the scheduler in an optimization problem. By analyzing the cost function, one can obtain valuable insights into how well the scheduler operates and achieves its objectives over the entire optimization horizon. This allows us to make an informed evaluation of the scheduler's performance. Based on it, the metric in (4.14) is computed and performance is reported in Table 4.1.

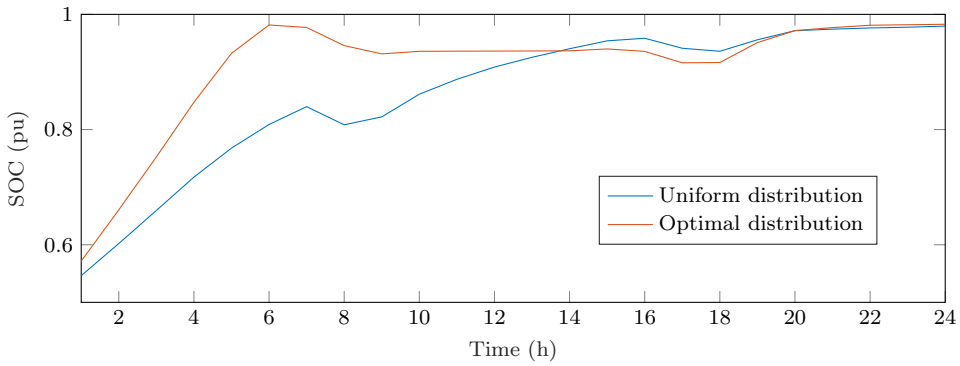

Figure 4.3: Comparison of mean SOC across the EVs population for different charging infrastructures with 20% higher demand than Fig 4.2.

$$\text{Metric} = \sum_{t=1}^{T} \sum_{v=1}^{V} (SOC_{vt} - SOC_v^*)^2 \tag{4.14}$$

Table 4.1: Metric performances for different charging infrastructures with smart charging.

	EV's discharging power	
	Original	20% higher than original
Optimal distribution	19.08	20.43
Uniform distribution	28.29	29.86

Based on the observations from Table 4.1, it can be concluded that in the case of optimally allocated infrastructure, the metric shows lower values for both the original discharging power of EVs and the 20% higher discharging power caused by driving demand. On the other hand, for uniformly allocated infrastructure, the metric yields higher values in both scenarios, indicating that the scheduler performs better with optimal distribution.

Impact on grid constraints

Upon solving the scheduling problem for both uniform and optimal distribution of charging infrastructure, it was observed that the grid constraints were respected. This outcome aligns with expectations since the scheduler implements grid constraints.

4.4 Conclusions

In conclusion, this chapter presents a methodology for validating the results of the optimal planning problem in the context of EVs charging scheduling. The proposed approach formulates the scheduling problem as a mixed-integer program (MIP) and utilizes the optimal power flow (OPF) technique. The MIP problem considers two scenarios: optimally distributed chargers and uniformly

distributed chargers across medium-voltage (MV) grid nodes. The empirical study conducted on the CIGRE MV grid case study demonstrates that the first scenario, where chargers are optimally distributed based on the results of the optimal planning problem, yields higher charge levels for the EV population compared to the second scenario with uniformly distributed chargers.

These findings emphasize the importance of considering optimal infrastructure placement for EV charging systems. By strategically locating chargers based on the results of the optimal planning problem, it is possible to shorten the charging times (as observed from the performance of the scheduler) and overall SOC levels of the EV population. It was also shown that the optimal deployment still achieve better results (shorter recharging times) with higher recharging demand. This information is critical for stakeholders involved in designing and implementing EV charging infrastructure, as it ensures effective and optimized operation. Additionally, it is important to note that this investigation did not consider nodal electricity prices. Future work should focus on investigating which charger deployment configuration is suitable while charging AEVs, taking into account nodal electricity prices. This aspect is crucial for optimizing the cost-effectiveness of charging strategies and maximizing the benefits of AEVs in the power grid. By incorporating pricing mechanisms into the optimization framework, it will be possible to determine the most cost-efficient charger deployment scenarios, considering both the grid constraints and the economic aspects of EV charging. Overall, the proposed methodology and its empirical validation contribute to advancing the field of EV charging scheduling and offer valuable insights for decision-makers to enhance the performance and sustainability of future transportation systems.

Chapter 5

Conclusions and future work

5.1 Conclusions

The conclusion chapter marks the culmination of this thesis, bringing together the key findings and insights obtained from the preceding chapters. Furthermore, this chapter provides a critical evaluation of the research outcomes. In Chapter 1, a thorough literature review was conducted. This comprehensive review served as the foundation for identifying research gaps, formulating the research objectives, and finally the methodological contributions presented throughout this thesis.

The Chapter 2 of this chapter covers the methods of charge scheduling for following EV charging policies: uncoordinated charging, smart or grid-aware coordinated or V1G charging, grid-aware coordinated bidirectional charging or V2G with (and without) reactive power support from the EV chargers. An integrated algorithmic framework is proposed in this chapter to formulate the scheduling problem at the grid level that facilitate integrating information of EVs. For all schedulers, formulation of scheduling problem is derived from a common (convex) optimization framework accounting for linearized power grid constraints (i.e. nodal voltage magnitudes, line currents etc.), charging/discharging efficiency, and 4-quadrant (and 2-quadrant unidirectional) chargers, that allow an efficient comparison among the charging policies. Through extensive investigations on a large population of EVs charging at different MV distribution grid nodes, valuable insights were obtained. The findings revealed that uncoordinated charging resulted in voltage constraint violations during the afternoon/evening periods, while smart charging showed effectiveness in reducing grid congestions during those periods. Interestingly, although the bidirectional charging (V2G) feature was not activated in the studied scenarios, the presence of reactive power support from EV chargers proved beneficial in reducing voltage congestions, allowing for increased EV charging and shorter charging times to achieve the desired state of charge. The insights gained from evaluating different charging policies provide valuable guidance for distribution system operators (DSOs). Furthermore, this thesis also highlighted the challenges associated with incorporating autonomous EVs (AEVs) into the power grid. The formulation of charging problems for different policies under a common framework was presented, acknowledging the increased computational burden due to the higher number of variables involved.

Chapter 3 of the thesis focuses on optimization methods for cost-optimal planning of EV charging infrastructure, taking into account the constraints of the distribution grid. The chapter explores various strategies to determine the optimal siting and sizing of chargers for EVs, considering factors such as charger types, vehicle-to-grid capabilities, and the flexibility of EV owners in plugging and unplugging their vehicles. To make the problem computationally tractable, the nonconvex constraints in the formulation are suitably modified to derive a mixed-integer linear programming (MILP) formulation. This allows the problem to be solved with off-the-shelf optimization libraries within a reasonable time frame. The method is applied to a 14-bus medium-voltage (MV) network with a population of 878 EVs and two different battery sizes (16 kWh and 60 kWh). The results demonstrate that for EVs with smaller batteries, multi-port chargers and cooperative EV owners contribute to reducing the number of chargers required. However, for EVs with larger batteries, the impact of EV owners' flexibility and multi-port chargers on the planning options is similar to that of forgetful EV owners and single-port chargers. The preference for slow chargers over fast chargers is observed in the proposed case study. The number of variables in the planning problem depends on the optimization horizon and the number of vehicles, and the computational time increases significantly with the number of decision variables. Thus, careful selection of the optimization horizon and input information is necessary to achieve manageable computation times. Another aspect explored in the chapter is the joint minimization of capital investments for EV charging infrastructure and maximization of self-consumption of local photovoltaic (PV) generation. The formulation considers operational constraints of the distribution grid, EV recharging demand, and the flexibility of EV owners. To examine the impact of various factors on the planning results, sensitivity analysis was performed. The results of the sensitivity analysis indicate that the duration of daytime parking has a significant impact on the planning of charging infrastructure and PV self-consumption. When daytime parking intervals are shorter, it is necessary to install a larger number of chargers in order to enhance PV self-consumption. However, this leads to higher infrastructure costs. On the other hand, extending the duration of daytime parking reveals a different outcome. In this case, a charging infrastructure focused on the nodes where EVs are parked during the day proves to be sufficient to meet the overall recharging demand. Consequently, this approach reduces the costs associated with EV charging infrastructure while also improving PV self-consumption. These findings highlight the importance of considering the duration of daytime parking when designing and planning charging infrastructure, as it can have a significant impact on both the financial aspects and the integration of renewable energy sources like PV. Additionally, when the objective is to minimize nodal EV charging prices, different results are obtained, albeit with higher installation costs for chargers. Overall, methods developed in Chapter 3 contributes to the efficient integration of EVs into the distribution grid while considering grid constraints, flexibility of EV owners, and renewable energy sources.

The Chapter 4 introduces a methodology for validating the results obtained from solving the optimal planning problem. The presented approach in this study formulates the scheduling problem as a mixed-integer program (MIP) and leverages the optimal power flow (OPF) technique. The MIP problem considers two scenarios: one with optimally distributed chargers and another with uniformly distributed chargers across medium-voltage (MV) grid nodes. By utilizing the results of the

optimal planning problem as input, the scheduling problem was efficiently solved, thereby offering valuable insights for decision-making purposes. An empirical study conducted on the CIGRE MV grid case study demonstrates that the first scenario, where chargers are optimally distributed based on the outcomes of the optimal planning problem, leads to higher SOC levels for the EV population compared to the second scenario with uniformly distributed chargers. These findings emphasize the importance of considering optimal infrastructure placement when designing EV charging systems. By strategically locating chargers based on the optimal planning problem's results, the recharging times the EV population was significantly improved. This information is crucial for stakeholders involved in the design and implementation of EV charging infrastructure, as it ensures effective and optimized operation. In summary, the proposed methodology, along with its empirical validation, contributes to the advancement of the field of EV's charging station planning.

5.2 Future work

Based on the presented work several potential avenues for future research is discussed in this section. In future works, the consideration of voltage-dependent power injections, as proposed in [132], will be explored and integrated into the linearized grid model. This enhancement aims to capture the influence of voltage variations on power injections and further improve the accuracy and realism of the model. Further work in this area could concentrate on refining the optimization models to accommodate additional factors. This may include the incorporation of more intricate charging patterns, such as stochastic charging behaviors and the influence of dynamic electricity pricing schemes. Furthermore, the integration of renewable energy sources and storage systems within the optimization model can enhance the sustainability and grid integration aspects of EV charging infrastructure. By addressing these aspects, future research can contribute to the development of more advanced and comprehensive optimization models for EV charging infrastructure.

Considering real-time information in the decision-making process can improve the responsiveness and adaptability of EV charging infrastructure. Therefore, future work could investigate the integration of real-time data, such as grid conditions, electricity demand, and EV availability, into the optimization model. This would enable more dynamic and optimized charging strategies that respond to current system conditions.

As the scale of EV adoption continues to increase, it becomes essential to develop scalable and tractable optimization algorithms that can handle larger networks and a higher number of decision variables. Therefore, future research can explore novel solution approaches or problem approximations that strike a balance between computational efficiency and solution quality. When EV charging infrastructure and smart grid technologies converge, there is an opportunity for synergistic optimization, leading to improved efficiency and effectiveness in managing both the charging of EVs and the operation of the electrical grid. So, future research in this area can explore how EV charging can be seamlessly integrated with advanced grid control mechanisms, demand response programs, and energy management systems. By integrating these technologies, it becomes possible

to develop coordinated and intelligent control strategies for EV charging. Such strategies can optimize the timing and distribution of charging loads based on real-time grid conditions, electricity demand, and available renewable energy resources. The integration of EV charging with advanced grid control mechanisms enables a more dynamic and flexible charging environment. For example, during periods of high electricity demand or when renewable energy generation is plentiful, the grid can intelligently direct EV charging to occur at optimal times, reducing strain on the grid and maximizing the utilization of clean energy sources.

In this Thesis, methods to plan charging infrastructures for *autonomous* EVs and assessing their impact on the MV grid have not been explored. Utilizing methods such as OPF, location optimization can ensure efficient planning of the charging infrastructure while minimizing the impact on the MV grid and advancing the transition towards a greener and more sustainable transportation system. Lastly, comprehensive studies on the long-term impacts of EV charging infrastructure deployment are needed. Future research can focus on evaluating the scalability and resilience of charging infrastructure under different scenarios, including varying EV adoption rates, changes in energy generation mix, and grid upgrades. Understanding the long-term implications will help policymakers, utility companies, and stakeholders make informed decisions regarding investments, infrastructure planning, and policy development.

Appendices

Appendix A

Accuracy of the linearized grid models

The accuracy of the linearized grid model can be evaluated by comparing the linear estimates with the corresponding ground-truth quantities. As the linear grid models use approximations, they inherently introduce errors. In the linear grid model, we consider day-ahead forecasts of the demand and renewable generation as the linearization points. It is worth mentioning that, this consideration does not incorporate any injections from EVs. In the next section, a case study is presented in which the accuracy of the linearized grid models is evaluated. Similarly, for the other case studies presented in Chapter 2 and Chapter 4, the accuracy of the linearized grid models can be measured.

Case study

We consider the case study from the Chapter 3, where the optimal planning problem was solved without considering the PV self consumption (see section 3.5.1). Specifically, we chose the case for Scenario A with single-port and multi-port chargers, solved with 1-day optimization horizon.

Nodal injections

The computation of nodal injections is done using Eq. 1.4. In the context of the case study, Fig.A.1 illustrates the active power injections over the time horizon at various MV grid nodes, which serve as the selected linearization points/working points. It is important to note that the power injections in Fig. A.1, solely represents the demand profile and do not incorporate the injections attributed to EVs recharge. Through the solution of the optimization problem, the nodal power contributions from EVs are determined over the time horizon. With this, perturbed nodal injections are computed, as shown in Fig. A.2. Subsequently, by computing the nodal injections, the ground-truth quantities of the grid model can be obtained through the execution of a nonlinear load flow analysis. From the plots, it can be observed that the nodal per-unit injection values are zero at grid nodes 2, 7, 9, and 13. The injection values at nodes 1 and 12 are high compared to other injections due to their proximity to the GCP, but they are not shown here as EVs are not connected to those nodes. The following section will address the errors in the voltage and current models.

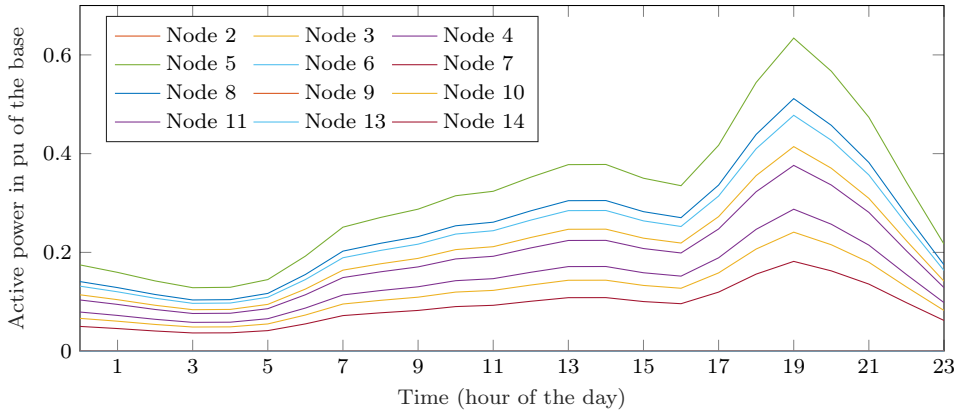

Figure A.1: Injections at different MV grid nodes serving as the selected linearization points for the case study.

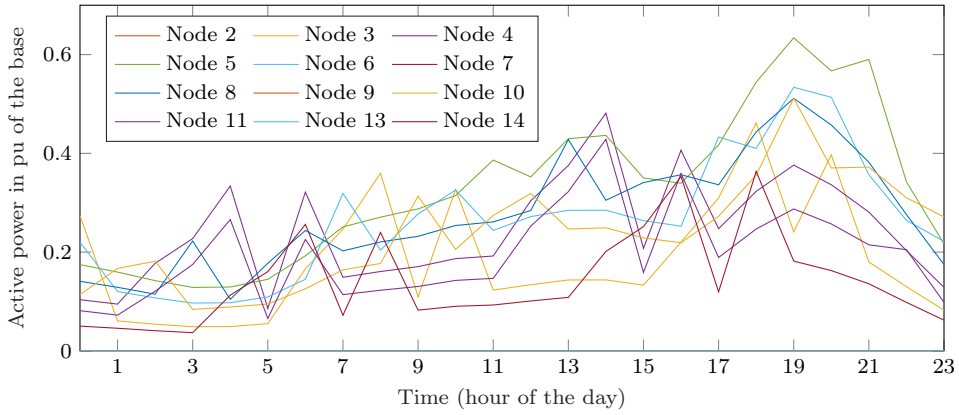

Figure A.2: The perturbed injections at different MV grid nodes for the case study.

Errors in linearized grid models

The linear estimation method relies on the utilization of SCs and the perturbed injections, as explained in the previous section. The histogram of the errors of the linear voltage and current estimations for the referred case study are shown in Figures A.3 and A.4, respectively. In this case study, the active constraints of the problem were the nodal injections in (3.18d). It was verified that grid's voltage and current constraints were not violated even when accounting for the estimation errors of the linear model. However, in order to (conservatively) hedge against these modeling errors, one could add back-off terms to voltage and current constraints in (3.18a) and (3.18b) considering, for example, worst-case modelling errors from these histograms.

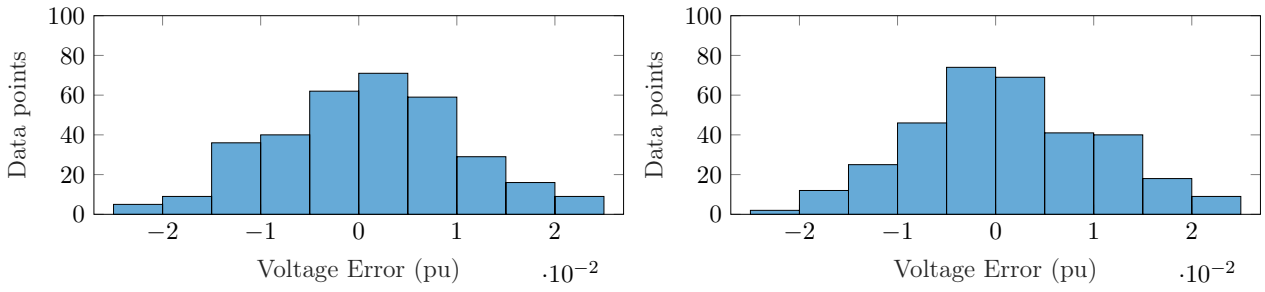

(a) Scenario A - SPC

(b) Scenario A - MPC

Figure A.3: Errors of the linear estimates of the nodal voltage magnitudes (in per unit of the base voltage).

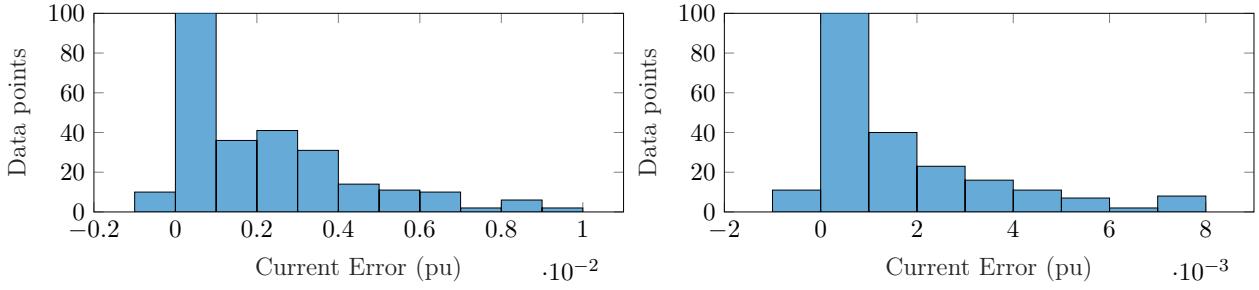

(a) Scenario A - SPC

(b) Scenario A - MPC

Figure A.4: Errors of the linear estimates of the lines' current magnitudes (per unit obtained by rescaling by the larger current observed in the grid).

Bibliography

[1] Katarina Knezovic. *Active integration of electric vehicles in the distribution network - theory, modelling and practice*. PhD thesis, 2017.

[2] IRENA. Innovation outlook: Smart charging for electric vehicles. Technical Report MSU-CSE-06-2, International Renewable Energy Agency, Abu Dhabi, 2019.

[3] Integration of electric vehicles into the power system in france. Technical report, RTE France, May 2019.

[4] IEA: Empowering electricity consumers to lower their carbon footprint. URL: https://www.iea.org/commentaries/empowering-electricity-consumers-to-lower-their-carbon-footprint. Accessed: 2022-09.

[5] Juan Van Roy. *Electric Vehicle Charging Integration in Buildings: Local Charging Coordination and DC Grids*. PhD thesis, KU Leuven, 2015.

[6] CIGRE' Task Force C6.04.02. Benchmark systems for network integration of renewable and distributed energy resources. Technical report, Cigre' International Council on large electric systems, July 2009.

[7] Biswarup Mukherjee and Fabrizio Sossan. Optimal planning of single-port and multi-port charging stations for electric vehicles in medium voltage distribution networks. *arXiv preprint arXiv:2111.07100*, 2021.

[8] Vehicle-to-Grid (V2G) power flow regulations and building codes review by the AVTA, september-2012, Idaho national laboratory. Online: https://bit.ly/30ZvNXr. Accessed: 2020-07.

[9] NASA. Online: https://climate.nasa.gov/effects/. Accessed: 2022-10.

[10] WEF: The countries most ready for the global energy transition. Online: https://www.weforum.org/agenda/2019/03/the-countries-most-ready-for-the-global-energy-transition/. Accessed: 2022-10.

[11] European legislation on climate change. Online: https://www.europarl.europa.eu/climatechange/doc/EU_Legislation_on_climate_change.pdf/, . Accessed: 2022-09.

[12] EU 2030 climate energy framework. Online: https://bit.ly/2P7PION, . Accessed: 2020-07.

[13] European Environment Agency (EEA). Online: https://bit.ly/2BIUYVv. Accessed: 2020-07.

[14] IEA: Transport, Energy and CO2. Online: https://iea.blob.core.windows.net/assets/34816408-681f-4dbb-9a1c-8bf787bf8ad3/transport2009.pdf. Accessed: 2020-06.

[15] Pia Grahn. *Electric Vehicle Charging Modeling*. PhD thesis, 2014.

[16] EU 2030 climate & energy framework. URL https://www.consilium.europa.eu/en/policies/climate-change/2030-climate-and-energy-framework/. Accessed: 2020-07.

[17] Marc-Olivier Metais, O. Jouini, Yannick Perez, Jaâfar Berrada, and Emilia Suomalainen. Too much or not enough? Planning electric vehicle charging infrastructure: a review of modeling options. working paper or preprint, February 2021. URL https://hal.archives-ouvertes.fr/hal-03127266.

[18] IEA, electric car stock by region and technology, 2013-2018, iea, paris. Online: https://www.iea.org/data-and-statistics/charts/electric-car-stock-by-region-and-technology-2013-2018. Accessed: 2020-06.

[19] J. A. P. Lopes, F. J. Soares, and P. M. R. Almeida. Integration of electric vehicles in the electric power system. *Proceedings of the IEEE*, 99(1):168–183, 2011.

[20] A. Ul-Haq, C. Buccella, C. Cecati, and H. A. Khalid. Smart charging infrastructure for electric vehicles. In *2013 International Conference on Clean Electrical Power (ICCEP)*, pages 163–169, 2013.

[21] Farhad Shahnia, Arindam Ghosh, Gerard Ledwich, and Firuz Zare. Voltage unbalance sensitivity analysis of plug-in electric vehicles in distributed networks. In G Ledwich, editor, *Proceedings of the 21st Australasian Universities Power Engineering Conference: Integrating Renewables into the Grid*, pages 1–6. IEEE, United States, 2011. URL https://eprints.qut.edu.au/80461/.

[22] Handbook of electric vehicle charging infrastructure implementation. Technical report, NITY Aayog, August 2021.

[23] B. Schucht. The development of e-mobility from the perspective of a german tso. 2017.

[24] Philipp Andreas Gunkel, Claire Bergaentzlé, Ida Græsted Jensen, and Fabian Scheller. From passive to active: Flexibility from electric vehicles in the context of transmission system development. *Applied Energy*, 277:115526, 2020. ISSN 0306-2619. doi: https://doi.org/10.1016/j.apenergy.2020.115526. URL https://www.sciencedirect.com/science/article/pii/S0306261920310382.

[25] IRENA. Innovation outlook: Smart charging for electric vehicles. Technical Report MSU-CSE-06-2, International Renewable Energy Agency, Abu Dhabi, 2019.

[26] Katarina Knezović, Alireza Soroudi, Andrew Keane, and Mattia Marinelli. Robust multi-objective pq scheduling for electric vehicles in flexible unbalanced distribution grids. *IET Generation, Transmission & Distribution*, 11(16):4031–4040, 2017. doi: https://doi.org/10.1049/iet-gtd.2017.0309. URL https://ietresearch.onlinelibrary.wiley.com/doi/abs/10.1049/iet-gtd.2017.0309.

[27] Sumit Paudyal, Oğuzhan Ceylan, Bishnu P. Bhattarai, and Kurt S. Myers. Optimal coordinated ev charging with reactive power support in constrained distribution grids. In *2017 IEEE Power Energy Society General Meeting*, pages 1–5, 2017. doi: 10.1109/PESGM.2017.8274266.

[28] Niels Leemput, Juan Van Roy, Frederik Geth, J. Driesen, and Sven De Breucker. Grid and fleet impact mapping of ev charge opportunities. *Data Science and Simulation in Transportation Research*, pages 364–390, 01 2013.

[29] O. Beaude, Y. He, and M. Hennebel. Introducing decentralized ev charging coordination for the voltage regulation. In *IEEE PES ISGT Europe 2013*, pages 1–5, 2013.

[30] J. Hu, S. You, M. Lind, and J. Østergaard. Coordinated charging of electric vehicles for congestion prevention in the distribution grid. *IEEE Transactions on Smart Grid*, 5(2):703–711, 2014.

[31] A. Masood, J. Hu, A. Xin, A. R. Sayed, and G. Yang. Transactive energy for aggregated electric vehicles to reduce system peak load considering network constraints. *IEEE Access*, 8:31519–31529, 2020. ISSN 2169-3536. doi: 10.1109/ACCESS.2020.2973284.

[32] Ministère de l'environnement de l'énergie et de lamer - La loi de transition Énergétique pour la croissance verte. URL https://bit.ly/3aRJ1Lb. Accessed: 2021-03.

[33] Estimating electric vehicle charging infrastructure costs across major U.S. metropolitan areas. URL https://theicct.org/publications/charging-cost-US. Accessed: 2021-03.

[34] Fabrizio Sossan. *Indirect control of flexible demand for power system applications.* PhD thesis, 2014.

[35] Joakim Widén, Ewa Wäckelgård, and Peter D. Lund. Options for improving the load matching capability of distributed photovoltaics: Methodology and application to high-latitude data. *Solar Energy*, 83(11):1953–1966, 2009. ISSN 0038-092X. doi: https://doi.org/10.1016/j.solener.2009.07.007. URL https://www.sciencedirect.com/science/article/pii/S0038092X09001741.

[36] Rasmus Luthander, Joakim Widén, Daniel Nilsson, and Jenny Palm. Photovoltaic self-consumption in buildings: A review. *Applied Energy*, 142:80–94, 2015. ISSN 0306-2619. doi: https://doi.org/10.1016/j.apenergy.2014.12.028. URL https://www.sciencedirect.com/science/article/pii/S0306261914012859.

[37] Guozhong Liu, Li Kang, Zeyu Luan, Jing Qiu, and Fenglei Zheng. Charging station and power network planning for integrated electric vehicles (EVs). *Energies*, 12(13), 2019.

[38] Yue Xiang, Junyong Liu, Ran Li, Furong Li, Chenghong Gu, and Shuoya Tang. Economic planning of electric vehicle charging stations considering traffic constraints and load profile templates. *Applied Energy*, 178:647–659, 2016. ISSN 0306-2619.

[39] J. Li, X. Sun, Q. Liu, W. Zheng, H. Liu, and J. A. Stankovic. Planning electric vehicle charging stations based on user charging behavior. In *2018 IEEE/ACM Third International Conference on Internet-of-Things Design and Implementation (IoTDI)*, pages 225–236, 2018. doi: 10.1109/IoTDI.2018.00030.

[40] Wei Gan, Mohammad Shahidehpour, Jianbo Guo, Wei Yao, Aleksi Paaso, Liuxi Zhang, and Jinyu Wen. Two-stage planning of network-constrained hybrid energy supply stations for electric and natural gas vehicles. *IEEE Transactions on Smart Grid*, 12(3):2013–2026, 2021. doi: 10.1109/TSG.2020.3039493.

[41] Wei Gan, Mohammad Shahidehpour, Mingyu Yan, Jianbo Guo, Wei Yao, Aleksi Paaso, Liuxi Zhang, and Jinyu Wen. Coordinated planning of transportation and electric power networks with the proliferation of electric vehicles. *IEEE Transactions on Smart Grid*, 11(5):4005–4016, 2020. doi: 10.1109/TSG.2020.2989751.

[42] Albert Y. S. Lam, Yiu-Wing Leung, and Xiaowen Chu. Electric vehicle charging station placement: Formulation, complexity, and solutions. *IEEE Transactions on Smart Grid*, 5(6): 2846–2856, 2014. doi: 10.1109/TSG.2014.2344684.

[43] Chao Luo, Yih-Fang Huang, and Vijay Gupta. Placement of EV charging stations—balancing benefits among multiple entities. *IEEE Transactions on Smart Grid*, 8(2):759–768, 2017. doi: 10.1109/TSG.2015.2508740.

[44] Zechun Hu and Yonghua Song. Distribution network expansion planning with optimal siting and sizing of electric vehicle charging stations. In *2012 47th International Universities Power Engineering Conference (UPEC)*, pages 1–6, 2012. doi: 10.1109/UPEC.2012.6398568.

[45] Xiong Yanhai, An Bo, and Kraus Sarit. Electric vehicle charging strategy study and the application on charging station placement. *Autonomous Agents and Multi-Agent Systems*, 35 (3), 2021. doi: https://doi.org/10.1007/s10458-020-09484-5.

[46] Jingqi Zhang, Shu Wang, Cuo Zhang, Fengji Luo, Zhao Yang Dong, and Yingliang Li. Planning of electric vehicle charging stations and distribution system with highly renewable penetrations. *IET Electrical Systems in Transportation*, 11(3):256–268, 2021. doi: https://doi.org/10.1049/els2.12022. URL https://ietresearch.onlinelibrary.wiley.com/doi/abs/10.1049/els2.12022.

[47] Hengsong Wang, Qi Huang, Changhua Zhang, and Aihua Xia. A novel approach for the layout of electric vehicle charging station. In *The 2010 International Conference on Apperceiving Computing and Intelligence Analysis Proceeding*, pages 64–70, 2010. doi: 10.1109/ICACIA.2010.5709852.

[48] Dongxiang Yan and Chengbin Ma. Stochastic planning of electric vehicle charging station integrated with photovoltaic and battery systems. *IET Generation, Transmission & Distribution*, 14(19):4217–4224, 2020. doi: https://doi.org/10.1049/iet-gtd.2019.1737. URL https://ietresearch.onlinelibrary.wiley.com/doi/abs/10.1049/iet-gtd.2019.1737.

[49] Fang Yao, Jiawei Wang, Fushuan Wen, Chung-Li Tseng, Xingyong Zhao, and Qiang Wang. An integrated planning strategy for a power network and the charging infrastructure of electric vehicles for power system resilience enhancement. *Energies*, 12(20), 2019. ISSN 1996-1073. doi: 10.3390/en12203918. URL https://www.mdpi.com/1996-1073/12/20/3918.

[50] Nataly Bañol Arias, Alejandra Tabares, John F. Franco, Marina Lavorato, and Rubén Romero. Robust joint expansion planning of electrical distribution systems and ev charging stations. *IEEE Transactions on Sustainable Energy*, 9(2):884–894, 2018. doi: 10.1109/TSTE.2017.2764080.

[51] Sahand Karimi-Arpanahi, Mohammad Jooshaki, Mahmud Fotuhi-Firuzabad, and Matti Lehtonen. Flexibility-oriented collaborative planning model for distribution network and ev parking lots considering uncertain behaviour of EVs. In *Proceedings of the 2020 International Conference on Probabilistic Methods Applied to Power Systems, PMAPS 2020*, United States, August 2020. IEEE. doi: 10.1109/PMAPS47429.2020.9183450.

[52] Chengcheng Shao, Tao Qian, Yanan Wang, and Xifan Wang. Coordinated planning of extreme fast charging stations and power distribution networks considering on-site storage. *IEEE Transactions on Intelligent Transportation Systems*, 22(1):493–504, 2021. doi: 10.1109/TITS.2020.3016765.

[53] Mohammad Mozaffari, Hossein Askarian Abyaneh, Mohammad Jooshaki, and Moein Moeini-Aghtaie. Joint expansion planning studies of ev parking lots placement and distribution network. *IEEE Transactions on Industrial Informatics*, 16(10):6455–6465, 2020. doi: 10.1109/TII.2020.2964049.

[54] Saeed Shojaabadi, Saeed Abapour, Mehdi Abapour, and Ali Nahavandi. Simultaneous planning of plug-in hybrid electric vehicle charging stations and wind power generation in distribution networks considering uncertainties. *Renewable Energy*, 99:237–252, 2016. ISSN 0960-1481. doi: https://doi.org/10.1016/j.renene.2016.06.032. URL https://www.sciencedirect.com/science/article/pii/S0960148116305560.

[55] Xu Wang, Mohammad Shahidehpour, Chuanwen Jiang, and Zhiyi Li. Coordinated planning strategy for electric vehicle charging stations and coupled traffic-electric networks. *IEEE Transactions on Power Systems*, 34(1):268–279, 2019. doi: 10.1109/TPWRS.2018.2867176.

[56] Weifeng Yao, Junhua Zhao, Fushuan Wen, Zhaoyang Dong, Yusheng Xue, Yan Xu, and Ke Meng. A multi-objective collaborative planning strategy for integrated power distribution and electric vehicle charging systems. *IEEE Transactions on Power Systems*, 29(4):1811–1821, 2014. doi: 10.1109/TPWRS.2013.2296615.

[57] Sebastian Hörl, F. Ciari, and K. Axhausen. Recent perspectives on the impact of autonomous vehicles. 2016.

[58] Ten ways autonomous driving could redefine the automotive world. Technical report, McKinsey&Company, June 2015.

[59] T. Donna Chen, Kara M. Kockelman, and Josiah P. Hanna. Operations of a shared, autonomous, electric vehicle fleet: Implications of vehicle charging infrastructure decisions. *Transportation Research Part A: Policy and Practice*, 94:243 – 254, 2016. ISSN 0965-8564. doi: https://doi.org/10.1016/j.tra.2016.08.020. URL http://www.sciencedirect.com/science/article/pii/S096585641630756X.

[60] Riccardo Iacobucci, Benjamin McLellan, and Tetsuo Tezuka. Modeling shared autonomous electric vehicles: Potential for transport and power grid integration. *Energy*, 158:148 – 163, 2018. ISSN 0360-5442. doi: https://doi.org/10.1016/j.energy.2018.06.024. URL http://www.sciencedirect.com/science/article/pii/S0360544218310776.

[61] Jeffery B. Greenblatt and Samveg Saxena. Autonomous taxis could greatly reduce greenhouse-gas emissions of us light-duty vehicles. *Nature Clim Change*, 5:860–863, 2015. ISSN 0360-5442. doi: https://doi.org/10.1038/nclimate2685. URL https://www.nature.com/articles/nclimate2685.

[62] Fabio ANTONIALLI. International benchmark on experimentations with Autonomous Shuttles for Collective Transport. In *27th International Colloquium of Gerpisa*, Paris, France, February 2019. URL https://hal-centralesupelec.archives-ouvertes.fr/hal-02489797.

[63] Camila Fernandes, Pablo Frías, and Jesús M. Latorre. Impact of vehicle-to-grid on power system operation costs: The spanish case study. *Applied Energy*, 96:194–202, 2012. ISSN 0306-2619. doi: https://doi.org/10.1016/j.apenergy.2011.11.058. URL https://www.sciencedirect.com/science/article/pii/S0306261911007641. Smart Grids.

[64] F. Sossan, B. Mukherjee, and Z. Hu. Impact of the charging demand of electric vehicles on distribution grids: a comparison between autonomous and non-autonomous driving. In *2020 Fifteenth International Conference on Ecological Vehicles and Renewable Energies (EVER)*, pages 1–6, 2020. doi: 10.1109/EVER48776.2020.9243122.

[65] Hongcai Zhang, Colin JR Sheppard, Timothy E Lipman, Teng Zeng, and Scott J Moura. Charging infrastructure demands of shared-use autonomous electric vehicles in urban areas. *Transportation Research Part D: Transport and Environment*, 78:102210, 2020.

[66] Mustafa Lokhandwala and Hua Cai. Siting charging stations for electric vehicle adoption in shared autonomous fleets. *Transportation Research Part D: Transport and Environment*, 80: 102231, 2020.

[67] Hamdi Abdi, Behnam Mohammadi-ivatloo, Saeid Javadi, Amir Reza Khodaei, and Ehsan Dehnavi. Chapter 7 - energy storage systems. In G.B. Gharehpetian and S. Mohammad Mousavi Agah, editors, *Distributed Generation Systems*, pages 333 – 368. Butterworth-Heinemann, 2017. ISBN 978-0-12-804208-3. doi: https://doi.org/10.1016/B978-0-12-804208-3.00007-8. URL http://www.sciencedirect.com/science/article/pii/B9780128042083000078.

[68] Is vehicle-to-home or vehicle-to-grid suitable for the electric vehicle user? discussion from a one year intensive experience, EVS29 Symposium 2016, Montréal.

[69] T.S. Kishore and S.K. Singal. Optimal economic planning of power transmission lines: A review. *Renewable and Sustainable Energy Reviews*, 39:949–974, 2014. ISSN 1364-0321. doi: https://doi.org/10.1016/j.rser.2014.07.125. URL https://www.sciencedirect.com/science/article/pii/S1364032114005772.

[70] Etta Grover Silva. *Optimization of the planning and operations of electric distribution grids in the context of high renewable energy penetration.* Theses, Université Paris sciences et lettres, December 2017. URL https://pastel.archives-ouvertes.fr/tel-01899752.

[71] S. Chatzivasileiadis. Lecture notes on optimal power flow (OPF). https://arxiv.org/pdf/1811.00943.pdf, 2018.

[72] Anton Vinkovic, Marko Suhadolc, and Rafael Mihalic. Current-based models of facts devices for three-phase load-flow calculations using the newton–raphson method. *International Journal of Electrical Power Energy Systems*, 45(1):117–128, 2013. ISSN 0142-0615. doi: https://doi.org/10.1016/j.ijepes.2012.08.070. URL https://www.sciencedirect.com/science/article/pii/S0142061512005200.

[73] Débora Rosana Ribeiro Penido, Leandro Ramos de Araujo, Sandoval Carneiro Júnior, and José Luiz Rezende Pereira. A new tool for multiphase electrical systems analysis based on current injection method. *International Journal of Electrical Power Energy Systems*, 44 (1):410–420, 2013. ISSN 0142-0615. doi: https://doi.org/10.1016/j.ijepes.2012.07.066. URL https://www.sciencedirect.com/science/article/pii/S0142061512004310.

[74] Hany E. Farag, E.F. El-Saadany, Ramadan El Shatshat, and Aboelsood Zidan. A generalized power flow analysis for distribution systems with high penetration of distributed generation. *Electric Power Systems Research*, 81(7):1499–1506, 2011. ISSN 0378-7796. doi: https://doi.org/10.1016/j.epsr.2011.03.001. URL https://www.sciencedirect.com/science/article/pii/S0378779611000642.

[75] W.C. Wu and B.M. Zhang. A three-phase power flow algorithm for distribution system power flow based on loop-analysis method. *International Journal of Electrical Power Energy Systems*, 30(1):8–15, 2008. ISSN 0142-0615. doi: https://doi.org/10.1016/j.ijepes.2007.06.005. URL https://www.sciencedirect.com/science/article/pii/S0142061507000774.

[76] Tsai-Hsiang Chen and Nien-Che Yang. Loop frame of reference based three-phase power flow for unbalanced radial distribution systems. *Electric Power Systems Research*, 80(7):799–806, 2010. ISSN 0378-7796. doi: https://doi.org/10.1016/j.epsr.2009.12.006. URL https://www.sciencedirect.com/science/article/pii/S0378779609003022.

[77] M. Abdel-Akher, K.M. Nor, and A.H.A. Rashid. Improved three-phase power-flow methods using sequence components. *IEEE Transactions on Power Systems*, 20(3):1389–1397, 2005. doi: 10.1109/TPWRS.2005.851933.

[78] Xiong Yang, Zhinong Wei, Guoqiang Sun, Yonghui Sun, Yang Yuan, Zigang Lu, Xiaohui Xu, and Li Huang. Power flow calculation for unbalanced three-phase distribution network with dgs based on phase-sequence hybrid modeling. In *2013 IEEE International Conference on Smart Energy Grid Engineering (SEGE)*, pages 1–6, 2013. doi: 10.1109/SEGE.2013.6707926.

[79] Stephen Boyd and Lieven Vandenberghe. *Convex optimization*. Cambridge university press, 2004.

[80] Prakornchai Phonrattanasak. Optimal placement of dg using multiobjective particle swarm optimization. In *2010 International Conference on Mechanical and Electrical Technology*, pages 342–346, 2010. doi: 10.1109/ICMET.2010.5598377.

[81] J.J. Jamian, M.W. Mustafa, H. Mokhlis, and M.A. Baharudin. Simulation study on optimal placement and sizing of battery switching station units using artificial bee colony algorithm. *International Journal of Electrical Power Energy Systems*, 55:592–601, 2014. ISSN 0142-0615. doi: https://doi.org/10.1016/j.ijepes.2013.10.009. URL https://www.sciencedirect.com/science/article/pii/S0142061513004262.

[82] Amany El-Zonkoly. Optimal placement and schedule of multiple grid connected hybrid energy systems. *International Journal of Electrical Power Energy Systems*, 61:239–247, 2014. ISSN 0142-0615. doi: https://doi.org/10.1016/j.ijepes.2014.03.040. URL https://www.sciencedirect.com/science/article/pii/S0142061514001422.

[83] Mohammad H. Moradi, Mohammad Abedini, S.M. Reza Tousi, and S. Mahdi Hosseinian. Optimal siting and sizing of renewable energy sources and charging stations simultaneously based on differential evolution algorithm. *International Journal of Electrical Power Energy Systems*, 73:1015–1024, 2015. ISSN 0142-0615. doi: https://doi.org/10.1016/j.ijepes.2015.06.029. URL https://www.sciencedirect.com/science/article/pii/S0142061515002859.

[84] Mahdi Sedghi, Ali Ahmadian, and Masoud Aliakbar-Golkar. Optimal storage planning in active distribution network considering uncertainty of wind power distributed generation. *IEEE Transactions on Power Systems*, 31(1):304–316, 2016. doi: 10.1109/TPWRS.2015.2404533.

[85] Sumit Paudyal, Claudio A. Cañizares, and Kankar Bhattacharya. Three-phase distribution opf in smart grids: Optimality versus computational burden. In *2011 2nd IEEE PES International*

Conference and Exhibition on Innovative Smart Grid Technologies, pages 1–7, 2011. doi: 10.1109/ISGTEurope.2011.6162628.

[86] Javad Lavaei and Steven H. Low. Zero duality gap in optimal power flow problem. *IEEE Transactions on Power Systems*, 27(1):92–107, 2012. doi: 10.1109/TPWRS.2011.2160974.

[87] X. Bai. Semi-definite programming-based method for security-constrained unit commitment with operational and optimal power flow constraints. *IET Generation, Transmission Distribution*, 3:182–197(15), February 2009. ISSN 1751-8687. URL https://digital-library.theiet.org/content/journals/10.1049/iet-gtd_20070516.

[88] Subhonmesh Bose, Steven H. Low, Thanchanok Teeraratkul, and Babak Hassibi. Equivalent relaxations of optimal power flow. *IEEE Transactions on Automatic Control*, 60(3):729–742, 2015. doi: 10.1109/TAC.2014.2357112.

[89] Masoud Farivar, Russell Neal, Christopher Clarke, and Steven Low. Optimal inverter var control in distribution systems with high pv penetration. In *2012 IEEE Power and Energy Society General Meeting*, pages 1–7, 2012. doi: 10.1109/PESGM.2012.6345736.

[90] Na Li, Lijun Chen, and Steven H. Low. Exact convex relaxation of opf for radial networks using branch flow model. In *2012 IEEE Third International Conference on Smart Grid Communications (SmartGridComm)*, pages 7–12, 2012. doi: 10.1109/SmartGridComm.2012.6485951.

[91] Lingwen Gan and Steven H. Low. Convex relaxations and linear approximation for optimal power flow in multiphase radial networks. In *2014 Power Systems Computation Conference*, pages 1–9, 2014. doi: 10.1109/PSCC.2014.7038399.

[92] S.Y. Abdelouadoud, R. Girard, F.P. Neirac, and T. Guiot. Optimal power flow of a distribution system based on increasingly tight cutting planes added to a second order cone relaxation. *International Journal of Electrical Power Energy Systems*, 69:9–17, 2015. ISSN 0142-0615. doi: https://doi.org/10.1016/j.ijepes.2014.12.084. URL https://www.sciencedirect.com/science/article/pii/S0142061515000095.

[93] Avirup Maulik and Debapriya Das. Optimal operation of microgrid using four different optimization techniques. *Sustainable Energy Technologies and Assessments*, 21:100–120, 2017. ISSN 2213-1388. doi: https://doi.org/10.1016/j.seta.2017.04.005. URL https://www.sciencedirect.com/science/article/pii/S221313881730228X.

[94] Simone Baldi, Athanasios Karagevrekis, Iakovos T. Michailidis, and Elias B. Kosmatopoulos. Joint energy demand and thermal comfort optimization in photovoltaic-equipped interconnected microgrids. *Energy Conversion and Management*, 101:352–363, 2015. ISSN 0196-8904. doi: https://doi.org/10.1016/j.enconman.2015.05.049. URL https://www.sciencedirect.com/science/article/pii/S019689041500504X.

[95] Nicholas Good, Efthymios Karangelos, Alejandro Navarro-Espinosa, and Pierluigi Mancarella. Optimization under uncertainty of thermal storage-based flexible demand response with quan-

tification of residential users' discomfort. *IEEE Transactions on Smart Grid*, 6(5):2333–2342, 2015. doi: 10.1109/TSG.2015.2399974.

[96] Zhaoyu Wang, Bokan Chen, Jianhui Wang, Miroslav M. Begovic, and Chen Chen. Coordinated energy management of networked microgrids in distribution systems. *IEEE Transactions on Smart Grid*, 6(1):45–53, 2015. doi: 10.1109/TSG.2014.2329846.

[97] K. R. Krishnanand, D. C. Hoang, S. K. Panda, and Rui Zhang. Optimal appliance scheduling in building operating systems for cost-effective energy management. In *IECON 2014 - 40th Annual Conference of the IEEE Industrial Electronics Society*, pages 5394–5399, 2014. doi: 10.1109/IECON.2014.7049324.

[98] Luhao Wang, Qiqiang Li, Ran Ding, Mingshun Sun, and Guirong Wang. Integrated scheduling of energy supply and demand in microgrids under uncertainty: A robust multi-objective optimization approach. *Energy*, 130:1–14, 2017. ISSN 0360-5442. doi: https://doi.org/10.1016/j.energy.2017.04.115. URL https://www.sciencedirect.com/science/article/pii/S0360544217306813.

[99] Vincenzo Trovato, Fei Teng, and Goran Strbac. Role and benefits of flexible thermostatically controlled loads in future low-carbon systems. *IEEE Transactions on Smart Grid*, 9(5):5067–5079, 2018. doi: 10.1109/TSG.2017.2679133.

[100] Yu Zhang, Nikolaos Gatsis, and Georgios B. Giannakis. Robust energy management for microgrids with high-penetration renewables. *IEEE Transactions on Sustainable Energy*, 4 (4):944–953, 2013. doi: 10.1109/TSTE.2013.2255135.

[101] Nima Nikmehr, Sajad Najafi-Ravadanegh, and Amin Khodaei. Probabilistic optimal scheduling of networked microgrids considering time-based demand response programs under uncertainty. *Applied Energy*, 198:267–279, 2017. ISSN 0306-2619. doi: https://doi.org/10.1016/j.apenergy.2017.04.071. URL https://www.sciencedirect.com/science/article/pii/S0306261917304774.

[102] John Peschon, Dean S. Piercy, William F. Tinney, and Odd J. Tveit. Sensitivity in power systems. *IEEE Transactions on Power Apparatus and Systems*, PAS-87(8):1687–1696, 1968. doi: 10.1109/TPAS.1968.292130.

[103] Qiong Zhou and Janusz W. Bialek. Simplified calculation of voltage and loss sensitivity factors in distribution networks. In *16th Power Systems Computation Conference, PSCC 2008*, 16th Power Systems Computation Conference, PSCC 2008. Power Systems Computation Conference (PSCC), 2008.

[104] J. W. Bandler and M. A. El-Kady. A new method for computerized solution of power flow equations. *IEEE Transactions on Power Apparatus and Systems*, PAS-101(1):1–10, 1982. doi: 10.1109/TPAS.1982.317249.

[105] L.A.F.M. Ferreira. Tellegen's theorem and power systems-new load flow equations, new solution methods. *IEEE Transactions on Circuits and Systems*, 37(4):519–526, 1990. doi: 10.1109/31.52753.

[106] Ravindranath Gurram and B. Subramanyam. Sensitivity analysis of radial distribution network – adjoint network method. *International Journal of Electrical Power Energy Systems*, 21(5):323–326, 1999. ISSN 0142-0615. doi: https://doi.org/10.1016/S0142-0615(98)00058-1. URL https://www.sciencedirect.com/science/article/pii/S0142061598000581.

[107] K. Christakou, J. LeBoudec, M. Paolone, and D. Tomozei. Efficient computation of sensitivity coefficients of node voltages and line currents in unbalanced radial electrical distribution networks. *IEEE Transactions on Smart Grid*, 4(2):741–750, 2013.

[108] Chunlei Sun, Xiangming Wen, Zhaoming Lu, Junshan Zhang, and Xi Chen. A graphical game approach to electrical vehicle charging scheduling: Correlated equilibrium and latency minimization. *IEEE Transactions on Intelligent Transportation Systems*, 22(1):505–517, 2021. doi: 10.1109/TITS.2020.3025721.

[109] Lingwen Gan, Ufuk Topcu, and Steven H. Low. Optimal decentralized protocol for electric vehicle charging. *IEEE Transactions on Power Systems*, 28(2):940–951, 2013. doi: 10.1109/TPWRS.2012.2210288.

[110] Hao Xing, Minyue Fu, Zhiyun Lin, and Yuting Mou. Decentralized optimal scheduling for charging and discharging of plug-in electric vehicles in smart grids. *IEEE Transactions on Power Systems*, 31(5):4118–4127, 2016. doi: 10.1109/TPWRS.2015.2507179.

[111] Mohammad Nikkhah Mojdehi and Prasanta Ghosh. An on-demand compensation function for an ev as a reactive power service provider. *IEEE Transactions on Vehicular Technology*, 65(6):4572–4583, 2016. doi: 10.1109/TVT.2015.2504264.

[112] Mithat C. Kisacikoglu, Burak Ozpineci, and Leon M. Tolbert. Examination of a phev bidirectional charger system for v2g reactive power compensation. In *2010 Twenty-Fifth Annual IEEE Applied Power Electronics Conference and Exposition (APEC)*, pages 458–465, 2010. doi: 10.1109/APEC.2010.5433629.

[113] Mithat C. Kisacikoglu, Metin Kesler, and Leon M. Tolbert. Single-phase on-board bidirectional pev charger for v2g reactive power operation. *IEEE Transactions on Smart Grid*, 6(2): 767–775, 2015. doi: 10.1109/TSG.2014.2360685.

[114] Lizi Luo, Pinquan He, Suyang Zhou, Guannan Lou, Bin Fang, and Puyu Wang. Optimal scheduling strategy of evs considering the limitation of battery state switching times. *Energy Reports*, 8:918–927, 2022. ISSN 2352-4847. doi: https://doi.org/10.1016/j.egyr.2022.02.199. URL https://www.sciencedirect.com/science/article/pii/S2352484722004462. ICPE 2021 - The 2nd International Conference on Power Engineering.

[115] Yifeng He, Bala Venkatesh, and Ling Guan. Optimal scheduling for charging and discharging of electric vehicles. *IEEE Transactions on Smart Grid*, 3(3):1095–1105, 2012. doi: 10.1109/TSG.2011.2173507.

[116] Niels Leemput, Frederik Geth, Juan Van Roy, Pol Olivella-Rosell, Johan Driesen, and Andreas Sumper. MV and LV residential grid impact of combined slow and fast charging of electric vehicles. *Energies*, 8(3), 2015. ISSN 1996-1073. doi: 10.3390/en8031760.

[117] Sylvester Johansson, Jonas Persson, Stavros Lazarou, and Andreas Theocharis. Investigation of the impact of large-scale integration of electric vehicles for a swedish distribution network. *Energies*, 12, 2019.

[118] Peter Bach Andersen. *Intelligent electric vehicle integration-domain interfaces and supporting informatics*. PhD thesis, Technical University of Denmark (DTU), 2013.

[119] Test-an-EV project: Electrical vehicle (EV) data. Online: http://mclabprojects.di.uniroma1.it/smarthgnew/Test-an-EV/?EV-code=EV8. Accessed: 2020-02.

[120] Garth P McCormick. Computability of global solutions to factorable nonconvex programs: Part i—convex underestimating problems. *Mathematical programming*, 10(1):147–175, 1976.

[121] Report on the integration of electric mobility, Enedis, France. URL https://bit.ly/3eWPjMQ. Accessed: 2021-03.

[122] Danilo J. Santini, Yan Zhou, Vetri Elango, Yanzhi Xu, and Randall Guensler. Daytime charging: What is the hierarchy of opportunities and customer needs? case study based on atlanta commute data. 2014.

[123] Laurent De Vroey, Rafael Jahn, Mohamed El Baghdadi, and Joeri Van Mierlo. Plug-to-wheel energy balance-results of a two years experience behind the wheel of electric vehicles. *World Electric Vehicle Journal*, 6(1):130–134, 2013.

[124] Kay W Axhausen, Andreas Horni, and Kai Nagel. *The multi-agent transport simulation MATSim*. Ubiquity Press, 2016.

[125] Marjan Gjelaj, Seyedmostafa Hashemi, Peter Bach Andersen, and Chresten Traeholt. Optimal infrastructure planning for ev fast-charging stations based on prediction of user behaviour. *IET Electrical Systems in Transportation*, 10(1):1–12, 2020. doi: https://doi.org/10.1049/iet-est.2018.5080. URL https://ietresearch.onlinelibrary.wiley.com/doi/abs/10.1049/iet-est.2018.5080.

[126] Mostafa Nick, Rachid Cherkaoui, and Mario Paolone. Optimal allocation of dispersed energy storage systems in active distribution networks for energy balance and grid support. *IEEE Transactions on Power Systems*, 29(5), 2014.

[127] Fabrizio Sossan, Enrica Scolari, Rahul Gupta, and Mario Paolone. Solar irradiance estimations for modeling the variability of photovoltaic generation and assessing violations of grid

constraints: A comparison between satellite and pyranometers measurements with load flow simulations. *Journal of Renewable and Sustainable Energy*, 11(5):056103, 2019.

[128] DA electricity prices in France - EPEXSpot. URL https://www.epexspot.com/en/market-data. Accessed: 2021-07.

[129] Spöttle, M., Jörling, K., Schimmel, M., Staats, M., Grizzel L., Jerram, L., Drier, W., Gartner, J. Research for TRAN committee - charging infrastructure for electric road vehicles. Technical report, European Parliament, Policy Department for Structural and Cohesion Policies, Brussels, 2018.

[130] Chris Nelder and Emily Rogers. Reducing EV charging infrastructure costs. Technical report, Rocky Mountain Institute, 2019.

[131] Schneider EVlink G4 smart charging station - EVB1A22P4ERI. URL https://bit.ly/3AVUWSO. Accessed: 2021-08.

[132] Sherif Fahmy and Mario Paolone. Analytical computation of power grids' sensitivity coefficients with voltage-dependent injections. In *2021 IEEE Madrid PowerTech*, pages 1–6, 2021. doi: 10.1109/PowerTech46648.2021.9494997.

RÉSUMÉ

Le nombre croissant de véhicules électriques (VE) représente un défi important pour les gestionnaires de réseaux de distribution (GRD) en raison de l'augmentation de la demande d'énergie nécessaire à la recharge. Cette thèse aborde le problème en développant des solutions algorithmiques pour aider les gestionnaires de réseaux de distribution à gérer efficacement la forte pénétration des véhicules électriques. La recherche se concentre sur deux aspects principaux : la programmation de la charge des VE et la planification de l'infrastructure de charge nécessaire. Pour la programmation de la charge des VE, la thèse se concentre sur le développement d'un cadre algorithmique unifié capable de prendre en compte différentes politiques de charge tout en considérant les contraintes opérationnelles du réseau. Ce cadre utilise une formulation OPF, incorporant un modèle linéarisé du réseau pour assurer la convexité et améliorer l'efficacité des calculs. Cette approche permet de comparer et d'analyser les performances de différentes stratégies de tarification. Pour planifier l'infrastructure de recharge en cas de forte pénétration des VE, une formulation MILP est proposée, étendant le cadre d'ordonnancement proposé. L'objectif est ici de calculer le nombre et l'emplacement des chargeurs de VE en satisfaisant la demande de charge des VE et les contraintes opérationnelles du réseau de distribution. La formulation proposée modélise explicitement la flexibilité des propriétaires dans le branchement et le débranchement de leurs VE. En outre, la méthode de planification prend en compte le concept de chargeurs à port unique et à ports multiples, en soulignant leur importance. En outre, une extension de la méthode est proposée pour encourager l'autoconsommation photovoltaïque et intégrer la fonctionnalité V2G. La validation des plans de déploiement proposés démontre la supériorité des chargeurs déployés de manière optimale pour atteindre des niveaux de charge plus élevés pour les VE par rapport aux scénarios de déploiement uniforme.

MOTS CLÉS

Véhicules électriques, Réseaux de distribution, Flux de puissance optimal, Programmation optimale, Planification optimale, Chargement intelligent, Véhicule-to-réseau, Stations de charge, Autoconsommation PV

ABSTRACT

The growing number of electric vehicles (EVs) poses a significant challenge for distribution grid operators (DSOs) due to their increased power demand required for charging. This thesis addresses the issue by developing algorithmic solutions to assist DSOs in effectively managing high EV penetration. The research focuses on two main aspects: scheduling EV charging and planning the necessary charging infrastructure. For scheduling the charge of EVs, the thesis focuses on the development of a unified algorithmic framework capable of accommodating various charging policies while considering operational constraints of the grid. This framework utilizes an OPF formulation, incorporating a linearized model of the grid to ensure convexity and improve computational efficiency. By employing this approach, the performance of different charging strategies can be compared and analyzed. To plan the charging infrastructure for large penetration of EVs, a MILP formulation is proposed, extending the proposed scheduling framework. Here the objective is to compute the number and the location of EV chargers by satisfying EVs' charging demand and the operational constraints of the distribution grid. The proposed formulation explicitly models flexibility of owners in plugging and unplugging their EVs. Additionally, the planning method considers the concept of single-port and multi-port chargers, highlighting their significance. Furthermore, an extension of the method is proposed to encourage PV self-consumption and incorporate V2G functionality. Validation of the proposed deployment plans demonstrates the superiority of optimally deployed chargers in achieving higher charging levels for EVs compared to uniform deployment scenarios.

KEYWORDS

Electric vehicles, Distribution networks, Optimal power flow, Optimal scheduling, Optimal planning, Smart charging, Vehicle-to-grid, Charging stations, PV self-consumption